Supporting Information

A heterologous expression platform in *Aspergillus nidulans* for the elucidation of cryptic secondary metabolism biosynthesis gene clusters: Discovery of the *Aspergillus fumigatus* sartorypyrone biosynthesis pathway

Shu-Yi Lin, C. Elizabeth Oakley, Cory B. Jenkinson, Yi-Ming Chiang, Ching-Kuo Lee, Christopher G. Jones, Paul M. Seidler, Hosea M. Nelson, Richard B. Todd, Clay C. C. Wang, and Berl R. Oakley

Correspondence should be addressed to clayw@usc.edu, boakley@ku.edu

Table of Contents

Detailed structural characterizations of new compounds from this study

Compound **1** has a molecular formula of $C_{26}H_{38}O_4$, as determined by its HRESIMS and ^{13}C-NMR data, representing eight indices of hydrogen deficiency (IHD). ^1H, ^{13}C, and HSQC NMR spectra showed signals for five methyl groups [δ_H 0.67, 0.75, 0.98, 1.73, and 2.10 (each 3H, s)], one carbinol methine group [δ_H 3.18 (1H, dd, J = 10.6, 5.4 Hz, H-3); δ_C 78.3 (C-3)], one downfield methylene [δ_H 3.02 (1H, dd, J = 13.9, 6.9 Hz, H-15) and 3.11 (1H, dd, J = 13.9, 7.7 Hz, H-15); δ_C 22.9 (C-15)], one terminal alkene [δ_H 4.52 and 4.80 (each 1H, br s, H-25); δ_C 106.7 (C-25)], and the α-pyrone moiety [δ_H 6.02 (1H, br d, J = 0.9 Hz, H-18), and 2.10 (3H, br s, H-20); δ_C 101.9 (C-16), 166.0 (C-17), 101.7 (C-18), 159.9 (C-19), 19.8 (C-20), and 167.4 (C-21)]. Besides the α-pyrone moiety, there are four additional sp2 carbons [δ_C 135.4 (C-13), 123.7 (C-14), 149.4 (C-8), and 106.7 (C-25)]. Considering that there are eight IHD in compound **1** with only one α-pyrone moiety and two olefins, compound **1** should contain a bicyclic diterpenoid moiety. Comparing the ^1H and ^{13}C NMR spectra of **1** with those of sartorypyrone D, the main differences are that one olefinic proton at ~ 5.03 ppm disappears, and one methyl group at ~ 1.59 ppm shifts to ~ 0.67 ppm in compound **1**, indicating the cyclization of one more ring in the diterpenoid moiety of compound **1**. In the HMBC spectrum, the long-range ^1H-^{13}C correlations between H_3-24 and C-1, C-5, C-9, and C-10 confirm the connectivity of the bicyclic structure. The correlations of H_2-15 to C-13, C-14, C-16, and C-17 further connect the bicyclic diterpenoid and the α-pyrone moiety to complete the planar structure of compound **1** (Table S2 and Fig S7-S11). The relative stereochemistry was determined by analysis of the NOESY spectrum (Table S2 and Fig S12). The H-5 signal exhibits correlations to H-3, H-9, and H_3-22, while showing no correlations with the methyl group at C-10 (H_3-24), suggesting a trans-decalin ring junction. Furthermore, since the NOESY spectral data also show cross peaks of H-14 to H_2-12 and H_2-15, the configuration of double bond at C-13 is 13*E*.

Compound **4** has a molecular formula of $C_{28}H_{40}O_5$, as deduced from its HRESIMS and ^{13}C-NMR data, implying nine IHD. The UV-Vis, ^1H and ^{13}C NMR spectrum were similar to those of compound **1**, indicating they are structural analogs. The main differences are the presence of an acetyl group [δ_H 2.00 (3H, s); δ_C 21.1, 170.8] and a mass difference of 42 units larger in compound **4**, suggesting compound **4** is an acetyl derivative of **1**. The COSY, HSQC, HMBC and NOESY spectrum analysis allowed the complete assignment of compound **4** as 3-O-acetylated compound **1** (Table S5 and Fig S17-S22).

Compound **5** has a molecular formula of $C_{26}H_{36}O_5$, which was found by means of HRESIMS and ^{13}C-NMR data, implying nine IHD. The UV-Vis, ^1H and ^{13}C NMR spectrum were similar to those of compound **6**, implying they are structural derivatives. The main differences are the disappearance of a methyl group [δ_H 1.65 (3H, s, H-27); δ_C 25.8 (C-27)] and the presence of a

carboxylic acid group [δ_C 169.2], suggesting compound **5** is a carboxylate derivative of **6** generated by carboxylation at C-27 (Table S6 and Fig S23-S27). The chemical shift values of compound **5** at the H_2-19 methylene [δ_H 2.31 (2H, m)] and at the H-20 olefinic proton [δ_H 6.77 (1H, tq, J = 7.3, 1.4 Hz)] are in good agreement with those for asiaticusin A, indicating the double bond at C-20 is 20*E*.[1] The NOESY correlation between H_2-19 and H_3-26 further confirmed the 20*E* configuration (Fig S28).

Compound **8** was determined to have a molecular formula of $C_{26}H_{38}O_4$, as determined through the utilization of HRESIMS and ^{13}C-NMR data. This molecular formula suggests the presence of eight degrees of unsaturation (IHD). The UV-Vis, ^{1}H, and ^{13}C NMR spectra of compound **8** exhibited similarities to those of compound **6**, indicating a structural relationship between the two compounds. The chemical shift values of compound **6** at C-20 [δ_C 125.0] and C-21 [δ_C 131.6] were observed to shift to different values in compound **8** at C-20 [δ_C 64.0] and C-21 [δ_C 58.1]. These shift values along with the mass difference of 16 units indicate that compound **8** was formed through the epoxidation of compound **6** at C-20 and C-21. Moreover, the configuration at C-20 was deduced to be *S*, based on the biosynthetic relationship with compound **7** (Table S9 and Fig S33-S37).

Compounds **9**, **10**, and **11** possess the molecular formulas $C_{21}H_{32}O_5$, $C_{22}H_{34}O_5$, and $C_{21}H_{30}O_4$, respectively, as determined through analysis of their HRESIMS and ^{13}C NMR data. The UV-Vis, ^{1}H, and ^{13}C NMR spectra exhibited similarities among compounds **7-11**, while the mass differences of 68 units between compounds **9** and **7**, as well as between compounds **11** and **8**, suggested that compounds **9** and **11** have one less prenyl group than compounds **7** and **8**. Additionally, a comparison of the ^{1}H and ^{13}C NMR between spectra between **9** and **10** revealed that **10** has one more ether group [δ_H 3.16 (3H, s); δ_C 49.2] than **9**. HMBC correlations confirmed the assigned structure of **10**. The relative arrangement of compounds **9-11** was inferred from their derivatives **7** based on the biosynthetic association (Table S10-S12 and Fig S38-S52).

Supplemental Materials and Methods

Molecular genetic techniques and strain construction

Transformation procedures were generally as previously described[2–4] except that 100 mg/mL VinoTaste Pro (Novozymes) was used for protoplasting. Transforming fragments were generated by fusion PCR as previously described[2–4] with the following modifications. The DNA polymerase used was Q5 Hot Start High-Fidelity 2X Master Mix (New England Biolabs). The annealing temperature was Tm (for the lowest melting temperature primer) + 3-5ºC. Tm was calculated as previously described[3] where Tm is the melting temperature of the primer with the lowest melting temperature. Extension time was 30 seconds per kb. Flanking

regions were ~1 kb with slight variations consistent with primer design. For the refactored BGC, at the *yA* locus (Fig. 1B) the *spyA* overlap was 1012 bp and the *AtpabaA* overlap was 1197 bp. At the *wA* locus the *AtriboB* overlap was 1012 bp (see Fig. S1). Miniprep DNA was prepared for diagnostic PCR following the procedure of Edgerton and Oakley.[5] The DNA polymerase was OneTaq Hot Start Quick Load 2X Master Mix (New England Biolabs). The annealing temperature was 55-60ºC and the extension time was one minute per kb. Multiple diagnostic PCR reactions were carried out for each gene. For the reconstruction of the BGC in *A. nidulans* (Fig. S3), the Afu8g02420 overlap was 1013 bp, the *spyD* overlap was 1086 bp and the *spyA* overlap was 1003 bp. Both the refactored cluster and the reconstructed cluster were made in strain LO11098. *SpyB* was refactored using two different start codons. Site 1 is the site annotated in FungiDB (ATGTGCATGGACCGTCTTGT). Site 2 is 593 bp downstream of site 1 (ATGCCTAGAAGAGAGCGTAG).

For deleting the individual genes of the refactored BGC, ~1kb flanking fragments were fused to a selectable marker and the resulting fragment was used for transformation with selection for the marker on the transforming fragment. Transforming fragments were designed to remove the promoter driving the target gene as well as the coding sequence and 3' untranslated DNA. For example, to delete *spyA*, a ~1 kb *yA* flanking sequence was fused to *AfpyroA aldA*(p) (~300 bp) and ~700 bp of the N-terminal coding region of Afu8g02440. Transformation with this fragment resulted in removal of *AfpyrG* and *spyA*, but left Afu8g02440 intact and under control of *aldA*(p).

For expression of SpyA alone, a fragment consisting of ~1 kb of *yA* flank, *AfpyrG*, the *alcA* promoter and a 5' portion of the *spyA* coding region was created by fusion PCR. A second fragment consisting of an overlapping 3' portion of the *spyA* coding region plus 3' untranslated region and ~1 kb of *yA* 3' flank was generated by fusion PCR. The two fragments shared an overlap region of 1003 bp. The two fragments were co-transformed into strain LO11945 which is LO11098 with the promoter of the *alcR* transcription factor (which drives expression of *alcA* and *aldA*) under control of the strong constitutive *gpdA* promoter. The *Aspergillus terreus biA* gene (*AtbiA*) gene was used as a selectable marker for the replacement of the *alcR* promoter with the *gpdA* promoter. We designated the resultant *spyA* expressing strain LO12091.

Fermentation and LC-MS analysis

Liquid LMM medium (15 g/L lactose, 6g/L $NaNO_3$, 0.52 g/L KCl, 0.52 g/L $MgSO_4 \cdot 7H_2O$, 1.52 g/L KH_2PO_4, 0.72 g/L fructose and 1 mL/L trace elements solution) was inoculated with 3×10^7 spores in a 30 mL volume and incubated at 37°C with shaking at 150 rpm in 125 mL flasks. Supplements such as riboflavin (2.5 mg/L), pyridoxine (0.5 mg/L), uracil (1 g/L), uridine (10 mM), p-aminobenzoic acid (1 mg/L), biotin (0.02 mg/L), L-lysine (200 mg/L) or choline HCl (20 mg/L) were added as needed. To induce *alcA*(p) and *aldA*(p), methyl ethyl ketone (MEK), was added into the medium at a final concentration of 50 mM, 42 hours after

inoculation. After 72 hours of MEK induction, the culture medium was collected by filtration and extracted with an equal volume of EtOAc. The mycelium was extracted with 30 mL 1:1 DCM/MeOH with 1 hour of sonication. The resulting extract was dried in vacuo to obtain an aqueous residue, which was then suspended in 30 ml H_2O and partitioned with 30 ml EtOAc. To extract acidic phenolic compounds, the water layer was extracted with the same volume of EtOAc after acidification to pH 2. The EtOAc extract from culture medium, acidified culture medium or mycelium was evaporated in vacuo, re-dissolved in 1 ml of 20% DMSO in MeOH, and a portion (10 μL) was subjected to high performance liquid chromatography-photodiode array detection-mass spectroscopy (HPLC-DAD-MS) analysis.

The HPLC-MS analysis was performed using an RP C18 column (Phenomenex Luna Omega 3 μm Polar C18 100 × 2.1 mm) on a ThermoFinnigan LCQ Advantage ion trap mass spectrometer. The flow rate used was 125 μL/min. The solvent gradient consisted of 95% MeCN/H_2O (solvent B) and 5% MeCN/H_2O (solvent A), both containing 0.05% formic acid. The gradient was run under the following conditions: 0% solvent B from 0 to 5 min, 0–100% solvent B from 5 min to 35 min, 100–0% solvent B from 40 to 45 min, and re-equilibration with 0% solvent B from 45 to 50 min.

Isolation and characterization of metabolites

To purify metabolites, EtOAc was used to extract the broth from a 5 L culture. Mycelia were also extracted with 800 mL 1:1 DCM/MeOH at ambient temperature overnight, and the resulting extract was concentrated and re-extracted with EtOAc. Both of the extracts were subjected to silica-gel column chromatography followed by further separation through semi-preparative HPLC (Phenomenex Luna 5 μm C18 (2), 250 × 10 mm), with a flow rate of 4.0 mL/min and monitored using a UV detector set at 254 nm. NMR spectra were recorded using a Varian VNMRS-600 spectrometer, while a high-resolution electrospray ionization mass spectrometer (HRESI-MS) was used to obtain mass spectra, and optical rotations were measured on a JASCO P-1010 digital polarimeter. The identity of previously reported compounds, including sartorypyrones A, D, and E, and geranylgeranyl-triacetate acid lactone (designated compounds **2-3** and **6-7**), was confirmed by comparing their HRESIMS, UV-vis, and ^{1}H-NMR data with published information (as shown in Tables S3-4 and S7-8†).

Purification conditions for compounds 1-4

For structural elucidation, compounds **1-4** were purified from 5 L of LMM medium inoculated with LO11839, grown and induced with MEK and extracted with EtOAc as described above. The mycelia which also containing compounds **1-4** were soaked in 800 mL DCM/MeOH (1:1) overnight, and the resulting extract was evaporated and re-extracted with EtOAc. Both extracts were pooled to get 1.36 g of crude extract. This extract was then applied to a silica gel (Sigma-Aldrich 70-230 mesh, 63-200 μm) column and eluted with DCM-MeOH mixtures of increasing polarity (fraction A, 100:0, 300 mL; fraction B, 100:1, 300 mL;

fraction C, 50:1, 300 mL; fraction D, 25:1, 300 mL). Fraction B (160 mg), which contained compounds **3**-**4**, and Fraction C (59 mg), which contained compounds **1-2**, were further purified by reverse phase HPLC [Phenomenex Luna 5μm C18 (2), 250 × 10 mm] with a flow rate of 4.0 mL/min and measured by a UV detector at 254 nm. The gradient system was 95% MeCN/H_2O (solvent B) in 5 % MeCN/H_2O (solvent A). Fraction B was separated with the following gradient condition: 90 % B from 0 to 5 min, 90 to 100 % B from 5 to 15 min, maintained at 100 % B from 15 to 17 min, 100 to 90 % B from 17 to 18 min, and re-equilibration with 90 % B from 18 to 22 min. Sartorypyrone A (**3**, 29.0 mg) and sartorypyrone G (**4**, 25.0 mg) were eluted at 10.5 and 11.5 min, respectively. Fraction C was separated with the following gradient conditions: 80 % B from 0 to 5 min, 80 to 100 % B from 5 to 15 min, maintained at 100 % B from 15 to 17 min, 100 to 80 % B from 17 to 18 min, and re-equilibration with 80 % B from 18 to 22 min. Sartorypyrone F (**1**, 5.6 mg) and sartorypyrone G (**2**, 15.6 mg) were eluted at 7.5 and 8.5 min, respectively.

Purification conditions for compounds 5-6

For structural elucidation, compound **5** was purified from 5 L of LMM medium inoculated with LO12126, grown and induced, and extracted with EtOAc as described above. The medium was extracted with EtOAc three times and the combined EtOAc layer was then evaporated in vacuo to obtain 217 mg of crude extract. This extract was then applied to a silica gel (Sigma-Aldrich 70-230 mesh, 63-200 μm) column and eluted with DCM-MeOH mixtures of increasing polarity (fraction A, 50:1, 50 mL; fraction B, 25:1, 80 mL; fraction C, 9:1, 50 mL; fraction D, 4:1, 50 mL). Fraction B (94 mg), which contained compound **5** was further purified by reverse phase HPLC [Phenomenex Luna 5μm C18 (2), 250 × 10 mm] with a flow rate of 4.0 mL/min and measured by a UV detector at 254 nm. The gradient system was 95% MeCN/H_2O (solvent B) in 5 % MeCN/H_2O (solvent A). Fraction B was separated with the following gradient conditions: 40 % B from 0 to 4 min, 40 to 75 % B from 4 to 20 min, 75 to 40 % B from 20 to 21 min, and re-equilibration with 40 % B from 21 to 25 min. Compound **5** (60.2 mg) was eluted at 19.5 min.

The mycelia which contained compound **6** were soaked in 800 mL DCM/MeOH (1:1) overnight, and the resulting extract was evaporated and re-extracted with EtOAc to obtain 1.1 g of crude extract. This extract was then applied to a silica gel (Sigma-Aldrich 70-230 mesh, 63-200 μm) column and eluted with DCM-MeOH mixtures of increasing polarity (fraction A, 100:0, 200 mL; fraction B, 100:1, 200 mL; fraction C, 50:1, 200 mL; fraction D, 4:1, 300 mL). Fraction B (227 mg), which contained compound **6** was further purified by reverse phase HPLC [Phenomenex Luna 5μm C18 (2), 250 × 10 mm] with a flow rate of 4.0 mL/min and measured by a UV detector at 254 nm. The gradient system was 95% MeCN/H_2O (solvent B) in 5 % MeCN/H_2O (solvent A). Fraction B was separated using the following gradient conditions: 0 % B from 0 to 5 min, 0 to 100 % B from 5 to 35 min, maintained at 100 % B from 35 to 40 min, 100 to 0 % B from 40 to 41 min, and re-equilibration with 0 % B from 41

to 45 min. Compound **6** (12.2 mg) was eluted at 40.0 min.

Purification conditions for compounds 7-8

For structural elucidation, compounds **7-8** were purified from 5 L of LMM medium inoculated with LO12107, grown, induced, and extracted with EtOAc as described above. The mycelia which also contained compounds **7-8** were soaked in 800 mL DCM/MeOH (1:1) overnight, and the resulting extract was evaporated and re-extracted with EtOAc. Both extracts were pooled to get 1.51 g of crude extract. This extract was then applied to a silica gel (Sigma-Aldrich 70-230 mesh, 63-200 μm) column and eluted with DCM-MeOH mixtures of increasing polarity (fraction A, 50:1, 300 mL; fraction B, 100:3, 300 mL; fraction C, 25:1, 300 mL; fraction D, 25:2, 300 mL; fraction E, 4:1, 300 mL). Fraction B (35.2 mg), which contained compound **8**, and Fraction D (311.1 mg), which contained compound **7**, were further purified by reverse phase HPLC [Phenomenex Luna 5μm C18 (2), 250 × 10 mm] with a flow rate of 4.0 mL/min and measured by a UV detector at 254 nm. The gradient system was 95% MeCN/H_2O (solvent B) in 5 % MeCN/H_2O (solvent A). Fraction B was separated with the following gradient condition: 40 % B from 0 to 4 min, 40 to 100 % B from 4 to 24 min, maintained at 100 % B from 24 to 25 min, 100 to 40 % B from 25 to 26 min, and re-equilibration with 40 % B from 26 to 30 min. Compound **7** (13.2 mg) was eluted at 22.0 min. Fraction D was separated with the following gradient condition: 45% B from 0 to 20 min, 45 to 100 % B from 20 to 21 min, maintained at 100 % B from 21 to 22 min, 100 to 45 % B from 22 to 23 min, and re-equilibration with 45 % B from 23 to 27 min. Compound **8** (142.3 mg) was eluted at 16.0 min.

Purification conditions for compounds 9-11

For structural elucidation, compounds **9-11** were purified from 5 L of LMM medium inoculated with LO12117, grown, induced, and extracted with EtOAc as described above. The medium was extracted with EtOAc three times and the combined EtOAc layer was then evaporated in vacuo to obtain 690 mg of crude extract. This extract was then applied to a silica gel (Sigma-Aldrich 70-230 mesh, 63-200 μm) column and eluted with DCM-MeOH mixtures of increasing polarity (fraction A, 100:1, 150 mL; fraction B, 50:1, 150 mL; fraction C, 25:1, 150 mL; fraction D, 25:2, 150 mL; fraction E, 4:1, 150 mL). Fraction B (270 mg), which contained compounds **9-11** was further purified by reverse phase HPLC [Phenomenex Luna 5μm C18 (2), 250 × 10 mm] with a flow rate of 4.0 mL/min and measured by a UV detector at 254 nm. The gradient system was 95% MeCN/H_2O (solvent B) in 5 % MeCN/H_2O (solvent A). Fraction B was separated using the following gradient conditions: 50 % B from 0 to 3 min, 50 to 60 % B from 3 to 20 min, 60 to 100 % B from 20 to 21 min, maintained at 100 % B from 21 to 22 min, 100 to 50 % B from 22 to 23 min, and re-equilibration with 50 % B from 23 to 27 min. Compound **9** (55.6 mg), compound **10** (3.0 mg), and compound **11** (11.6 mg) were eluted at 6.7, 12.0, and 17.0 min, respectively.

Crystallization of compound 1

Compound **1** was crystallized by the hanging drop vapor diffusion crystallization method. First, compound **1** was dissolved in acetone at a concentration of 20 mg/mL. A series of polyethylene glycols (PEGs) ranging in mass from 300-20,000 were screened as precipitants at various concentrations (18, 25, and 32%). Vapor diffusion was set up by transferring 100 µL of PEG into each well of a 96-well plate. On a cover slip 0.4 µL of PEG precipitants from each reservoir was mixed with 0.4 µL of compound **1**. The cover slide was used to seal the reservoir using a silicone grease ring around the edge of the well. Crystals appeared in 1-3 days and drops containing crystals were harvested from multiple wells and combined for MicroED.

Electron diffraction data collection, refinement, and statistics for compound 1

A slurry of microcrystals was pipetted onto a lacey carbon grid and then briefly blotted using a Kimwipe. The grid containing dried crystals was mounted in a Gatan 626 cryo-holder at room temperature and inserted into a FEI Tecnai F200C transmission electron microscope prior to cooling the cryo holder to avoid icing. The microscope was operated at a voltage of 200 keV and a wavelength of 0.025 Å. After insertion, the sample was cooled down to a cryogenic temperature of 100 K. Data acquisition, conversion, and reduction were carried out as described previously,[6] and data from eight crystals were merged and scaled to obtain a complete data set for compound **1**. Diffraction data were indexed and merged using XDS Phases.[7] Compound **1** was solved using direct methods in SHELXD, and initial maps were refined in ShelXle with SHELXL,[8–10] where all non-hydrogen atoms were refined anisotropically, and hydrogen atoms were placed using the riding model.

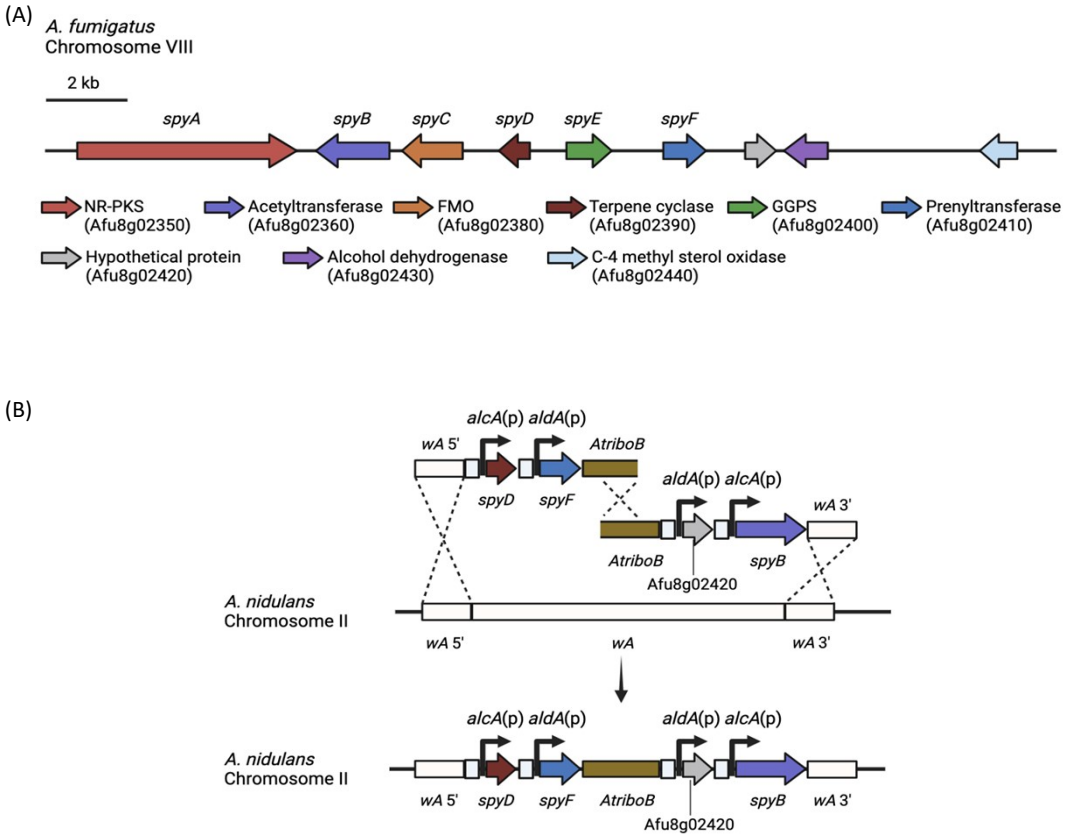

Figure S1. (A) The *spy* BGC from *A. fumigatus.* (B) Refactoring the *spyB, D* and *F* genes at the *wA* locus in *A. nidulans.* Afu8g02420 was also refactored at the *wA* locus, but it proved not to be a component of the *spy* BGC.

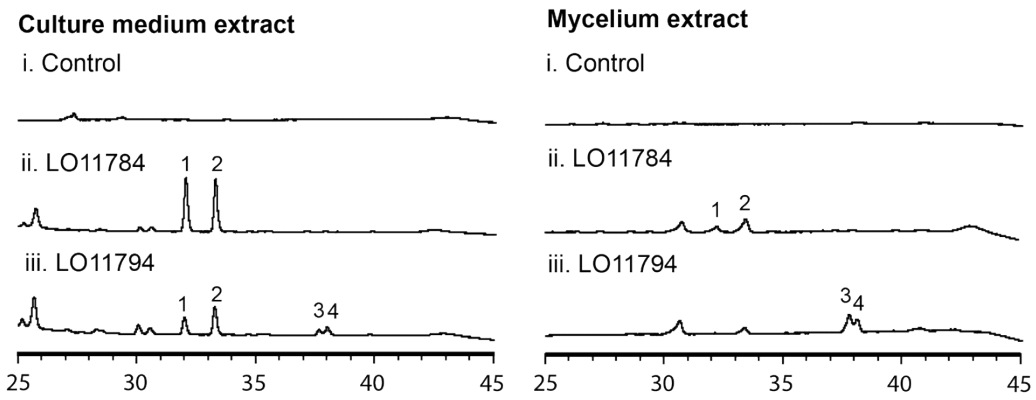

Figure S2. HPLC profiles of culture medium and mycelium extracts from *A. nidulans* transformants. Afu8g02360 (*spyB*) in LO11784 was refactored by fusing *alcA*(p) at start site 1; Afu8g02360 (*spyB*) in LO11794 was refactored by fusing *alcA*(p) at start site 2. The control strain is LO11098, which lacked the *A. fumigatus* BGC genes.

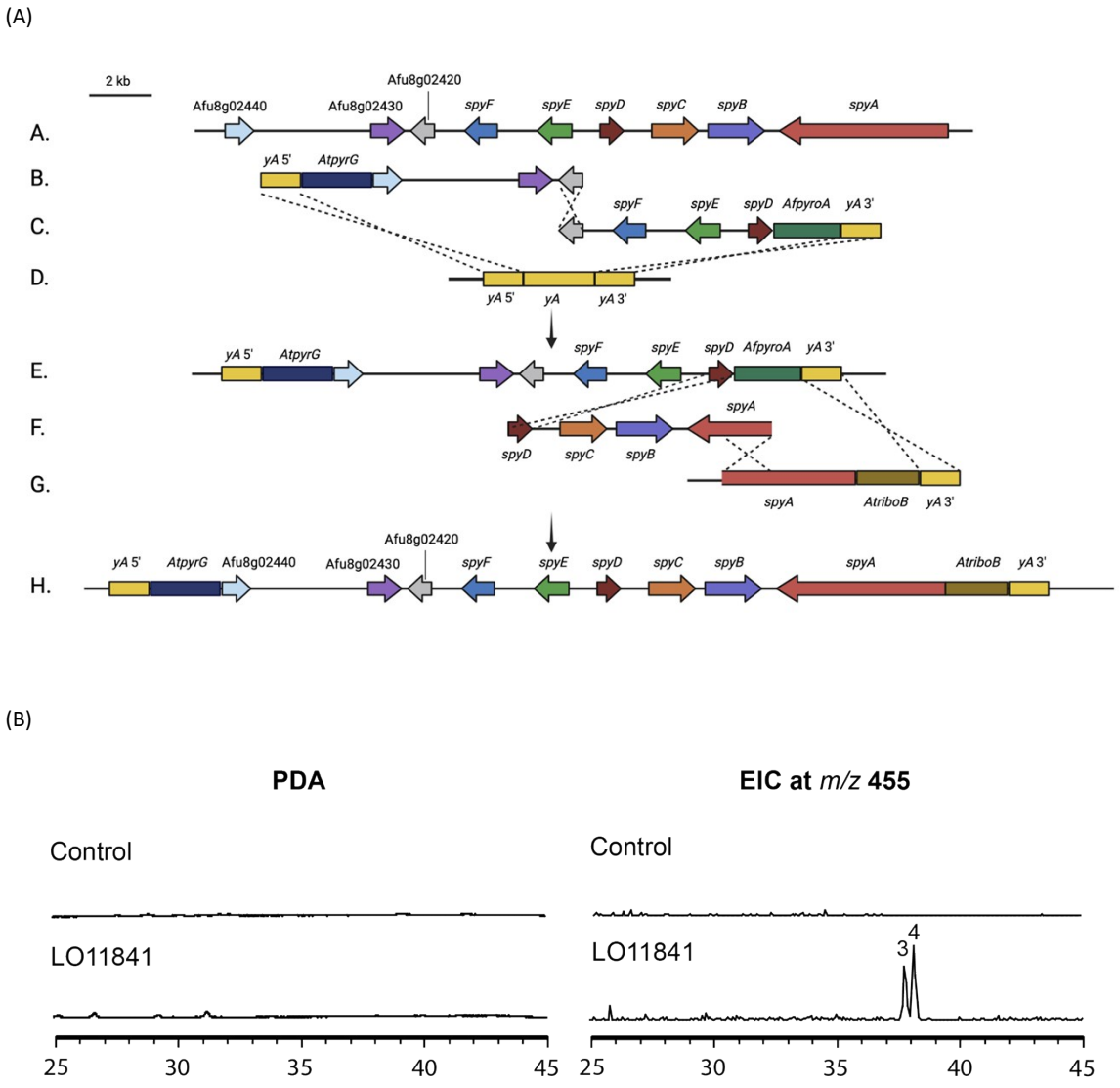

Figure S3. (A) Reconstructing the *spy* BGC from *A. fumigatus* into *A. nidulans*. The entire sequence transferred into *A. nidulans* was 25,832 bp. (B) HPLC profiles of extracts from the parental strain and a strain carrying the reconstructed BGC overexpressing *laeA* and *llmG* (LO11841) as detected by PDA and mass spectrometry in negative mode of extracted ion chromatogram (EIC) and *m/z* = 455.

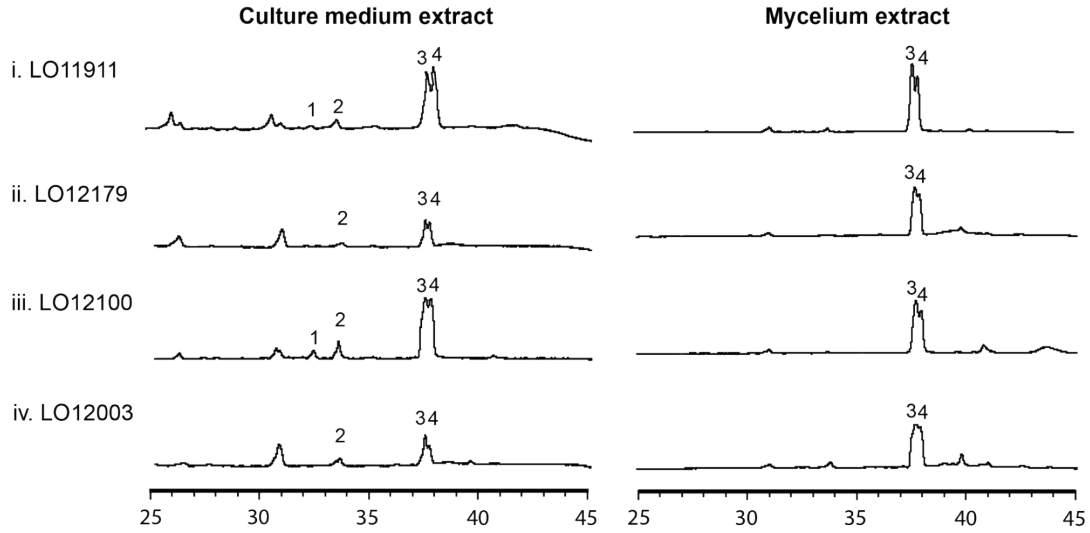

Figure S4. HPLC profiles of culture medium and mycelium extracts from *A. nidulans* transformants. LO11911 carried the entire *spy* BGC and three additional adjacent genes (Afu8g02420, Afu8g02430, and Afu8g02440); LO12179, LO12100, and LO12003 were Afu8g02420, Afu8g02430, and Afu8g02440 deletants from LO11911, respectively.

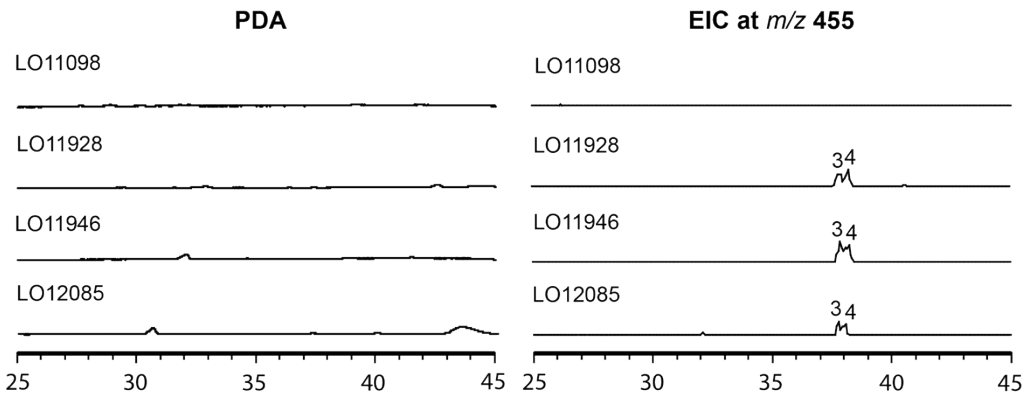

Figure S5. HPLC profiles of extracts from a control strain (LO11098), *spyA* deletant strain (LO11928), *spyA* /AN12440 double deletant strain (LO11946), and *spyA*/AN6448 double deletant strain (LO12085) as detected by PDA and mass spectrometry in negative mode of extracted ion chromatogram (EIC) and *m/z* = 455.

Table S1. Strains used in this study. Some of the types of constructs are novel and there is no standard nomenclature for them. We have chosen to use brackets to indicate that multiple genes have been inserted or refactored at a particular locus. For example, [*wA*Δ:: *alcA*(p)*spyD*, *aldA*(p)*spyF, AtRiboB, aldA*(p)Afu8g02420, *alcA*(p)*spyB* start site 1], indicates that the *wA* gene has been replaced with *spyD* under control of the *alcA* promoter, *spyF* under control of the *aldA* promoter, the *Aspergillus terreus riboB* gene, Afu8g02420 under control of the *aldA* promoter, and *spyB* under control of the *alcA* promoter driving expression from start site 1.

Strain	Description	Genotype
LO11098	Multi-marker dereplication strain	*pyrG89, pyroA4, riboB2, pabaA*Δ, *biA*Δ, *lysB*Δ, *choA*Δ, *nkuA*Δ*::argB*, sterigmatocystin cluster (AN7804-AN7825)Δ, emericellamide cluster (AN2545-AN2549)Δ, asperfuranone cluster (AN1039-AN1029)Δ, monodictyphenone cluster (AN10023-AN10021)Δ, terrequinone cluster (AN8512-AN8520)Δ, austinol cluster part 1 (AN8379-AN8384)Δ, austinol cluster part 2 (AN9246-AN9259)Δ, F9775 cluster (AN7906-AN7915)Δ, asperthecin cluster (AN6000-AN6002)Δ.
LO11784 - 11793	Refactored *A. fumigatus* sartorypyrone cluster, with start site 1 for Afu8g02360 (*spyB*), in LO11098	[*wA*Δ:: *alcA*(p)*spyD*, *aldA*(p)*spyF, AtRiboB, aldA*(p)Afu8g02420, *alcA*(p)*spyB* start site 1], [*yA*Δ*:: AfpyrG, alcA*(p)*spyA, aldA*(p)Afu8g02440*, alcA*(p)*spyE, AtpabaA, alcA*(p)*spyC, aldA*(p)Afu8g02430], *pyrG89, pyroA4, riboB2, pabaA*Δ, *biA*Δ, *lysB*Δ, *choA*Δ, *nkuA*Δ*::argB*, sterigmatocystin cluster (AN7804-AN7825)Δ, emericellamide cluster (AN2545-AN2549)Δ, asperfuranone cluster (AN1039-AN1029)Δ, monodictyphenone cluster (AN10023-AN10021)Δ, terrequinone cluster (AN8512-AN8520)Δ, austinol cluster part 1 (AN8379-AN8384)Δ, austinol cluster part 2 (AN9246-AN9259)Δ, F9775 cluster (AN7906-AN7915)Δ, asperthecin cluster (AN6000-AN6002)Δ.
LO11794 - 11803	Refactored *A. fumigatus* sartorypyrone cluster, with start site 2 for Afu8g02360 (*spyB*), in LO11098	[*wA*Δ:: *alcA*(p)*spyD*, *aldA*(p)*spyF, AtRiboB, aldA*(p)Afu8g02420, *alcA*(p)*spyB* start site 2], [*yA*Δ*:: AfpyrG, alcA*(p)*spyA, aldA*(p)Afu8g02440*, alcA*(p)*spyE, AtpabaA, alcA*(p)*spyC, aldA*(p)Afu8g02430], *pyrG89, pyroA4, riboB2, pabaA*Δ, *biA*Δ, *lysB*Δ, *choA*Δ, *nkuA*Δ*::argB*, sterigmatocystin cluster (AN7804-AN7825)Δ, emericellamide cluster (AN2545-AN2549)Δ, asperfuranone cluster (AN1039-AN1029)Δ, monodictyphenone cluster (AN10023-AN10021)Δ, terrequinone cluster (AN8512-AN8520)Δ, austinol cluster part 1 (AN8379-AN8384)Δ, austinol cluster part 2 (AN9246-

		AN9259)Δ, F9775 cluster (AN7906-AN7915)Δ, asperthecin cluster (AN6000-AN6002)Δ.
LO11839	*agsB*Δ::*ptrA* in LO11794	*agsB*Δ::*ptrA* (pyrithiamine resistance gene from *Aspergillus oryzae*), [*wA*Δ:: *alcA*(p)*spyD*, *aldA*(p)*spyF, AtRiboB, aldA*(p)Afu8g02420, *alcA*(p)*spyB* start site 2], [*yA*Δ*:: AfpyrG, alcA*(p)*spyA, aldA*(p)Afu8g02440*, alcA*(p)*spyE, AtpabaA, alcA(*p)*spyC, aldA*(p)Afu8g02430], *pyrG89, pyroA4, riboB2, pabaA*Δ*, biA*Δ*, lysB*Δ*, choA*Δ*, nkuA*Δ*::argB*, sterigmatocystin cluster (AN7804-AN7825)Δ, emericellamide cluster (AN2545-AN2549)Δ, asperfuranone cluster (AN1039-AN1029)Δ, monodictyphenone cluster (AN10023-AN10021)Δ, terrequinone cluster (AN8512-AN8520)Δ, austinol cluster part 1 (AN8379-AN8384)Δ, austinol cluster part 2 (AN9246-AN9259)Δ, F9775 cluster (AN7906-AN7915)Δ, asperthecin cluster (AN6000-AN6002)Δ.
LO11841	Entire *A. fumigatus* sartorypyrone cluster, from 5' TTGGCTGTTGCCGCTGCG……to.....GTGGCAACGCCCTGCCTT 3', replacing the *yA* coding sequence, *alcA*(p)*laeA*, *alcA*(p)*llmG* in LO11098	*Atpaba-alcA*(p)*laeA, AtlysB-alcA*(p)*llmG,* [*yA*Δ*::AfpyrG,* Afu8g02440, Afu8g02430, Afu8g02420, *spyF, spyE, spyD, spyC, spyB, spyA*], *pyrG89, pyroA4, riboB2, pabaA*Δ*, biA*Δ*, lysB*Δ*, choA*Δ*, nkuA*Δ*::argB*, sterigmatocystin cluster (AN7804-AN7825)Δ, emericellamide cluster (AN2545-AN2549)Δ, asperfuranone cluster (AN1039-AN1029)Δ, monodictyphenone cluster (AN10023-AN10021)Δ, terrequinone cluster (AN8512-AN8520)Δ, austinol cluster part 1 (AN8379-AN8384)Δ, austinol cluster part 2 (AN9246-AN9259)Δ, F9775 cluster (AN7906-AN7915)Δ, asperthecin cluster (AN6000-AN6002)Δ.
LO11911	*AtbiA-gpdA*(p)*alcR* in LO11839	*AtbiA-gpdA*(p)*alcR*, *agsB*Δ::*ptrA*, [*wA*Δ:: *alcA*(p)*spyD*, *aldA*(p)*spyF, AtRiboB, aldA*(p)Afu8g02420, *alcA*(p)*spyB* start site 2], [*yA*Δ*:: AfpyrG, alcA*(p)*spyA, aldA*(p)Afu8g02440*, alcA*(p)*spyE, AtpabaA, alcA*(p)*spyC, aldA*(p)Afu8g02430], *pyrG89, pyroA4, riboB2, pabaA*Δ*, biA*Δ*, lysB*Δ*, choA*Δ*, nkuA*Δ*::argB*, sterigmatocystin cluster (AN7804-AN7825)Δ, emericellamide cluster (AN2545-AN2549)Δ, asperfuranone cluster (AN1039-AN1029)Δ, monodictyphenone cluster (AN10023-AN10021)Δ, terrequinone cluster (AN8512-AN8520)Δ, austinol cluster part 1 (AN8379-AN8384)Δ, austinol cluster part 2 (AN9246-

		AN9259)Δ, F9775 cluster (AN7906-AN7915)Δ, asperthecin cluster (AN6000-AN6002)Δ.
LO11928	*AfpyrG*-*alcA*(p)*spyA*Δ::*AtbiA* in LO11839	*agsB*Δ::*ptrA*, [*wA*Δ:: *alcA*(p)*spyD*, *aldA*(p)*spyF, AtRiboB, aldA*(p)Afu8g02420, *alcA*(p)*spyB* start site 2], [*yA*Δ*:: AtbiA, aldA*(p)Afu8g02440*, alcA*(p)*spyE, AtpabaA, alcA*(p)*spyC, aldA*(p)Afu8g02430], *pyrG89, pyroA4, riboB2, pabaA*Δ*, biA*Δ*, lysB*Δ*, choA*Δ*, nkuA*Δ*::argB*, sterigmatocystin cluster (AN7804-AN7825)Δ, emericellamide cluster (AN2545-AN2549)Δ, asperfuranone cluster (AN1039-AN1029)Δ, monodictyphenone cluster (AN10023-AN10021)Δ, terrequinone cluster (AN8512-AN8520)Δ, austinol cluster part 1 (AN8379-AN8384)Δ, austinol cluster part 2 (AN9246-AN9259)Δ, F9775 cluster (AN7906-AN7915)Δ, asperthecin cluster (AN6000-AN6002)Δ.
LO11945	*AtbiA*-*gpdA*(p)*alcR* in LO11098	*AtbiA*-*gpdA*(p)*alcR, pyrG89, pyroA4, riboB2, pabaA*Δ*, biA*Δ*, lysB*Δ*, choA*Δ*, nkuA*Δ*::argB*, sterigmatocystin cluster (AN7804-AN7825)Δ, emericellamide cluster (AN2545-AN2549)Δ, asperfuranone cluster (AN1039-AN1029)Δ, monodictyphenone cluster (AN10023-AN10021)Δ, terrequinone cluster (AN8512-AN8520)Δ, austinol cluster part 1 (AN8379-AN8384)Δ, austinol cluster part 2 (AN9246-AN9259)Δ, F9775 cluster (AN7906-AN7915)Δ, asperthecin cluster (AN6000-AN6002)Δ.
LO11946	AN12440Δ::*AtpyrG* in LO11928	AN12440Δ::*AtpyrG*, *agsB*Δ::*ptrA*, [*wA*Δ:: *alcA*(p)*spyD*, *aldA*(p)*spyF, AtRiboB, aldA*(p)Afu8g02420, *alcA*(p)*spyB* start site 2], [*yA*Δ*:: AtbiA, aldA*(p)Afu8g02440*, alcA*(p)*spyE, AtpabaA, alcA*(p)*spyC, aldA*(p)Afu8g02430], *pyrG89, pyroA4, riboB2, pabaA*Δ*, biA*Δ*, lysB*Δ*, choA*Δ*, nkuA*Δ*::argB*, sterigmatocystin cluster (AN7804-AN7825)Δ, emericellamide cluster (AN2545-AN2549)Δ, asperfuranone cluster (AN1039-AN1029)Δ, monodictyphenone cluster (AN10023-AN10021)Δ, terrequinone cluster (AN8512-AN8520)Δ, austinol cluster part 1 (AN8379-AN8384)Δ, austinol cluster part 2 (AN9246-AN9259)Δ, F9775 cluster (AN7906-AN7915)Δ, asperthecin cluster (AN6000-AN6002)Δ.

LO12003	*aldA*(p)Afu8g02440Δ:: *AfpyroA* in LO11911	*AtbiA-gpdA*(p)*alcR*, *agsB*Δ::*ptrA*, [*wA*Δ:: *alcA*(p)*spyD*, *aldA*(p)*spyF, AtRiboB, aldA*(p)Afu8g02420, *alcA*(p)*spyB* start site 2], [*yA*Δ*:: AfpyrG, alcA*(p)*spyA, AfpyroA, alcA*(p)*spyE, AtpabaA, alcA*(p)*spyC, aldA*(p)Afu8g02430], *pyrG89, pyroA4, riboB2, pabaA*Δ*, biA*Δ*, lysB*Δ*, choA*Δ*, nkuA*Δ*::argB*, sterigmatocystin cluster (AN7804-AN7825)Δ, emericellamide cluster (AN2545-AN2549)Δ, asperfuranone cluster (AN1039-AN1029)Δ, monodictyphenone cluster (AN10023-AN10021)Δ, terrequinone cluster (AN8512-AN8520)Δ, austinol cluster part 1 (AN8379-AN8384)Δ, austinol cluster part 2 (AN9246-AN9259)Δ, F9775 cluster (AN7906-AN7915)Δ, asperthecin cluster (AN6000-AN6002)Δ.
LO12085	AN6448Δ::*AtpyrG* in LO11927 (sister transformant of LO11928)	AN6448Δ::*AtpyrG*, *agsB*Δ::*ptrA*, [*wA*Δ:: *alcA*(p)*spyD*, *aldA*(p)*spyF, AtRiboB, aldA*(p)Afu8g02420, *alcA*(p)*spyB* start site 2], [*yA*Δ*:: AtbiA, aldA*(p)Afu8g02440*, alcA*(p)*spyE, AtpabaA, alcA*(p)*spyC, aldA*(p)Afu8g02430], *pyrG89, pyroA4, riboB2, pabaA*Δ*, biA*Δ*, lysB*Δ*, choA*Δ*, nkuA*Δ*::argB*, sterigmatocystin cluster (AN7804-AN7825)Δ, emericellamide cluster (AN2545-AN2549)Δ, asperfuranone cluster (AN1039-AN1029)Δ, monodictyphenone cluster (AN10023-AN10021)Δ, terrequinone cluster (AN8512-AN8520)Δ, austinol cluster part 1 (AN8379-AN8384)Δ, austinol cluster part 2 (AN9246-AN9259)Δ, F9775 cluster (AN7906-AN7915)Δ, asperthecin cluster (AN6000-AN6002)Δ.
LO12091	*yA*Δ::*AtpyrG-alcA*(p) *spyA* in LO11945	*yA*Δ::*AtpyrG-alcA*(p)*spyA, AtbiA-gpdA*(p)*alcR*, *pyrG89, pyroA4, riboB2, pabaA*Δ, *biA*Δ, *lysB*Δ, *choA*Δ, *nkuA*Δ::*argB*, sterigmatocystin cluster (AN7804-AN7825)Δ, emericellamide cluster (AN2545-AN2549)Δ, asperfuranone cluster (AN1039-AN1029)Δ, monodictyphenone cluster (AN10023-AN10021)Δ, terrequinone cluster (AN8512-AN8520)Δ, austinol cluster part 1 (AN8379-AN8384)Δ, austinol cluster part 2 (AN9246-AN9259)Δ, F9775 cluster (AN7906-AN7915)Δ, asperthecin cluster (AN6000-AN6002)Δ.

LO12096	*alcA*(p)*spyB*Δ::*AtlysB*	*AtbiA-gpdA*(p)*alcR*, *agsB*Δ::*ptrA*, [*wA*Δ:: *alcA*(p)*spyD*, *aldA*(p)*spyF, AtRiboB, aldA*(p)Afu8g02420, *AtlysB*], [*yA*Δ*:: AfpyrG, alcA(p)spyA, aldA*(p)Afu8g02440*, alcA*(p)*spyE, AtpabaA, alcA*(p)*spyC, aldA*(p)Afu8g02430], *pyrG89, pyroA4, riboB2, pabaA*Δ*, biA*Δ*, lysB*Δ*, choA*Δ*, nkuA*Δ*::argB*, sterigmatocystin cluster (AN7804-AN7825)Δ, emericellamide cluster (AN2545-AN2549)Δ, asperfuranone cluster (AN1039-AN1029)Δ, monodictyphenone cluster (AN10023-AN10021)Δ, terrequinone cluster (AN8512-AN8520)Δ, austinol cluster part 1 (AN8379-AN8384)Δ, austinol cluster part 2 (AN9246-AN9259)Δ, F9775 cluster (AN7906-AN7915)Δ, asperthecin cluster (AN6000-AN6002)Δ.
LO12100	*aldA*(p)Afu8g02430Δ:: *AtlysB* in LO11911	*AtbiA-gpdA*(p)*alcR*, *agsB*Δ::*ptrA*, [*wA*Δ:: *alcA*(p)*spyD*, *aldA*(p)*spyF, AtRiboB, aldA*(p)Afu8g02420, *alcA*(p)*spyB* start site 2], [*yA*Δ*:: AfpyrG, alcA*(p)*spyA, aldA*(p)Afu8g02440*, alcA*(p)*spyE, AtpabaA, alcA*(p)*spyC, AtlysB*], *pyrG89, pyroA4, riboB2, pabaA*Δ*, biA*Δ*, lysB*Δ*, choA*Δ*, nkuA*Δ*::argB*, sterigmatocystin cluster (AN7804-AN7825)Δ, emericellamide cluster (AN2545-AN2549)Δ, asperfuranone cluster (AN1039-AN1029)Δ, monodictyphenone cluster (AN10023-AN10021)Δ, terrequinone cluster (AN8512-AN8520)Δ, austinol cluster part 1 (AN8379-AN8384)Δ, austinol cluster part 2 (AN9246-AN9259)Δ, F9775 cluster (AN7906-AN7915)Δ, asperthecin cluster (AN6000-AN6002)Δ.
LO12107	*alcA*(p)*spyD*Δ::*AtlysB* in LO11911	*AtbiA-gpdA*(p)*alcR*, *agsB*Δ::*ptrA*, [*wA*Δ:: *AtlysB*, *aldA*(p)*spyF, AtRiboB, aldA*(p)Afu8g02420, *alcA*(p)*spyB* start site 2], [*yA*Δ*:: AfpyrG, alcA*(p)*spyA, aldA*(p)Afu8g02440*, alcA*(p)*spyE, AtpabaA, alcA*(p)*spyC, aldA*(p)Afu8g02430], *pyrG89, pyroA4, riboB2, pabaA*Δ*, biA*Δ*, lysB*Δ*, choA*Δ*, nkuA*Δ*::argB*, sterigmatocystin cluster (AN7804-AN7825)Δ, emericellamide cluster (AN2545-AN2549)Δ, asperfuranone cluster (AN1039-AN1029)Δ, monodictyphenone cluster (AN10023-AN10021)Δ, terrequinone cluster (AN8512-AN8520)Δ, austinol cluster part 1 (AN8379-AN8384)Δ, austinol cluster part 2 (AN9246-AN9259)Δ, F9775 cluster (AN7906-AN7915)Δ, asperthecin cluster (AN6000-AN6002)Δ.

LO12117	*alcA*(p)*spyE, AtpabaA*Δ::*AtlysB* in LO11911	*AtbiA-gpdA*(p)*alcR*, *agsB*Δ::*ptrA*, [*wA*Δ:: *alcA*(p)*spyD*, *aldA*(p)*spyF, AtRiboB, aldA*(p)Afu8g02420, *alcA*(p)*spyB* start site 2], [*yA*Δ*:: AfpyrG, alcA*(p)*spyA, aldA*(p)Afu8g02440*, AtlysB, alcA*(p)*spyC, aldA*(p)Afu8g02430], *pyrG89, pyroA4, riboB2, pabaA*Δ*, biA*Δ*, lysB*Δ*, choA*Δ*, nkuA*Δ*::argB*, sterigmatocystin cluster (AN7804-AN7825)Δ, emericellamide cluster (AN2545-AN2549)Δ, asperfuranone cluster (AN1039-AN1029)Δ, monodictyphenone cluster (AN10023-AN10021)Δ, terrequinone cluster (AN8512-AN8520)Δ, austinol cluster part 1 (AN8379-AN8384)Δ, austinol cluster part 2 (AN9246-AN9259)Δ, F9775 cluster (AN7906-AN7915)Δ, asperthecin cluster (AN6000-AN6002)Δ.
LO12126	*AtpabaA-alcA*(p)*spyC*Δ::*AtlysB* in LO11911	*AtbiA-gpdA*(p)*alcR*, *agsB*Δ::*ptrA*, [*wA*Δ:: *alcA*(p)*spyD*, *aldA*(p)*spyF, AtRiboB, aldA*(p)Afu8g02420, *alcA*(p)*spyB* start site 2], [*yA*Δ*:: AfpyrG, alcA*(p)*spyA, aldA*(p)Afu8g02440*, alcA*(p)*spyE, AtlysB, aldA*(p)Afu8g02430], *pyrG89, pyroA4, riboB2, pabaA*Δ*, biA*Δ*, lysB*Δ*, choA*Δ*, nkuA*Δ*::argB*, sterigmatocystin cluster (AN7804-AN7825)Δ, emericellamide cluster (AN2545-AN2549)Δ, asperfuranone cluster (AN1039-AN1029)Δ, monodictyphenone cluster (AN10023-AN10021)Δ, terrequinone cluster (AN8512-AN8520)Δ, austinol cluster part 1 (AN8379-AN8384)Δ, austinol cluster part 2 (AN9246-AN9259)Δ, F9775 cluster (AN7906-AN7915)Δ, asperthecin cluster (AN6000-AN6002)Δ.
LO12178	*aldA*(p)*spyF-AtriboB*Δ::*AfpyroA* in LO11911	*AtbiA-gpdA*(p)*alcR*, *agsB*Δ::*ptrA*, [*wA*Δ:: *alcA*(p)*spyD*, *Afpyro, aldA*(p)Afu8g02420, *alcA*(p)*spyB* start site 2], [*yA*Δ*::AfpyrG, alcA*(p)*spyA, aldA*(p)Afu8g02440*, alcA*(p)*spyE, AtpabaA, alcA*(p)*spyC, aldA*(p)Afu8g02430], *pyrG89, pyroA4, riboB2, pabaA*Δ*, biA*Δ*, lysB*Δ*, choA*Δ*, nkuA*Δ*::argB*, sterigmatocystin cluster (AN7804-AN7825)Δ, emericellamide cluster (AN2545-AN2549)Δ, asperfuranone cluster (AN1039-AN1029)Δ, monodictyphenone cluster (AN10023-AN10021)Δ, terrequinone cluster (AN8512-AN8520)Δ, austinol cluster part 1 (AN8379-AN8384)Δ, austinol cluster part 2 (AN9246-AN9259)Δ, F9775 cluster (AN7906-AN7915)Δ, asperthecin cluster (AN6000-AN6002)Δ.

LO12179	*Atribo-aldA*(p)Afu8g02420Δ::*AfpyroA* in LO11911	*AtbiA-gpdA*(p)-*alcR*, *agsB*Δ::*ptrA*, [*wA*Δ:: *alcA*(p)*spyD*, *aldA*(p)*spyF, AfpyroA*, *alcA*(p)*spyB* start site 2], [*yA*Δ*:: AfpyrG, alcA*(p)*spyA, aldA*(p)Afu8g02440*, alcA*(p)*spyE, AtpabaA, alcA*(p)*spyC, aldA*(p)Afu8g02430], *pyrG89, pyroA4, riboB2, pabaA*Δ*, biA*Δ*, lysB*Δ*, choA*Δ*, nkuA*Δ*::argB*, sterigmatocystin cluster (AN7804-AN7825)Δ, emericellamide cluster (AN2545-AN2549)Δ, asperfuranone cluster (AN1039-AN1029)Δ, monodictyphenone cluster (AN10023-AN10021)Δ, terrequinone cluster (AN8512-AN8520)Δ, austinol cluster part 1 (AN8379-AN8384)Δ, austinol cluster part 2 (AN9246-AN9259)Δ, F9775 cluster (AN7906-AN7915)Δ, asperthecin cluster (AN6000-AN6002)Δ.

Table S2. NMR data for sartorypyrone F (**1**)

^{1}H NMR spectrum (400 MHz), ^{13}C NMR spectrum (100 MHz), acetone-d_6

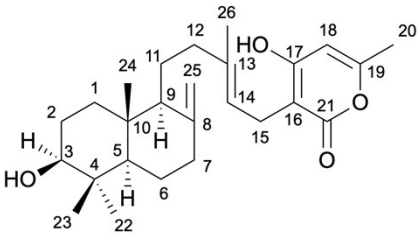

Compound 1, Sartorypyrone F

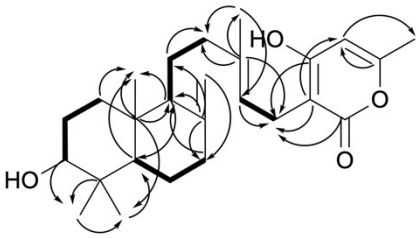

Key COSY (bold line) and HMBC (arrow) correlations of **1**

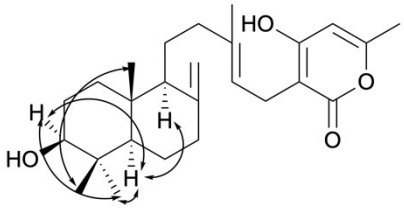

Key NOESY correlations of **1**

position	δ_C, **type**	δ_H **mult (*J* in Hz)**
1	37.7, CH_2	1.13, m
		1.71, m
2	28.8, CH_2	1.55-1.61, m
3	78.3, CH	3.18, dd (10.6, 5.4)
4	39.9, qC	-
5	55.4, CH	1.08, dd (12.5, 2.7)
6	24.9, CH_2	1.35, m
		1.71, m
7	38.9, CH_2	1.90, m
		2.34, ddd (12.7, 4.2, 2.4)
8	149.4, qC	-
9	55.8, CH	1.60, m
10	39.8, qC	-
11	22.4, CH_2	1.43, m
		1.58, m
12	38.9, CH_2	1.81, m
		2.06, m
13	135.4, qC	-
14	123.7, CH	5.20, dd (7.7, 6.9)
15	22.9, CH_2	3.02, dd (13.9, 6.9)
		3.11, dd (13.9, 7.7)
16	101.9, qC	-
17	166.0, qC	-
18	101.7, CH	6.02, br d (0.9)
19	159.9, qC	-
20	19.8, CH_3	2.10, br s
21	167.4, qC	-
22	28.8, CH_3	0.98, s
23	16.1, CH_3	0.75, s
24	15.1, CH_3	0.67, s
25	106.7, CH_2	4.52, br s
		4.80, br s
26	16.4, CH_3	1.73, s

HRMS-ESI (*m/z*) found 415.2846 $[M+H]^+$ (calculated for $C_{26}H_{39}O_4$, 415.2843).

Yellowish white amorphous; $[\alpha]_D^{27} = -9.87$ (c = 0.15, acetone).

Table S3. Comparison of experimental and literature[11] NMR data for sartorypyrone D (**2**) ^{1}H NMR spectrum (400 MHz), ^{13}C NMR spectrum (100 MHz), $CDCl_3$

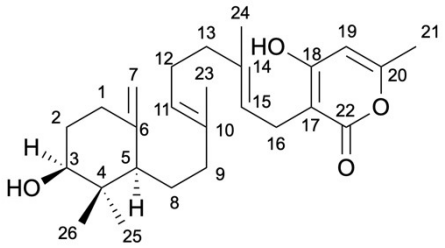

Compound 2, Sartorypyrone D

position	**Literature δ_H mult (*J* in Hz)**	**Observed δ_H mult (*J* in Hz)**	**Literature δ_C, type**	**Observed δ_C, type**
1	1.98, ddd (13.0, 12.0, 5.0)	1.99, m	32.4, CH_2	32.4, CH_2
	2.33, ddd (13.0, 5.0, 5.0)	2.34, dt (13.2, 5.2)		
2	1.52, m	1.52, m	32.0, CH_2	32.0, CH_2
	1.86, dddd (13.0, 5.0, 5.0, 5.0)	1.87, m		
3	3.43, dd (10.0, 5.0)	3.43, dd (9.3, 4.2)	77.3, CH	77.2, CH
4	-	-	40.4, qC	40.4, qC
5	1.63, br d (11.0)	1.62, m	51.2, CH	51.2, CH
6	-	-	147.3, qC	147.3, qC
7	4.60, s	4.60, s	108.5, CH_2	108.6, CH_2
	4.86, s	4.86, s		
8	1.55, m	1.57, m	23.9, CH_2	23.9, CH_2
	1.60, m	1.60, m		
9	1.75, m	1.75, m	38.6, CH_2	38.6, CH_2
	2.05, m	2.05, m		
10	-	-	136.3, qC	136.4, qC
11	5.03, br t (7.0)	5.02, m	123.2, CH	123.2, CH
12	2.10, br t (7.0)	2.11, m	26.0, CH_2	26.0, CH_2
13	2.09, br t (7.0)	2.09, m	39.6, CH_2	39.6, CH_2
14	-	-	140.6, qC	141.1, qC
15	5.32, br t (7.0)	5.33, br t (7.5)	120.4, CH	120.5, CH
16	3.23, br d (7.0)	3.24, d (7.5)	22.9, CH_2	23.0, CH_2
17	-	-	100.7, qC	100.6, qC
18	-	-	165.8, qC	165.7, qC
19	5.82, s	5.78, br d (1.0)	100.7, CH	100.6, CH
20	-	-	160.3, qC	160.3, qC
21	2.18, s	2.19, br s	19.7, CH_3	19.7, CH_3
22	-	-	165.9, qC	165.8, qC
23	1.59, s	1.59, s	16.2, CH_3	16.2, CH_3
24	1.78, s	1.78, s	16.3, CH_3	16.4, CH_3
25	1.02, s	1.02, s	26.1, CH_3	26.1, CH_3
26	0.74, s	0.74, s	16.2, CH_3	16.2, CH_3

Table S4. Comparison of experimental and literature NMR data for sartorypyrone A (**3**)
^{1}H NMR spectrum (400 MHz), ^{13}C NMR spectrum (100 MHz), $CDCl_3$

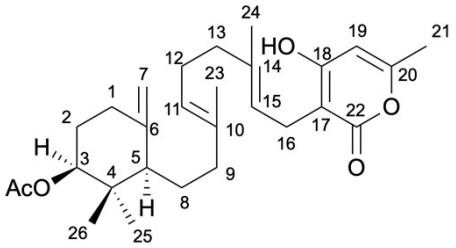

Compound 3, Sartorypyrone A

position	**Literature δ_H mult (*J* in Hz)**	**Observed δ_H mult (*J* in Hz)**	**Literature δ_C, type**	**Observed δ_C, type**
1	2.03, m	2.03, m	31.7, CH_2	31.8, CH_2
	2.31, m	2.31, m		
2	1.55, m	1.56, m	28.6, CH_2	28.6, CH_2
	1.85, m	1.83, m		
3	4.66, dd (8.9, 4.1)	4.66, dd (9.0, 4.2)	78.9, CH	78.9, CH
4	-	-	39.1, qC	39.1, qC
5	1.72, dd (9.1, 3.1)	1.72, dd (9.9, 3.2)	51.0, CH	51.0, CH
6	-	-	146.6, qC	146.5, qC
7	4.62, br s	4.62, br s	109.2, CH_2	109.1, CH_2
	4.88, br s	4.88, br s		
8	1.59, m	1.58, m	23.6, CH_2	23.5, CH_2
9	1.80, m	1.78, m	38.2, CH_2	38.2, CH_2
10	-	-	135.4, qC	135.7, qC
11	5.05, dd (5.6, 6.5)	5.04, m	124.1, CH	123.8, CH
12	2.08, m	2.08, m	26.3, CH_2	26.1, CH_2
13	2.04, m	2.04, m	39.7, CH_2	39.6, CH_2
14	-	-	138.2, qC	139.4, qC
15	5.29, ddd (7.2, 7.2, 1.0)	5.32, tq (7.4, 1.3)	120.5, CH	120.4, CH
16	3.20, d (7.2)	3.22, d (7.4)	22.4, CH_2	22.6, CH_2
17	-	-	101.7, qC	101.2, qC
18	-	-	166.1, qC	165.7, qC
19	6.00, d (0.7)	5.92, br d (1.0)	101.1, CH	100.8, CH
20	-	-	159.9, qC	160.0, qC
21	2.19, s	2.19, br s	19.6, CH_3	19.6, CH_3
22	-	-	166.8, qC	166.2, qC
23	1.58, s	1.58, br s	15.9, CH_3	15.9, CH_3
24	1.77, s	1.77, br s	16.3, CH_3	16.3, CH_3
25	0.94, s	0.94, s	26.0, CH_3	25.9, CH_3
26	0.79, s	0.79, s	17.5, CH_3	17.4, CH_3
OAc	-		171.1, qC	171.0, qC
	2.07, s	2.07, s	21.3, CH_3	21.3, CH_3

Table S5. NMR data for sartorypyrone G (**4**)

^{1}H NMR spectrum (400 MHz), ^{13}C NMR spectrum (100 MHz), acetone-d_6

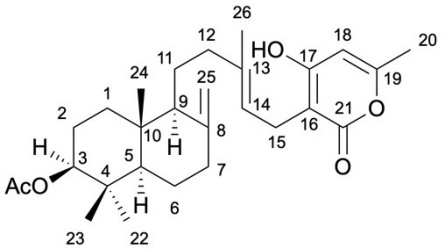

Compound 4, Sartorypyrone G

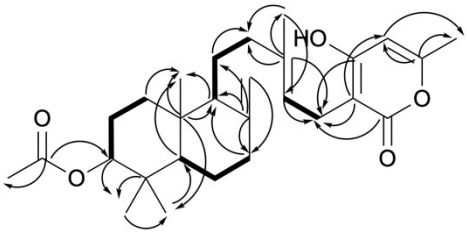

Key COSY (bold line) and HMBC (arrow) correlations of **4**

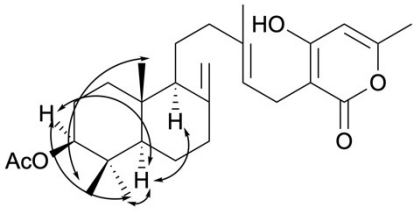

Key NOESY correlations of **4**

position	δ_C, type	δ_H mult (*J* in Hz)
1	37.3, CH_2	1.17, m
		1.74, m
2	25.1, CH_2	1.55-1.65, m
3	81.0, CH	4.47, dd (10.9, 5.5)
4	38.7, qC	-
5	55.3, CH	1.18, m
6	24.6, CH_2	1.36, m
		1.75, m
7	38.7, CH_2	1.90, m
		2.35, ddd (12.8, 4.2, 2.5)
8	148.9, qC	-
9	55.3, CH	1.65, m
10	39.7, qC	-
11	22.3, CH_2	1.45, m
		1.58, m
12	38.7, CH_2	1.81, m
		2.05, m
13	136.0, qC	-
14	123.1, CH	5.18, ddq (7.7, 6.8, 1.5)
15	22.7, CH_2	3.02, dd (14.0, 6.8)
		3.12, dd (14.0, 7.7)
16	102.6, qC	-
17	165.1, qC	-
18	100.7, CH	6.04, br d (0.9)
19	160.8, qC	-
20	19.7, CH_3	2.13, br s
21	165.6, qC	-
22	28.6, CH_3	0.87, s
23	16.9, CH_3	0.84, s
24	15.1, CH_3	0.71, s
25	107.1, CH_2	4.54, br s
		4.82, br s
26	16.3, CH_3	1.73, s
OAc	170.8, qC	-
	21.1, CH_3	2.00, s

HRMS-ESI (*m/z*) found 457.2950 $[M+H]^+$ (calculated for $C_{28}H_{41}O_5$, 457.2949).

Yellowish white plate, mp 175-177 °C; $[\alpha]_D^{27} = -12.34$ (c = 1.05, acetone).

Table S6. NMR data for geranylgeranyl-triacetate lactone carboxylic acid (**5**)
^{1}H NMR spectrum (400 MHz), ^{13}C NMR spectrum (100 MHz), acetone-d_6

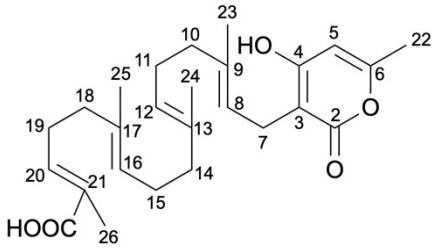

Compound 5

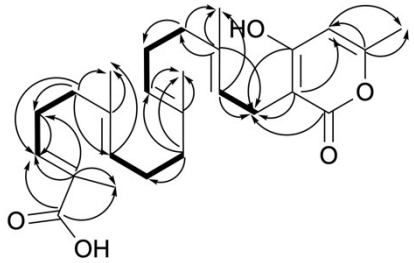

Key COSY (bold line) and HMBC (arrow) correlations of **5**

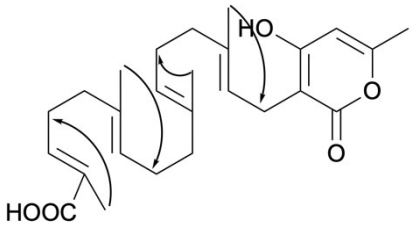

Key NOESY correlations of **5**

position	δ_C, type	δ_H mult (*J* in Hz)
1		
2	165.6, qC	-
3	102.6, qC	-
4	165.0, qC	-
5	100.7, CH	6.01, br s
6	160.8, qC	-
7	22.8, CH_2	3.08, d (7.2)
8	122.6, CH	5.23, m
9	135.8, qC	-
10	40.5*, CH_2	1.97, m
11	27.3, CH_2	2.07, m
12	125.2, CH	5.12, tq (7.1, 1.4)
13	135.4, qC	-
14	40.4*, CH_2	1.97, m
15	27.3, CH_2	2.07, m
16	125.9, CH	5.17, m
17	134.7, qC	-
18	39.0, CH_2	2.11, m
19	27.9, CH_2	2.31, m
20	142.8, CH	6.77, tq (7.3, 1.4)
21	128.4, qC	-
22	19.7, CH_3	2.14, br s
23	16.3, CH_3	1.73, br s
24	16.1, CH_3	1.58, br s
25	16.1, CH_3	1.63, br s
26	12.5, CH_3	1.80, br s
COOH	169.2, qC	-

*The values are interchangeable

HRMS-ESI (*m/z*) found 429.2629 $[M+H]^+$ (calculated for $C_{26}H_{37}O_5$, 429.2636).
White amorphous powder.

Table S7. Comparison of experimental and literature[13] NMR data for geranylgeranyl-triacetate lactone (**6**)

^{1}H NMR spectrum (400 MHz), ^{13}C NMR spectrum (100 MHz), acetone-d_6

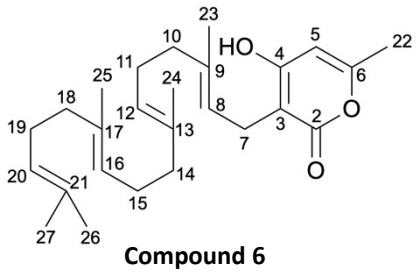

Compound 6

position	**Literature δ_H mult (*J* in Hz)**	**Observed δ_H mult (*J* in Hz)**	**Literature δ_C, type**	**Observed δ_C, type**
1				
2	-	-	165.7, qC	165.9, qC
3	-	-	102.4, qC	102.2, qC
4	-	-	165.4, qC	165.7, qC
5	5.98, s	6.01, br d (1.0)	100.8, CH	101.0, CH
6	-	-	160.7, qC	160.4, qC
7	3.09, d (7.0)	3.08, d (7.2)	22.7, CH_2	22.8, CH_2
8	5.23, t (7.0)	5.24, tq (7.2, 1.3)	122.6, CH	122.9, CH
9	-	-	135.3, qC	135.3, qC
10	1.93, m	1.97, m	40.4, CH_2	40.4, CH_2
11	2.05, m	2.05, m	27.2, CH_2	27.3, CH_2
12	5.12, m	5.11, m	125.1, CH	125.2, CH
13	-	-	135.6, qC	135.4, qC
14	2.04, m	2.05, m	40.4, CH_2	40.4, CH_2
15	1.93, m	1.97, m	27.2, CH_2	27.3, CH_2
16	5.12, m	5.11, m	125.1, CH	125.1, CH
17	-	-	135.4, qC	135.4, qC
18	1.93, m	1.97, m	40.5, CH_2	40.5, CH_2
	2.04, m	2.05, m		
19	1.93, m	1.97, m	27.4, CH_2	27.4, CH_2
	2.04, m	2.05, m		
20	5.12, m	5.11, m	125.0, CH	125.1, CH
21	-	-	131.5, qC	131.6, qC
22	2.14, s	2.12, br s	19.6, CH_3	19.6, CH_3
23	1.59, s	1.59, s	16.1, CH_3	16.1, CH_3
24	1.59, s	1.59, s	16.1, CH_3	16.1, CH_3
25	1.74, s	1.74, s	16.3, CH_3	16.3, CH_3
26	1.59, s	1.59, s	17.7, CH_3	17.7, CH_3
27	1.65, s	1.65, s	25.8, CH_3	25.8, CH_3

Table S8. Comparison of experimental and literature[14] NMR data for sartorypyrone E (**7**)
^{1}H NMR spectrum (400 MHz), ^{13}C NMR spectrum (100 MHz), CD_3OD

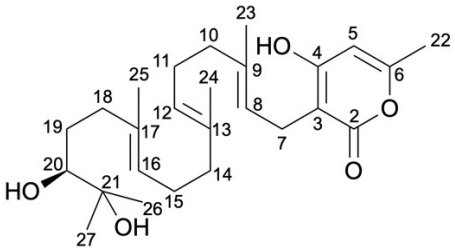

Compound 7, Sartorypyrone E

position	**Literature δ_H mult (*J* in Hz)**	**Observed δ_H mult (*J* in Hz)**	**Literature δ_C, type**	**Observed δ_C, type**
1				
2	-	-	168.8, qC	168.8, qC
3	-	-	103.2, qC	103.3, qC
4	-	-	168.2, qC	167.8, qC
5	5.97, s	5.97, br d (1.0)	102.0, CH	101.8, CH
6	-	-	161.8, qC	161.8, qC
7	3.06, d (7.0)	3.06, d (7.2)	22.9, CH_2	22.9, CH_2
8	5.16, dt (7.5, 1.5)	5.15, tq (7.2, 1.3)	122.9, CH	122.8, CH
9	-	-	136.4, qC	136.5, qC
10	1.95, m	1.95, m	41.0, CH_2	41.0, CH_2
	2.03, m	2.04, m		
11	1.98, m	1.98, m	27.9, CH_2	27.9, CH_2
	2.07, m	2.07, m		
12	5.08, dt (7.0, 1.0)	5.07, tq (7.1, 1.3)	125.5, CH	125.5, CH
13	-	-	136.0, qC	136.0, qC
14	1.95, m	1.95, m	41.0, CH_2	41.0, CH_2
15	2.07, m	2.07, m	27.6, CH_2	27.6, CH_2
16	5.16, dt (7.5, 1.5)	5.15, tq (7.2, 1.3)	125.8, CH	125.8, CH
17	-	-	136.1, qC	136.1, qC
18	2.24, ddd (14.0, 9.5, 4.5)	2.24, ddd (14.4, 10.3, 4.6)	38.1, CH_2	38.1, CH_2
	2.00, m	1.98, m		
19	1.70, m	1.70, m	31.0, CH_2	31.0, CH_2
	1.34, m	1.34, m		
20	3.23, dd (10.5, 1.5)	3.23, dd (10.6, 1.8)	79.2, CH	79.2, CH
21	-	-	73.9, qC	73.9, qC
22	2.19, s	2.18, br s	19.8, CH_3	19.8, CH_3
23	1.73, s	1.72, br s	16.4, CH_3	16.4, CH_3
24	1.57, s	1.57, br s	16.3, CH_3	16.3, CH_3
25	1.61, s	1.60, br s	16.3, CH_3	16.3, CH_3
26	1.12, s	1.12, s	25.1, CH_3	25.1, CH_3
27	1.15, s	1.15, s	25.8, CH_3	25.8, CH_3

Table S9. NMR data for epoxygeranylgeranyl-triacetate lactone (**8**)

^{1}H NMR spectrum (400 MHz), ^{13}C NMR spectrum (100 MHz), acetone-d_6

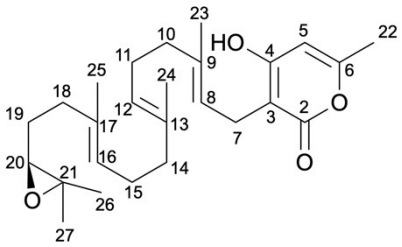

Compound 8

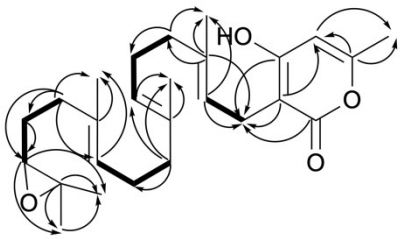

Key COSY (bold line) and HMBC (arrow) correlations of **8**

position	δ_C, **type**	δ_H **mult (*J* in Hz)**
1		
2	165.6, qC	-
3	102.4, qC	-
4	165.2, qC	-
5	100.8, CH	6.02, br s
6	160.7, qC	-
7	22.8, CH_2	3.08, d (7.2)
8	122.7, CH	5.23, tq (7.2, 1.3)
9	135.6, qC	-
10	40.5, CH_2	1.97, m
11	27.3, CH_2	2.07, m
12	125.1, CH	5.12, m
13	135.4, qC	-
14	40.4, CH_2	1.97, m
15	27.3, CH_2	2.07, m
16	125.5, CH	5.17, ddq (8.2, 6.9, 1.2)
17	135.0, qC	-
18	37.1, CH_2	2.09, m
19	28.4, CH_2	1.58, m
20	64.0, CH	2.63, t (6.2)
21	58.1, qC	-
22	19.7, CH_3	2.13, br s
23	16.3, CH_3	1.74, br s
24	16.1, CH_3	1.59, br s
25	16.1, CH_3	1.62, br s
26	19.0, CH_3	1.21, s
27	25.1, CH_3	1.22, s

HRMS-ESI (*m/z*) found 415.2831 $[M+H]^+$ (calculated for $C_{26}H_{39}O_4$, 415.2843).

White amorphous powder; $[\alpha]_D^{20} = -5.94$ (c = 0.12, MeOH).

Table S10. NMR data for dihydroxyfarnesyl-triacetate lactone (**9**)

^{1}H NMR spectrum (400 MHz), ^{13}C NMR spectrum (100 MHz), CD_3OD

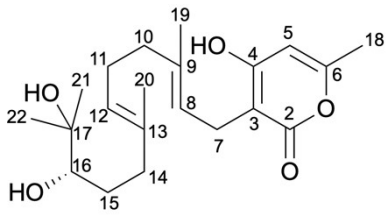

Compound 9

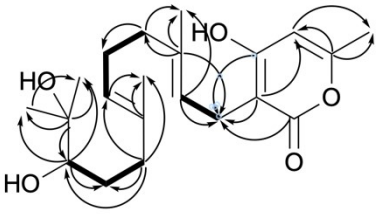

Key COSY (bold line) and HMBC (arrow) correlations of **9**

position	δ_C, **type**	δ_H **mult (*J* in Hz)**
1		
2	168.8, qC	-
3	103.2, qC	-
4	167.9, qC	-
5	101.9, CH	5.99, br s
6	161.8, qC	-
7	22.9, CH_2	3.06, d (7.1)
8	122.7, CH	5.15, m
9	136.6, qC	-
10	41.0, CH_2	1.98, m
11	27.7, CH_2	2.07, m
12	125.7, CH	5.15, m
13	136.1, qC	-
14	38.0, CH_2	1.98, m
		2.22, m
15	30.9, CH_2	1.32, m
		1.69, m
16	79.2, CH	3.23, dd (10.5, 1.7)
17	74.0, qC	-
18	19.8, CH_3	2.19, br s
19	16.5, CH_3	1.72, br s
20	16.3, CH_3	1.59, br s
21	25.1, CH_3	1.12, s
22	25.8, CH_3	1.15, s

HRMS-ESI (*m/z*) found 365.2324 $[M+H]^+$ (calculated for $C_{21}H_{33}O_5$, 365.2323).

Yellowish white amorphous powder; $[\alpha]_D^{20} = -17.83$ (c = 0.12, MeOH).

Table S11. NMR data for 17-methoxy-16-hydroxyfarnesyl-triacetate lactone (**10**)
^{1}H NMR spectrum (400 MHz), ^{13}C NMR spectrum (100 MHz), acetone-d_6

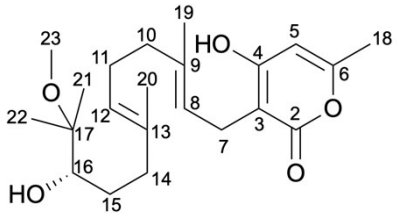

Compound 10

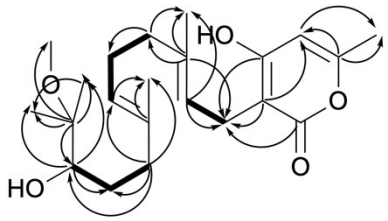

Key COSY (bold line) and HMBC (arrow) correlations of **10**

position	δ_C, **type**	δ_H **mult (*J* in Hz)**
1		
2	166.2, qC	-
3	102.1, qC	-
4	165.8, qC	-
5	101.2, CH	6.02, br s
6	160.4, qC	-
7	22.8, CH_2	3.08, d (7.1)
8	123.1, CH	5.24, tq (6.4, 1.4)
9	135.4, qC	-
10	40.5, CH_2	1.98, m
11	27.2, CH_2	2.07, m
12	125.0, CH	5.15, tq (6.8, 1.3)
13	135.8, qC	-
14	37.6, CH_2	1.98, m
		2.23, ddd (14.3, 9.7, 4.8)
15	30.1, CH_2	1.31, m
		1.64, m
16	76.4, CH	3.35, dd (10.4, 1.8)
17	77.9, qC	-
18	19.7, CH_3	2.12, br s
19	16.2, CH_3	1.73, br s
20	16.3, CH_3	1.58, br s
21	20.3, CH_3	1.07, s
22	20.8, CH_3	1.10, s
23	49.2, CH_3	3.16, s

HRMS-ESI (*m/z*) found 379.2470 $[M+H]^+$ (calculated for $C_{22}H_{35}O_5$, 379.2479).
Yellow oil; $[\alpha]_D^{20} = -17.76$ (c = 0.07, MeOH).

Table S12. NMR data for epoxyfarnesyl-triacetate lactone (**11**)

^{1}H NMR spectrum (400 MHz), ^{13}C NMR spectrum (100 MHz), acetone-d_6

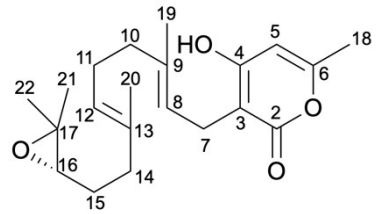

Compound 11

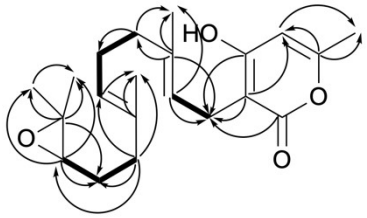

Key COSY (bold line) and HMBC (arrow) correlations of **11**

position	δ_C, **type**	δ_H **mult (*J* in Hz)**
1		
2	165.6, qC	-
3	102.5, qC	-
4	165.2, qC	-
5	100.7, CH	6.02, br s
6	160.8, qC	-
7	22.8, CH_2	3.09, d (7.2)
8	122.8, CH	5.23, tq (7.2, 1.3)
9	135.6, qC	-
10	40.4, CH_2	1.98, m
11	27.2, CH_2	2.08, m
12	125.4, CH	5.17, tq (7.1, 1.3)
13	135.0, qC	-
14	37.1, CH_2	2.08, m
15	28.3, CH_2	1.57, m
16	64.1, CH	2.63, t (6.3)
17	58.1, qC	-
18	19.7, CH_3	2.15, br s
19	16.3, CH_3	1.74, br s
20	16.1, CH_3	1.61, br s
21	19.0, CH_3	1.21, s
22	25.1, CH_3	1.23, s

HRMS-ESI (*m/z*) found 347.2210 $[M+H]^+$ (calculated for $C_{21}H_{31}O_4$, 347.2217).

White amorphous powder; $[\alpha]_D^{20} = -7.96$ (c = 0.09, MeOH).

Table S13. Tabulated MicroED data statistics for sartorypyrone F (**1**)

Stoichiometric Formula	$C_{26}H_{38}O_4$
Data Collection	
Temperature (K)	100(2)
Space group	C2
Cell dimensions	
a, *b*, *c* (Å)	50.1(2), 6.67(2), 12.670(10)
α, *β*, *γ* (°)	90, 98.52(6), 90
Resolution (Å)	1.00
Observed reflections	13017
Unique reflections	2065
R_{obs} (%)	13.7
R_{meas} (%)	14.8
I/σI	8.22
$CC_{1/2}$ (%)	99.1
Completeness (%)	84.1
Refinement	
R_1	0.1502
wR_2	0.3363
GooF	1.285

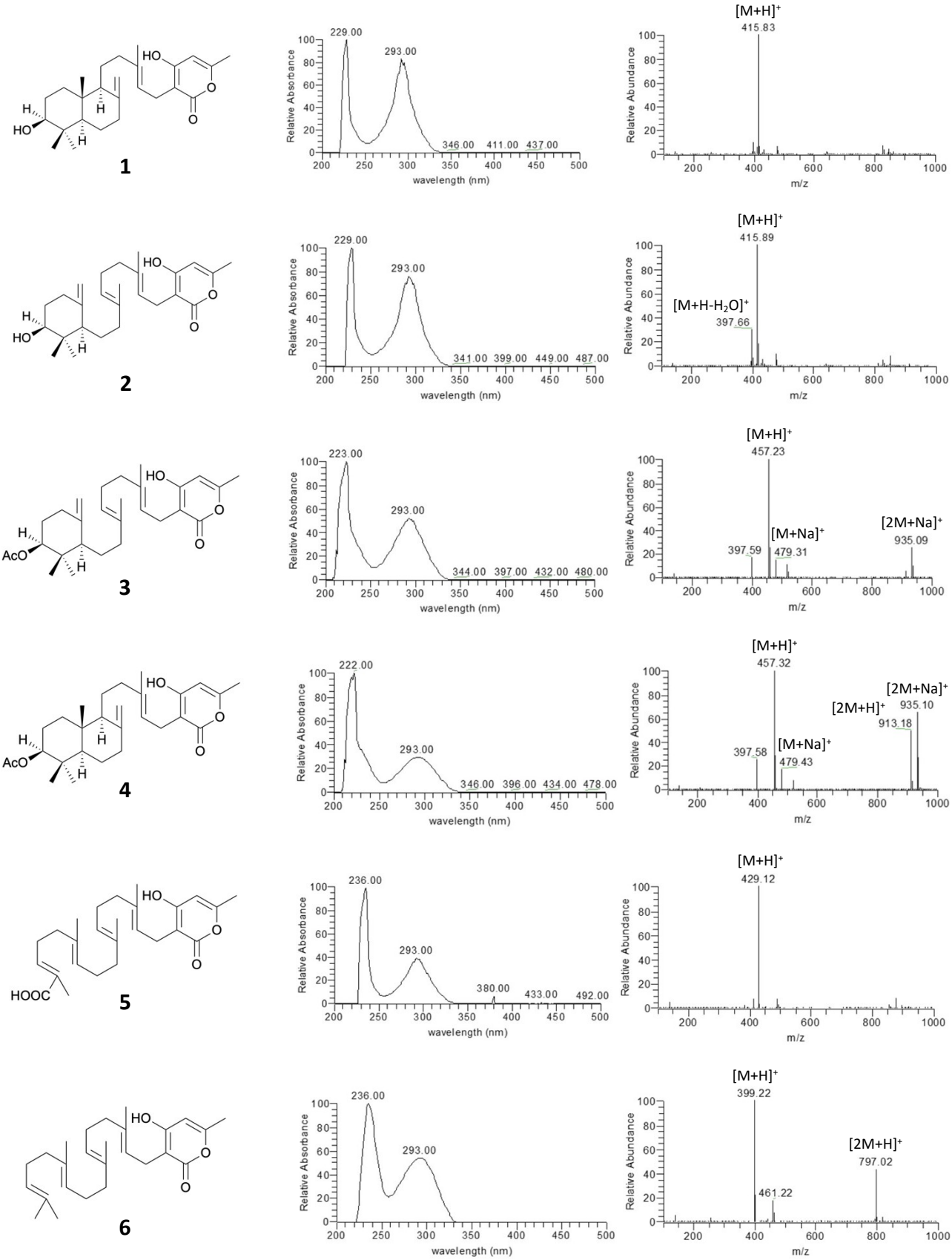

Figure S6. UV-Vis and ESIMS spectra of compounds **1-12**

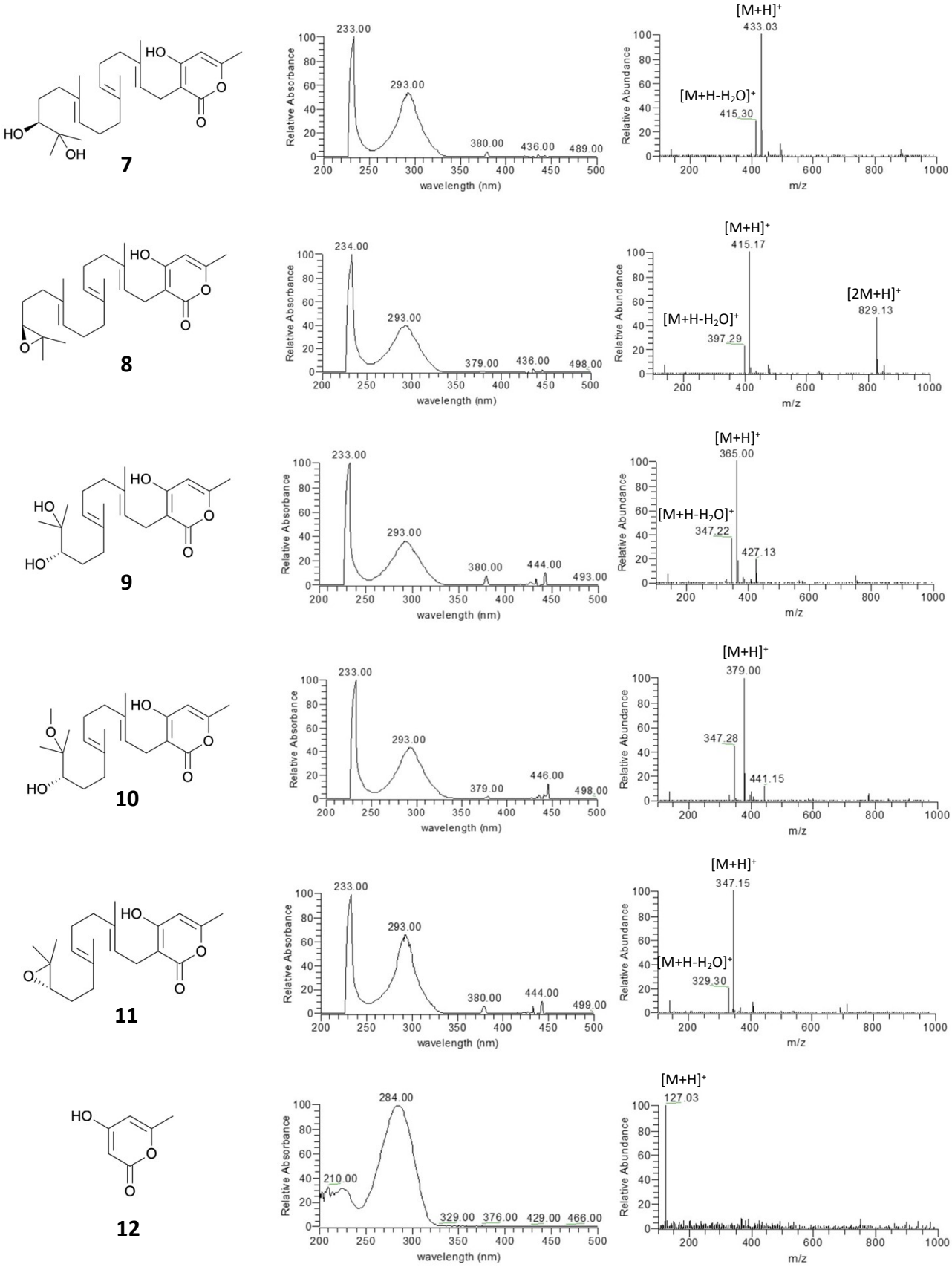

Figure S6. UV-Vis and ESIMS spectra of compounds **1-12** (continued)

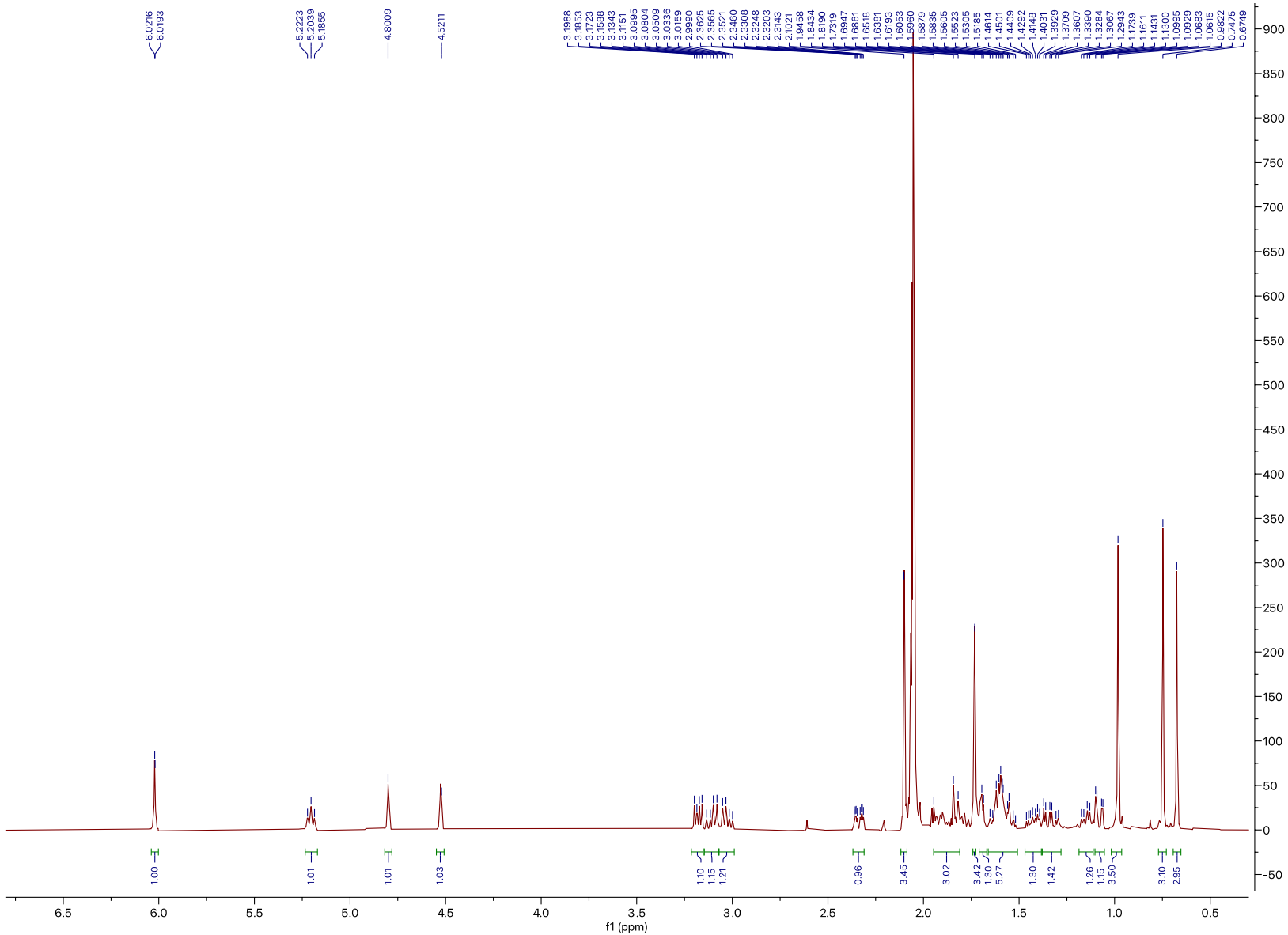

Figure S7. ^{1}H NMR of compound **1** in acetone-d_6

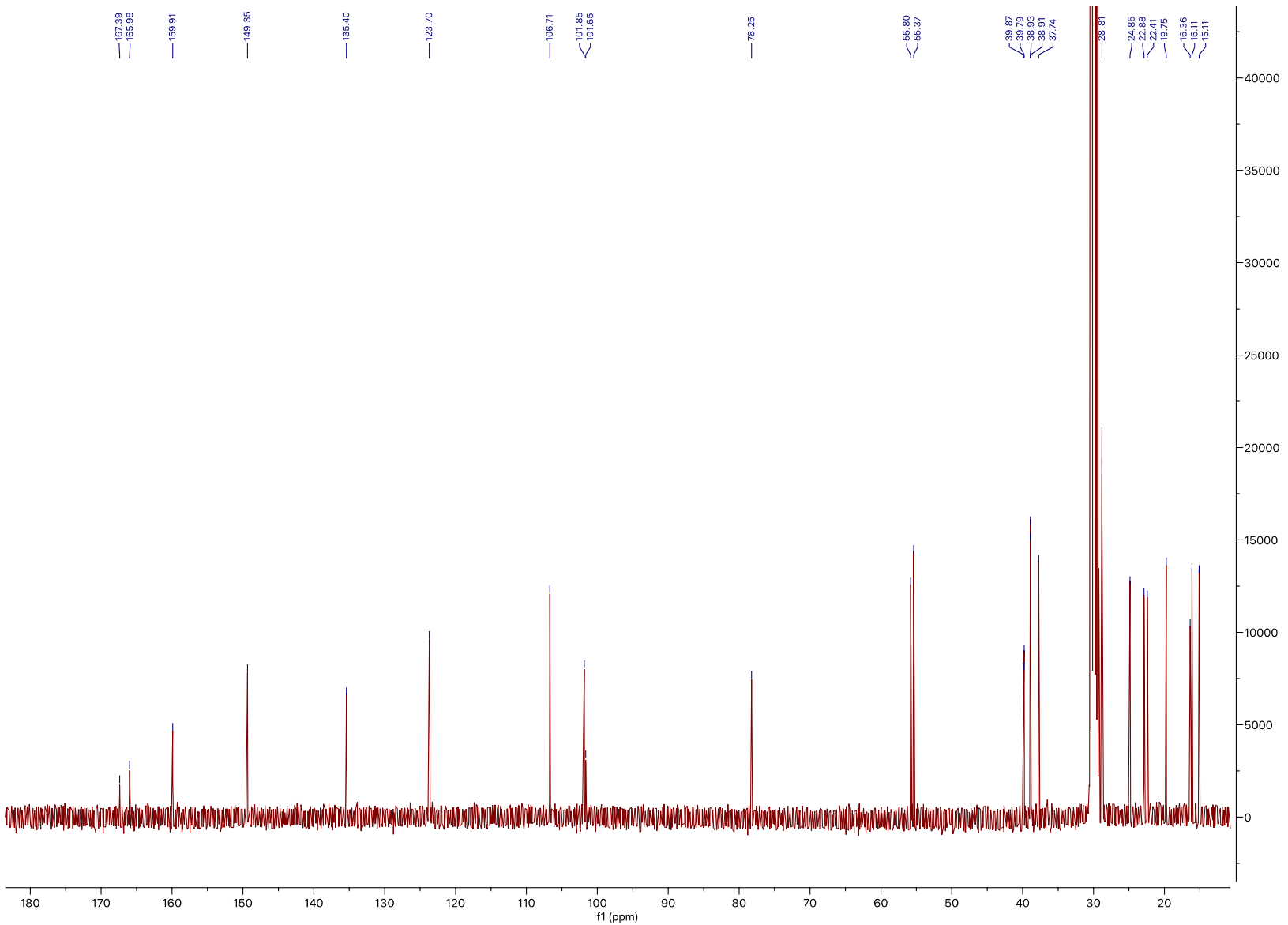

Figure S8. ^{13}C NMR of compound **1** in acetone-d_6

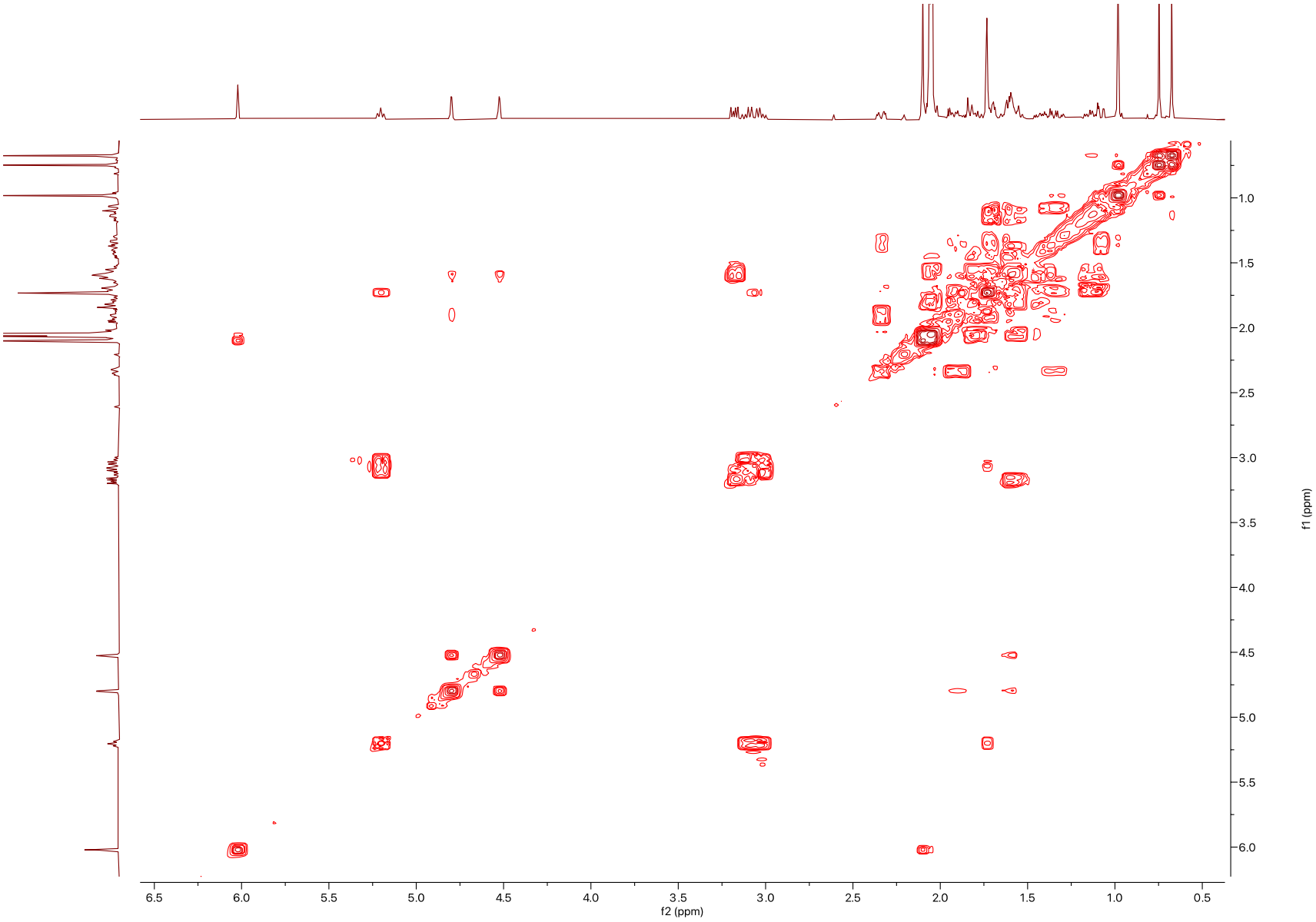

Figure S9. COSY of compound **1** in acetone-d_6

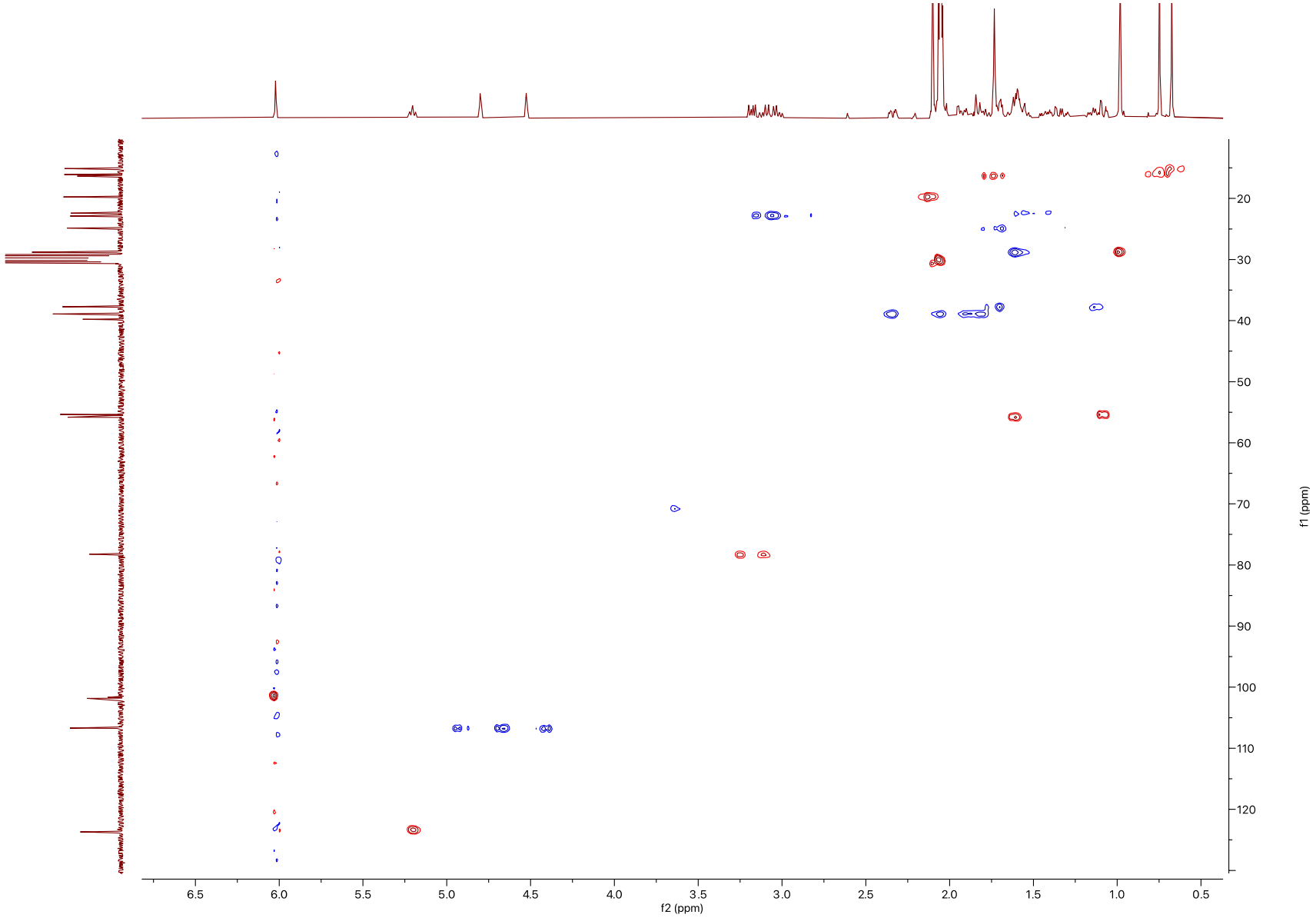

Figure S10. HSQC of compound **1** in acetone-d_6

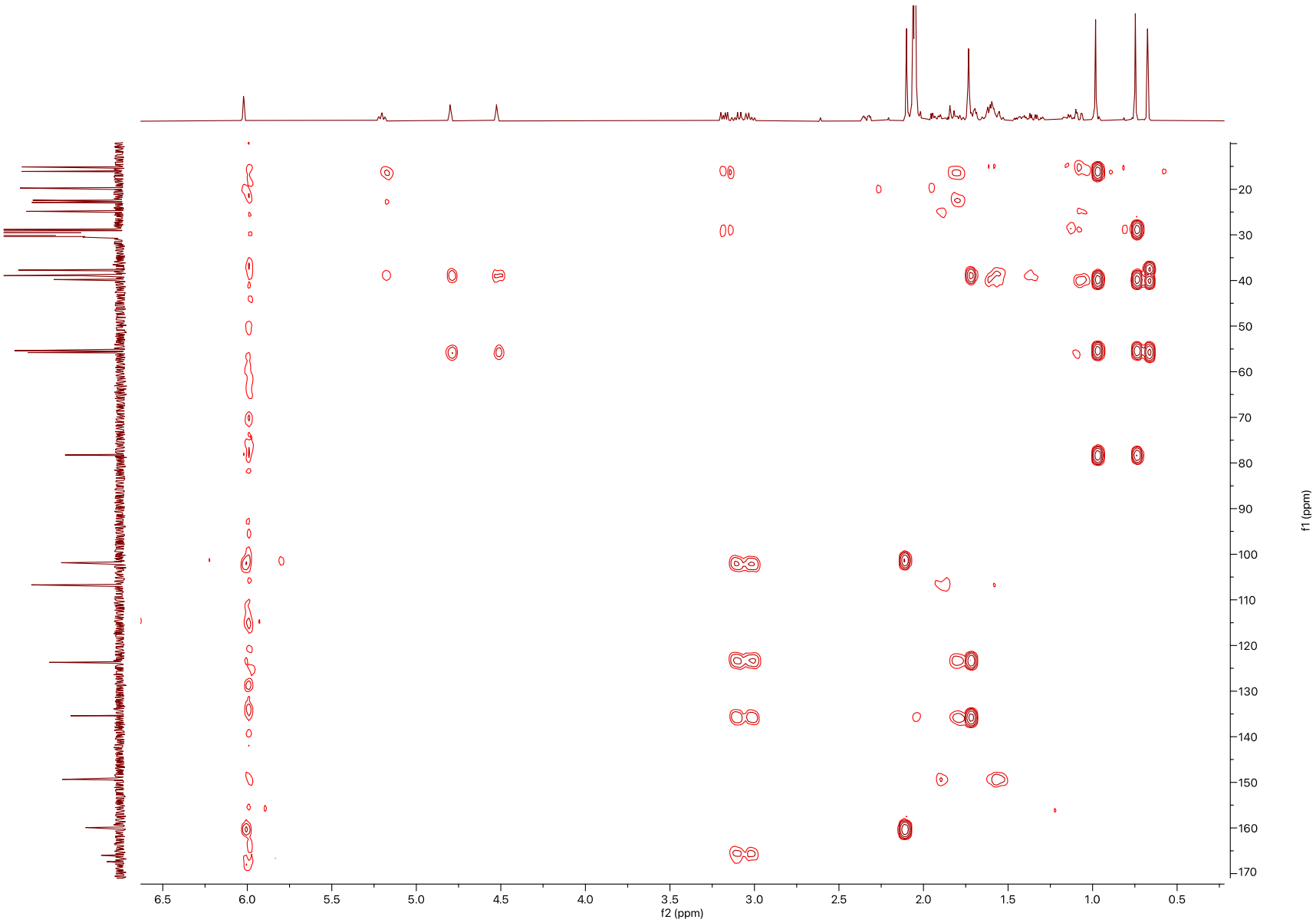

Figure S11. HMBC of compound **1** in acetone-d_6

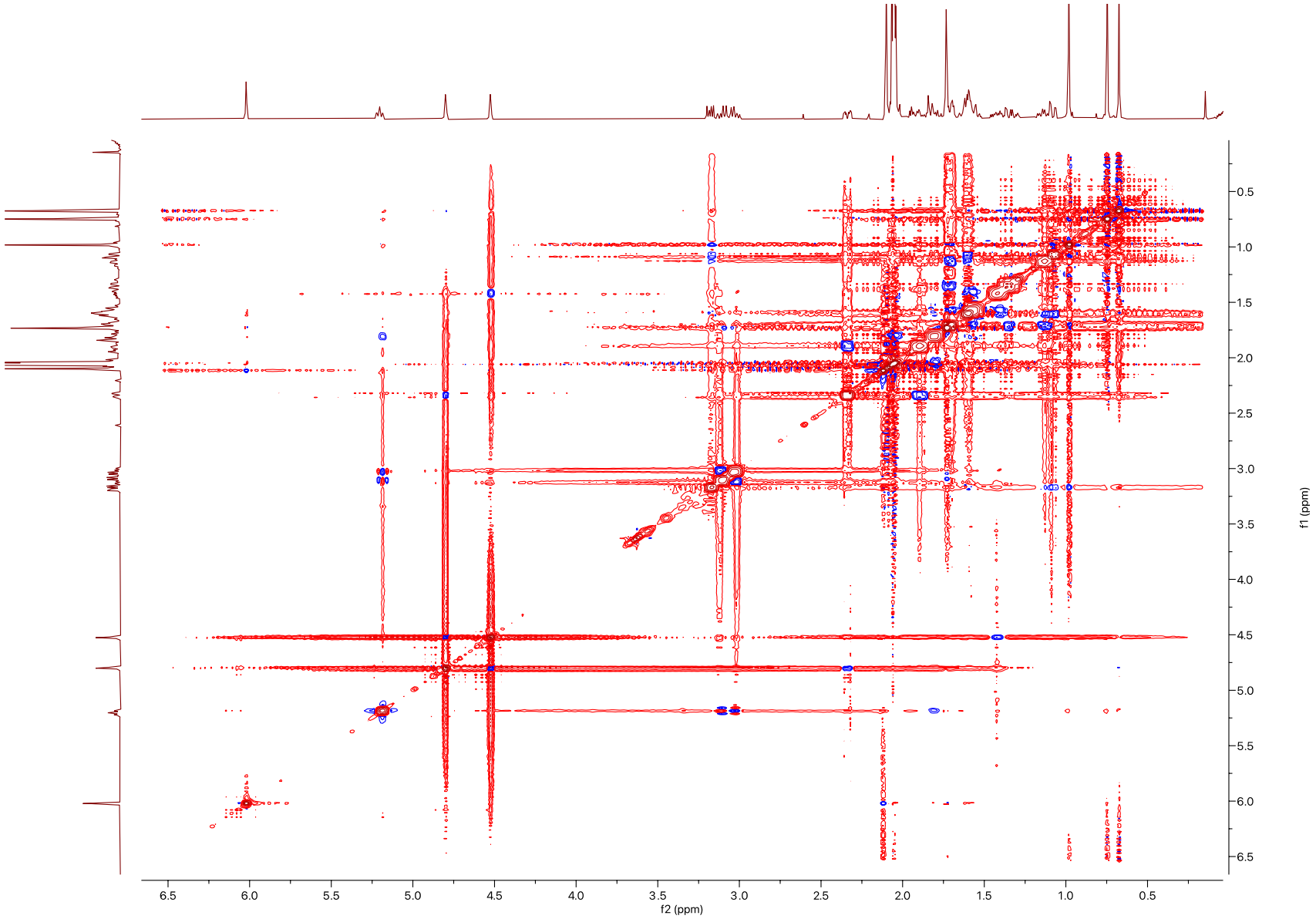

Figure S12. NOESY of compound **1** in acetone-d_6

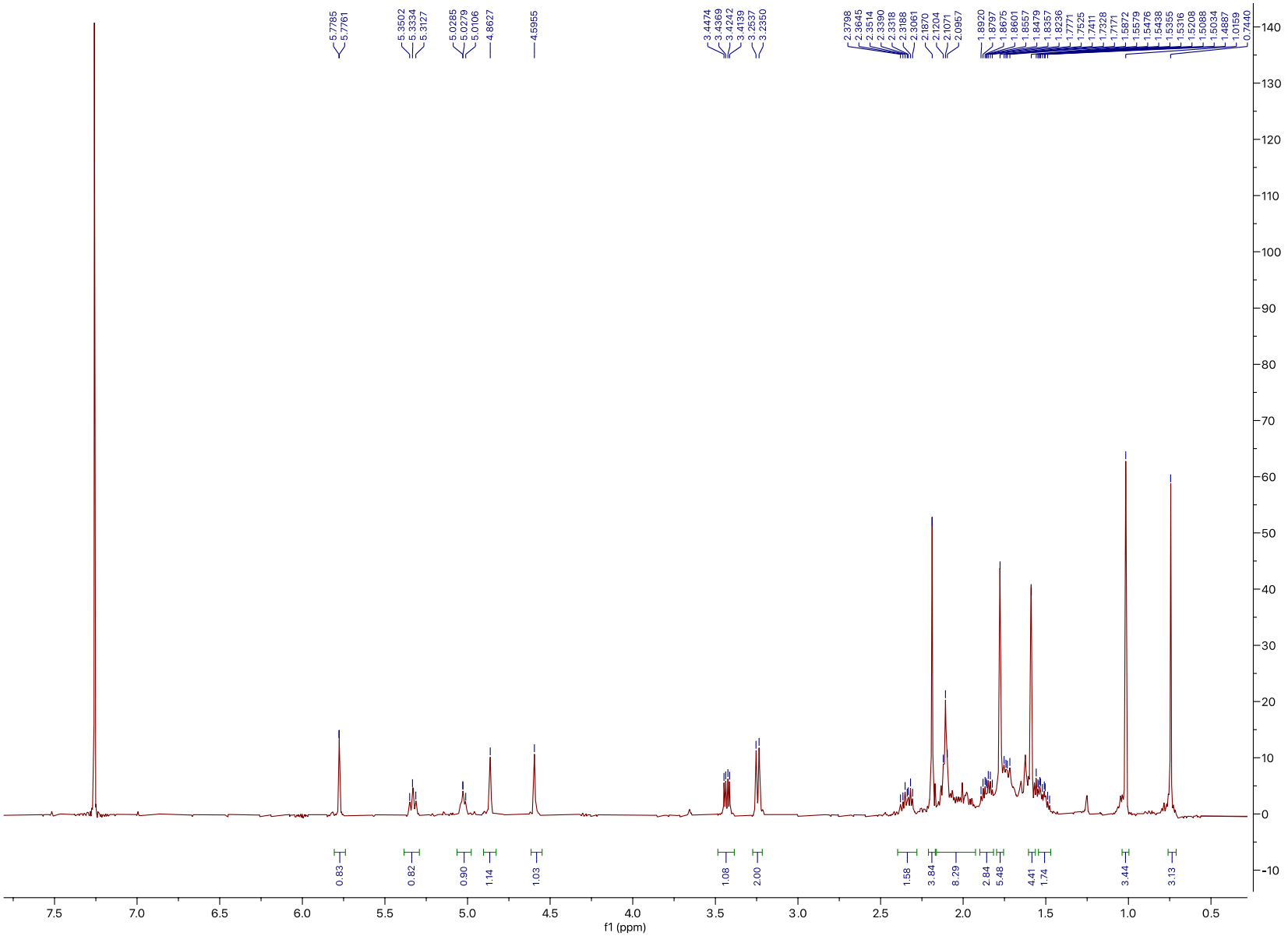

Figure S13. ^{1}H NMR of compound **2** in $CDCl_3$

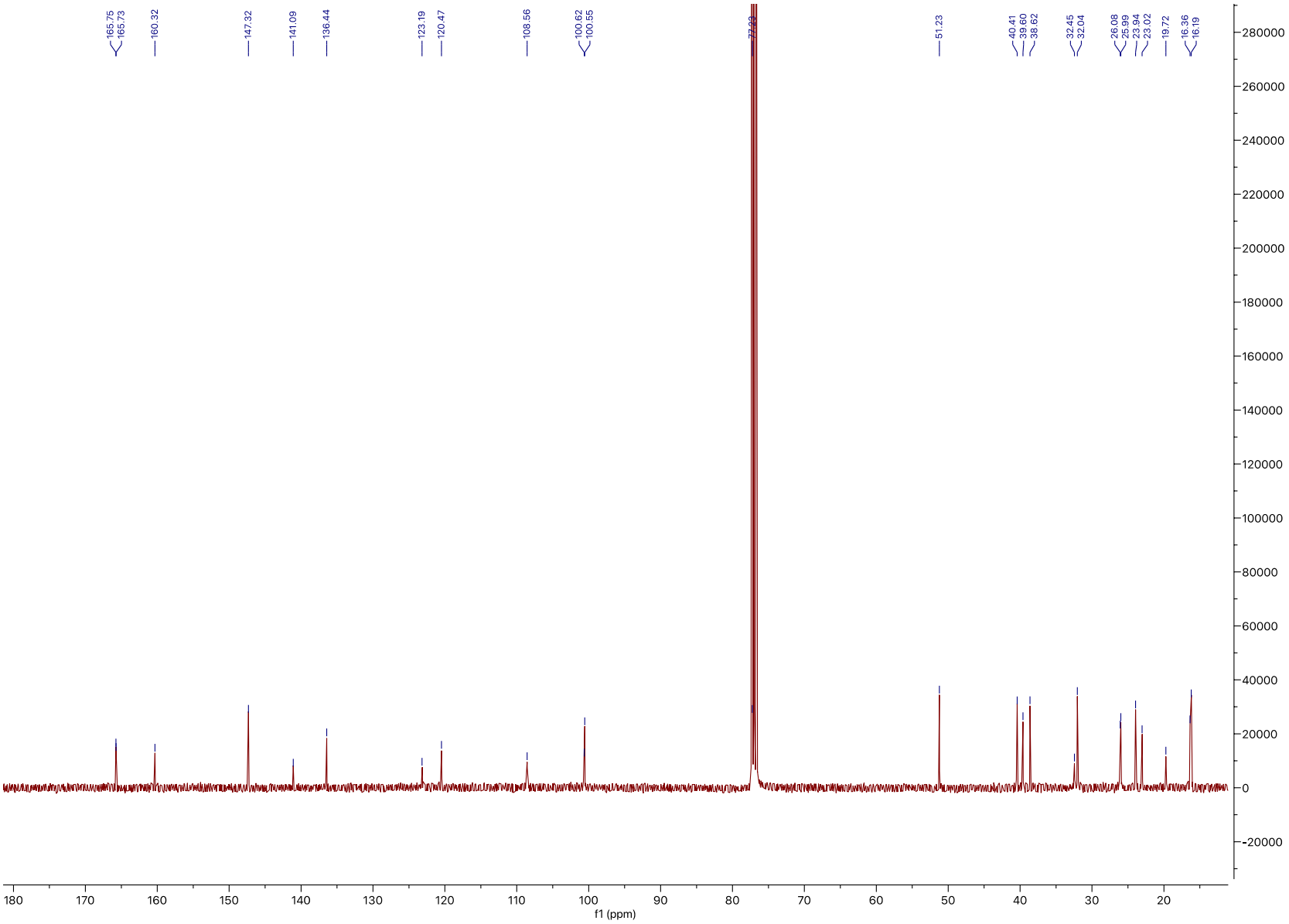

Figure S14. ^{13}C NMR of compound **2** in $CDCl_3$

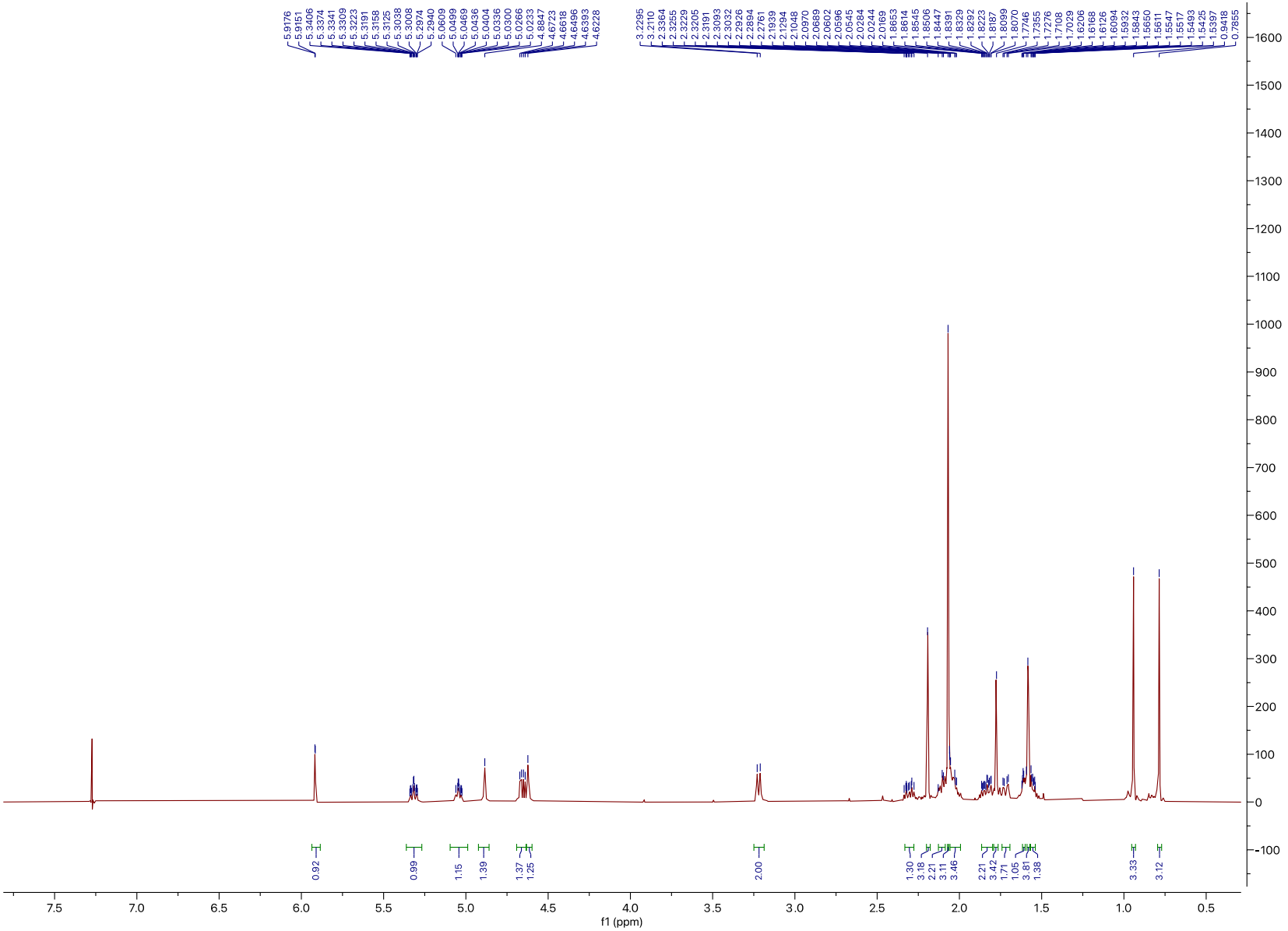

Figure S15. ^{1}H NMR of compound **3** in $CDCl_3$

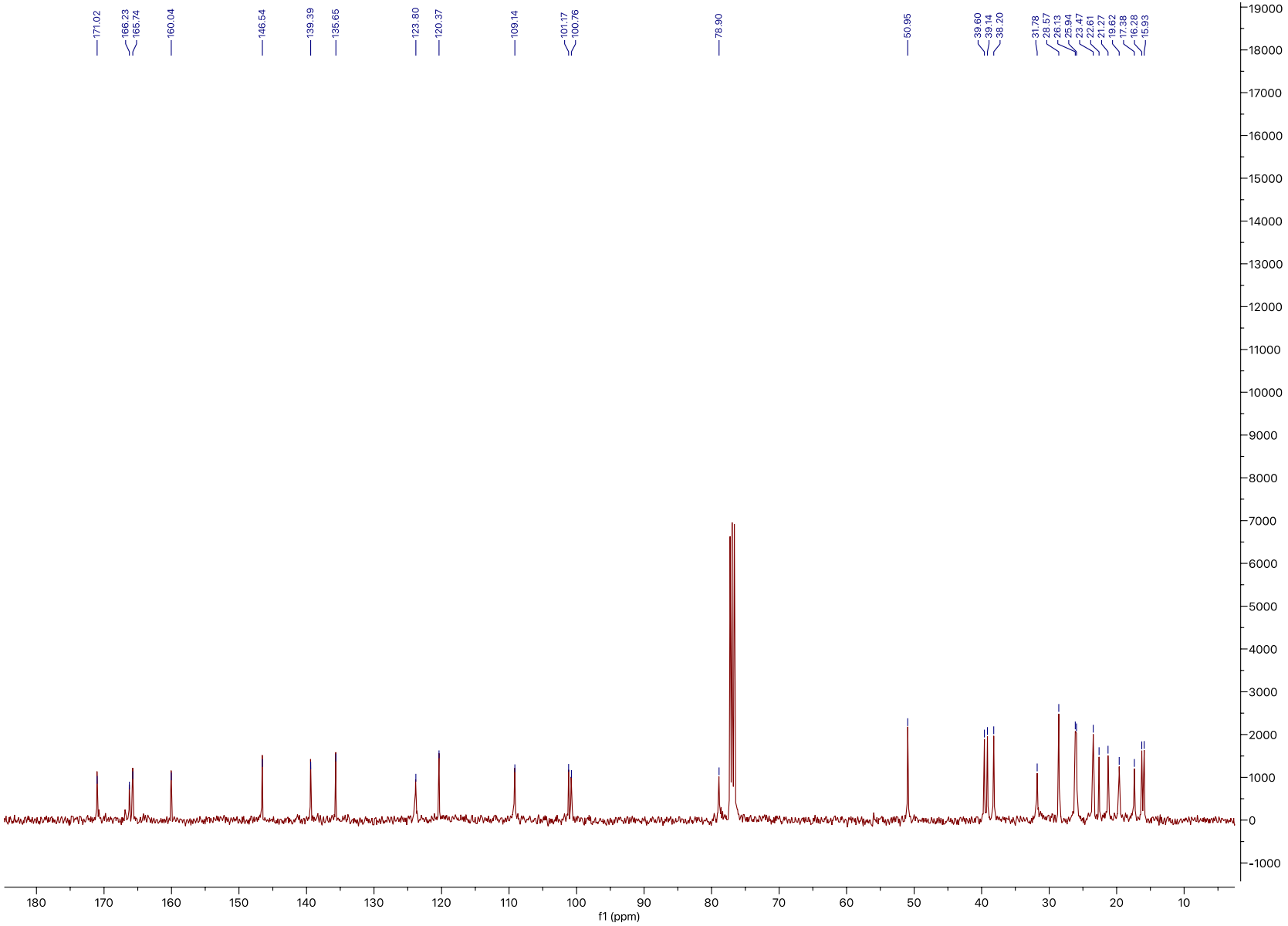

Figure S16. ^{13}C NMR of compound **3** in $CDCl_3$

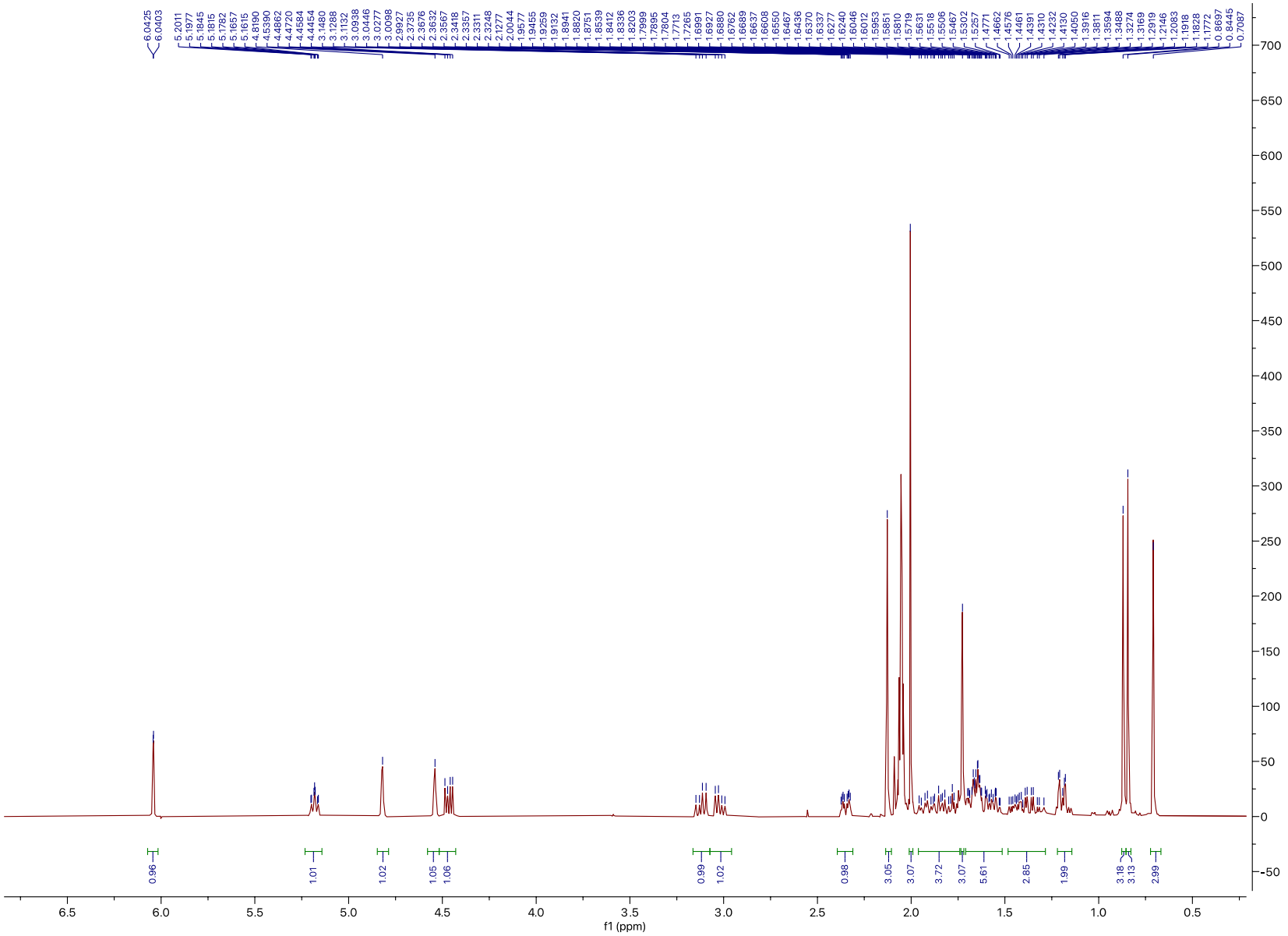

Figure S17. ^{1}H NMR of compound **4** in acetone-d_6

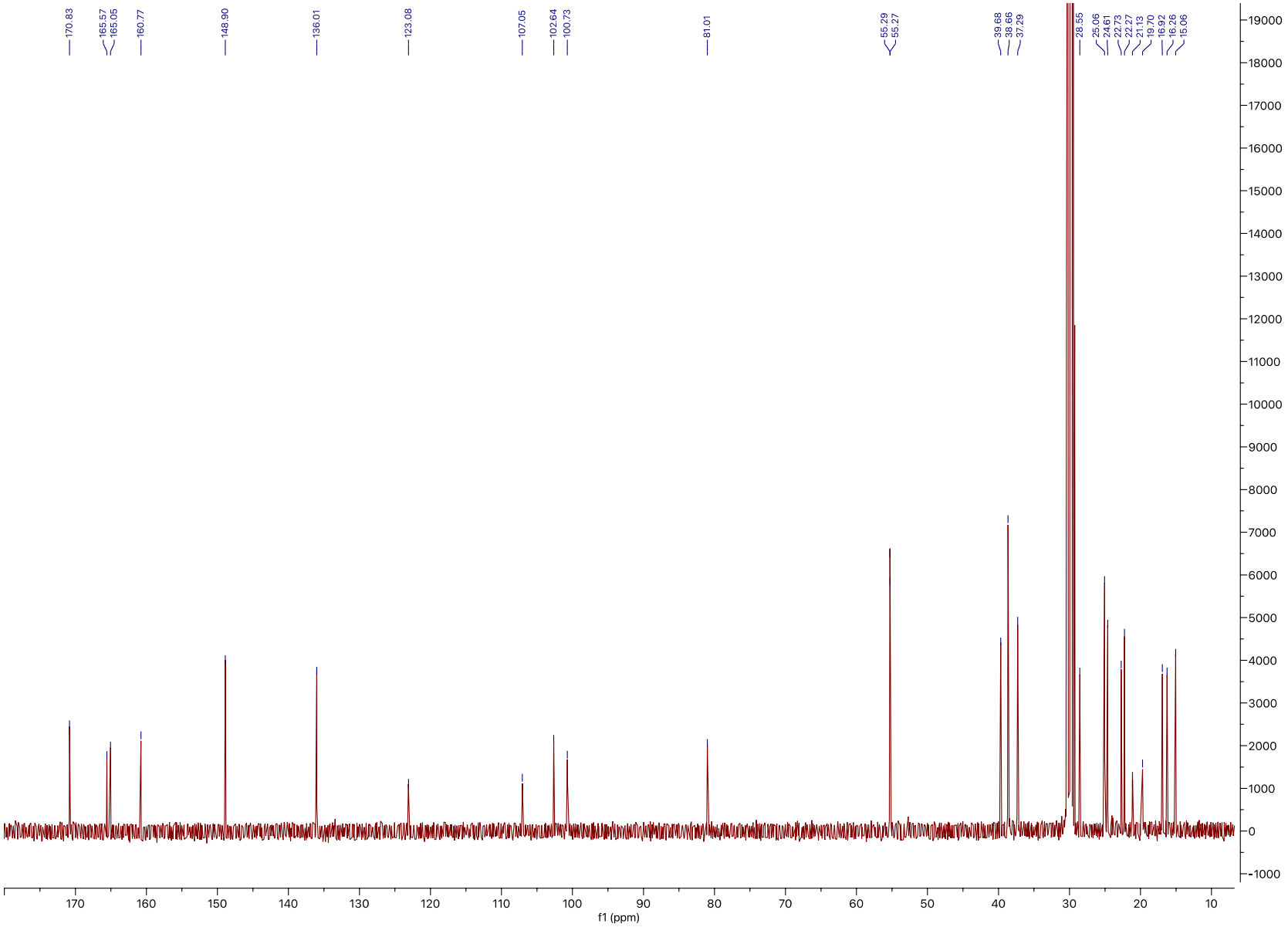

Figure S18. ^{13}C NMR of compound **4** in acetone-d_6

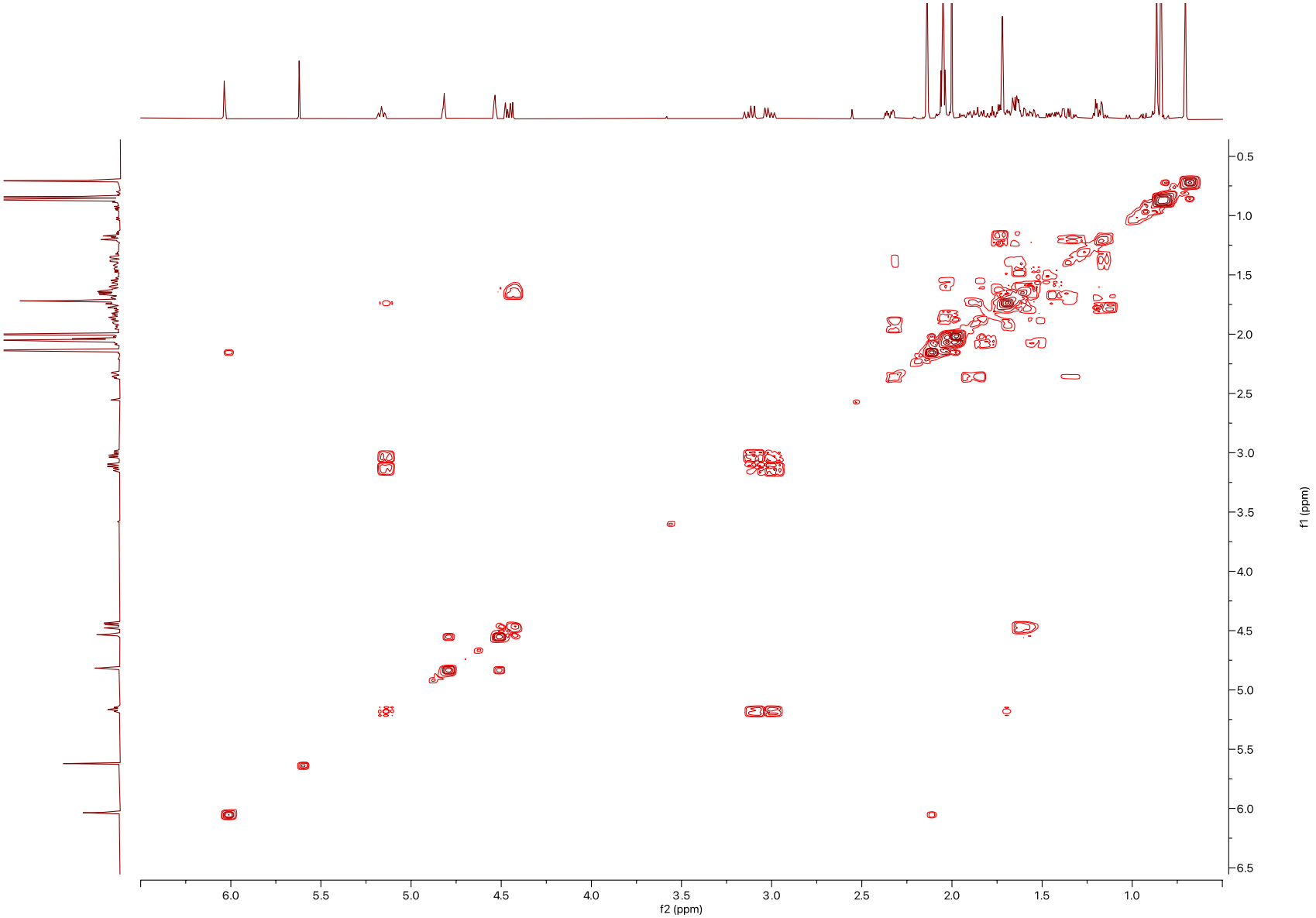

Figure S19. COSY of compound **4** in acetone-d_6

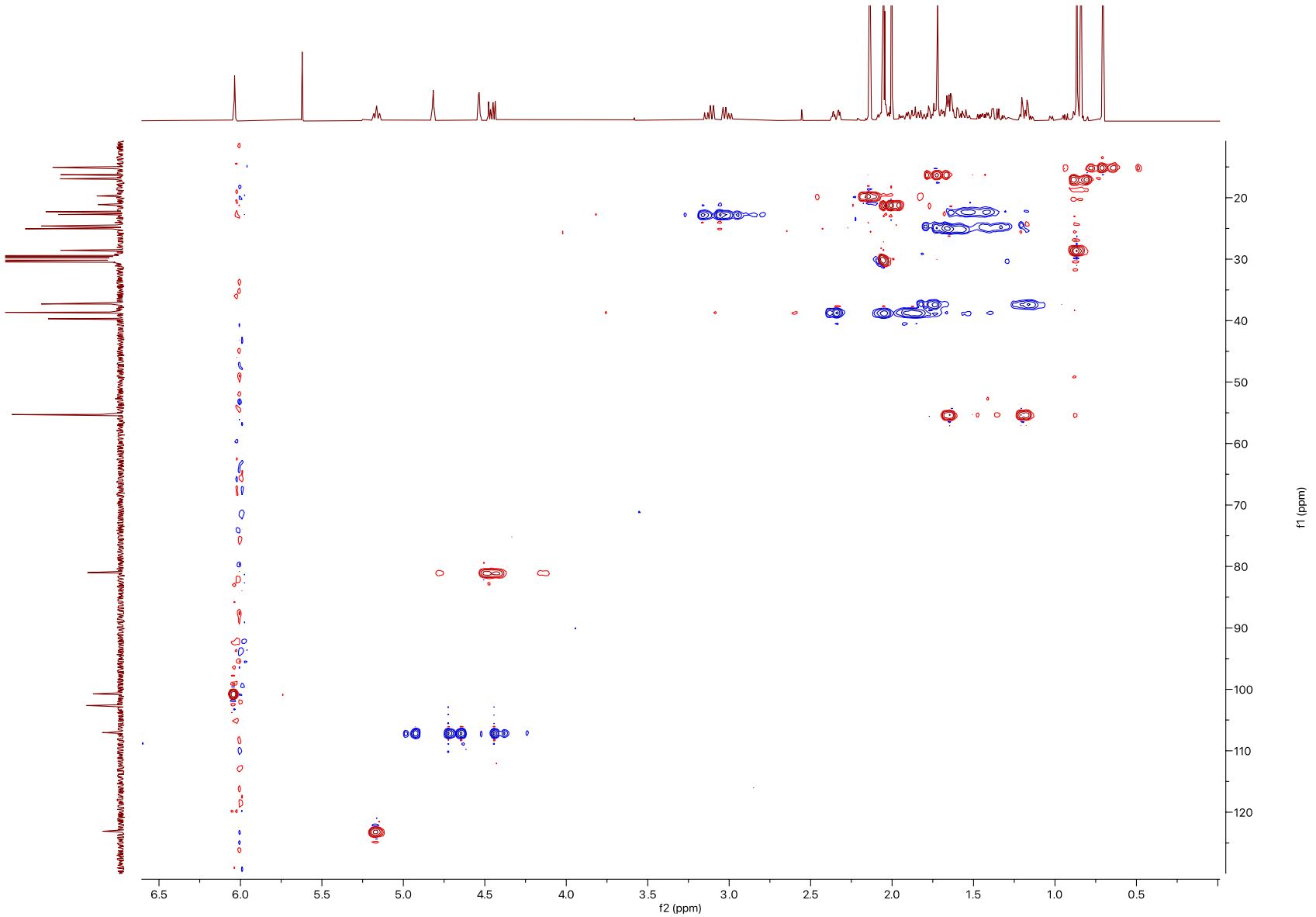

Figure S20. HSQC of compound **4** in acetone-d_6

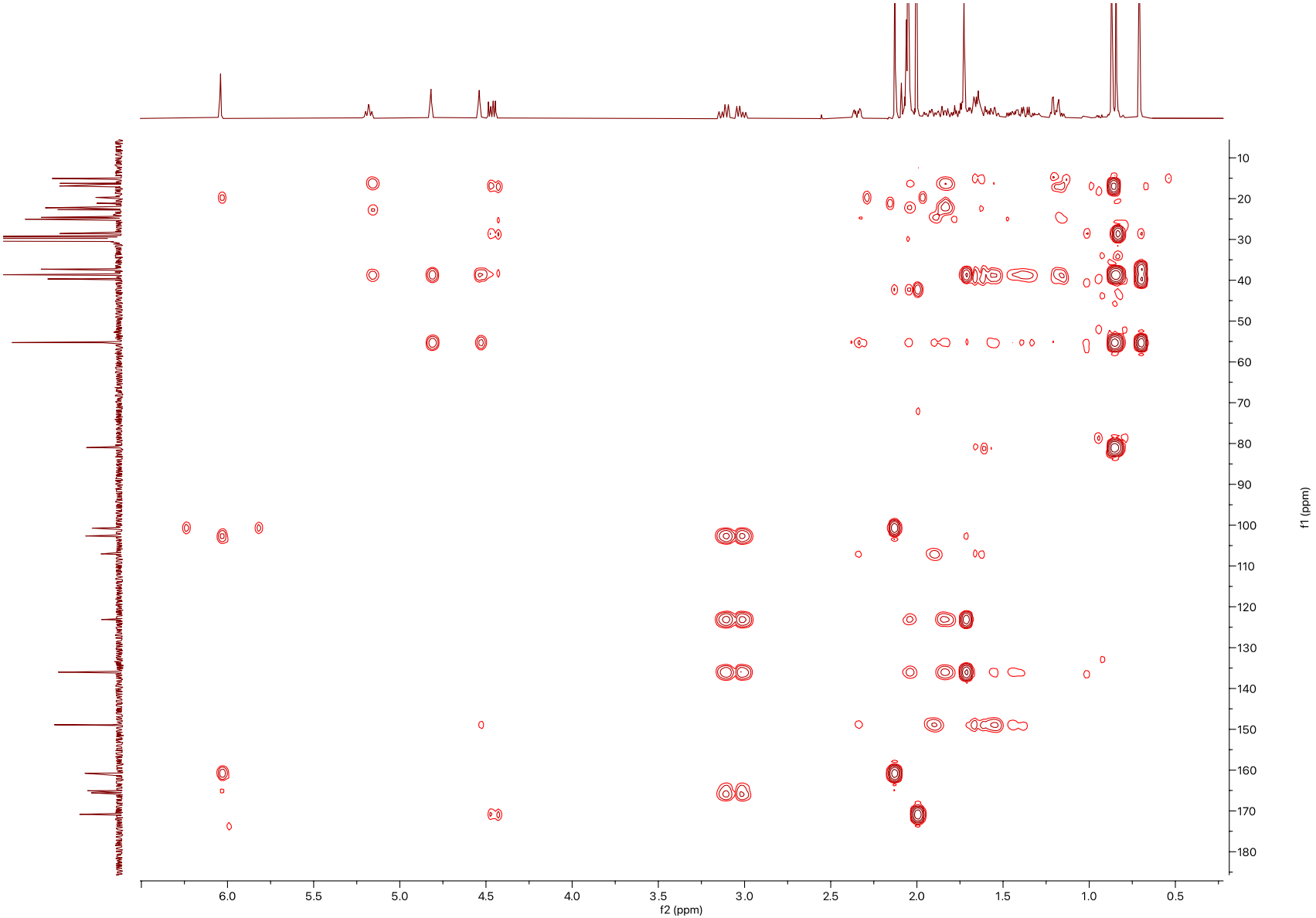

Figure S21. HMBC of compound **4** in acetone-d_6

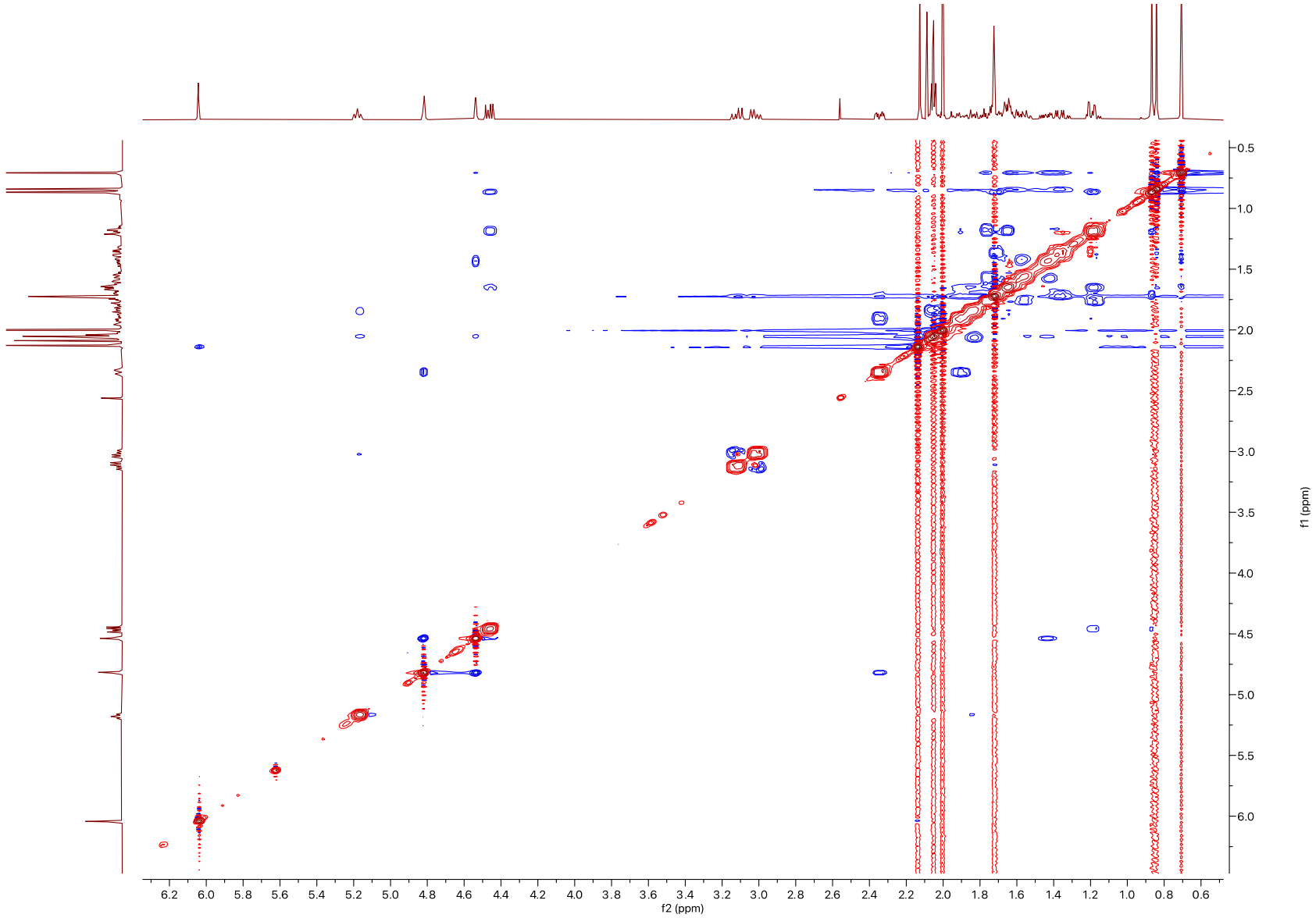

Figure S22. NOESY of compound **4** in acetone-d_6

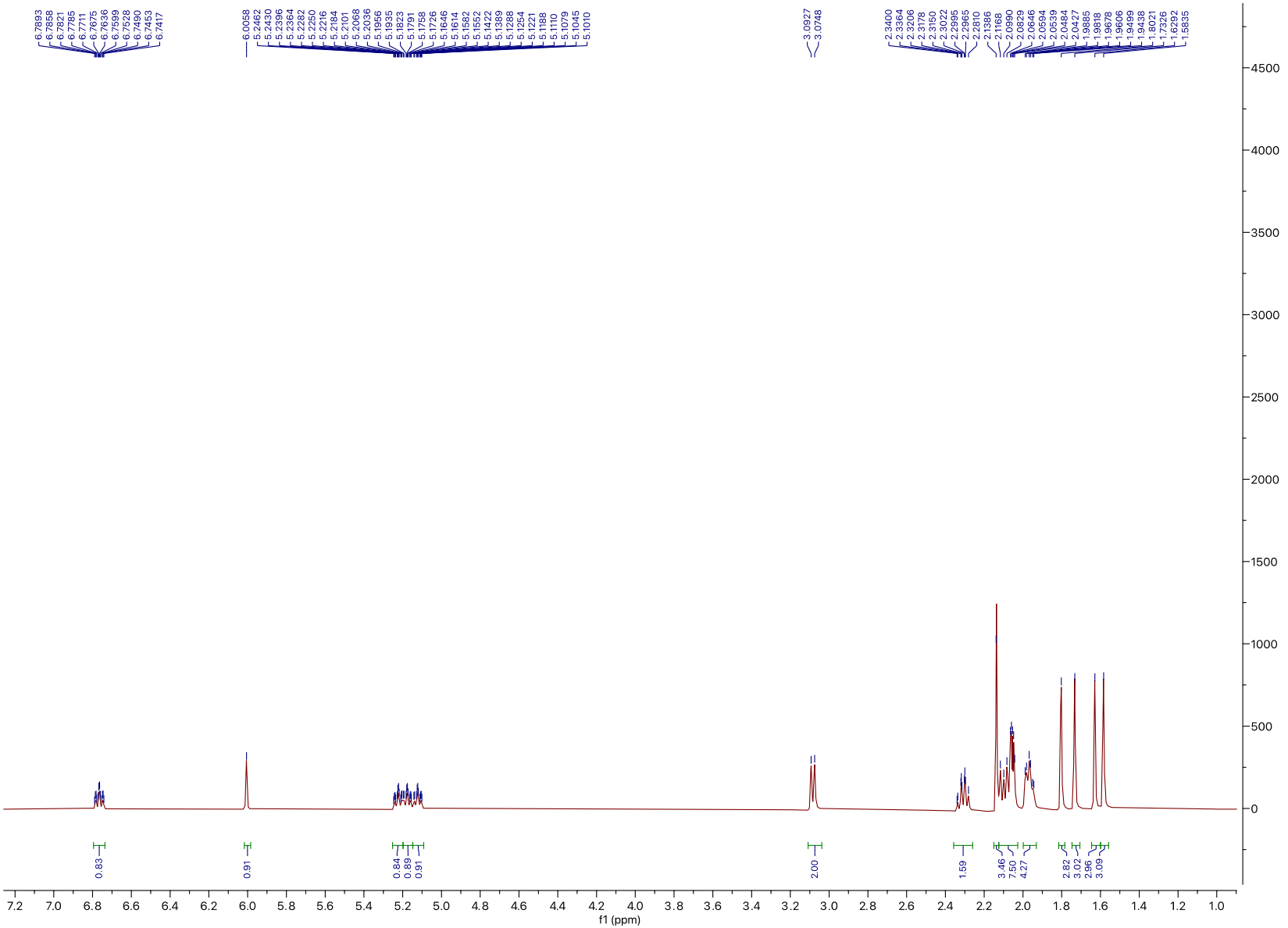

Figure S23. ^{1}H NMR of compound **5** in acetone-d_6

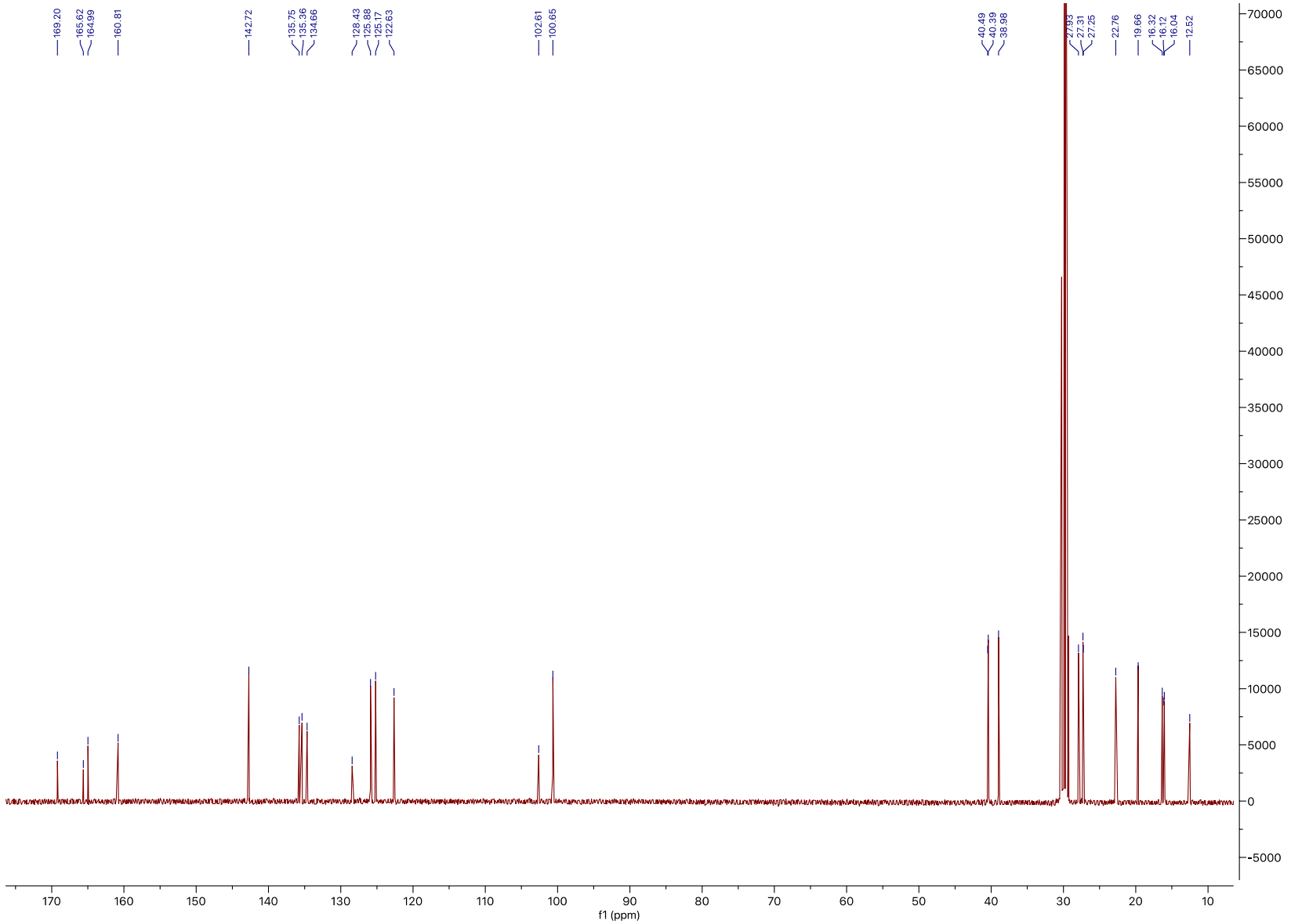

Figure S24. ^{13}C NMR of compound **5** in acetone-d_6

Figure S25. COSY of compound **5** in acetone-d_6

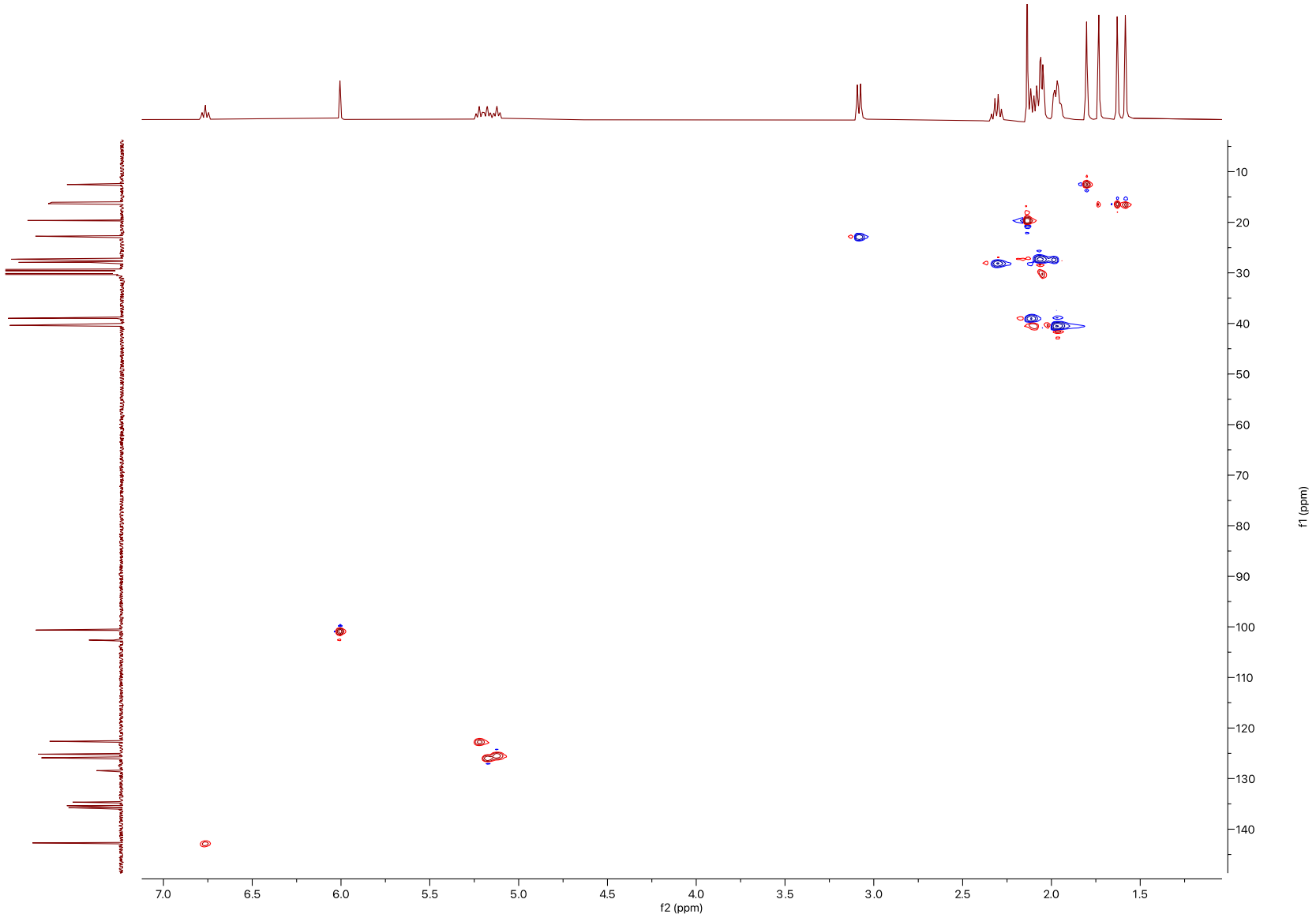

Figure S26. HSQC of compound **5** in acetone-d_6

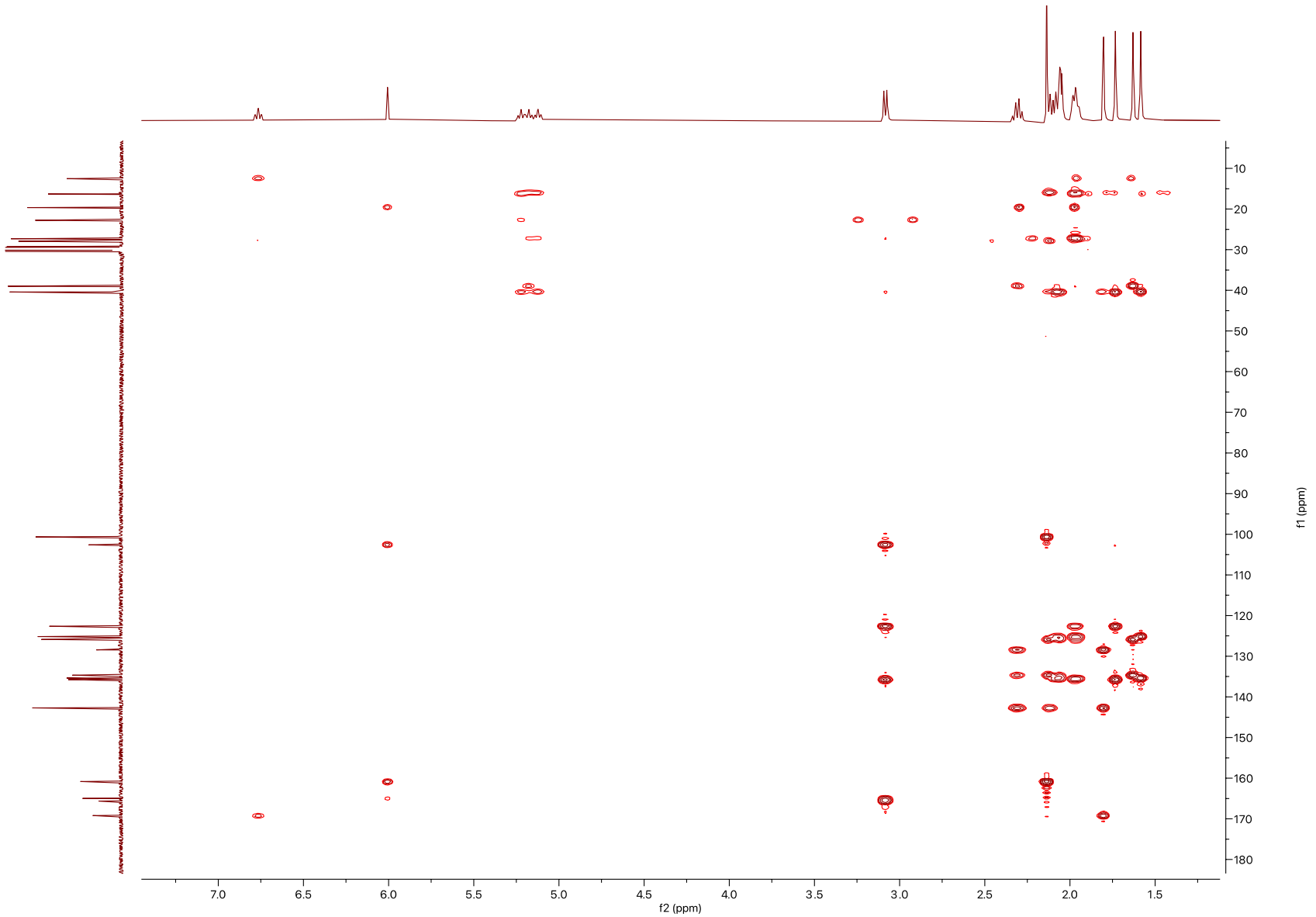

Figure S27. HMBC of compound **5** in acetone-d_6

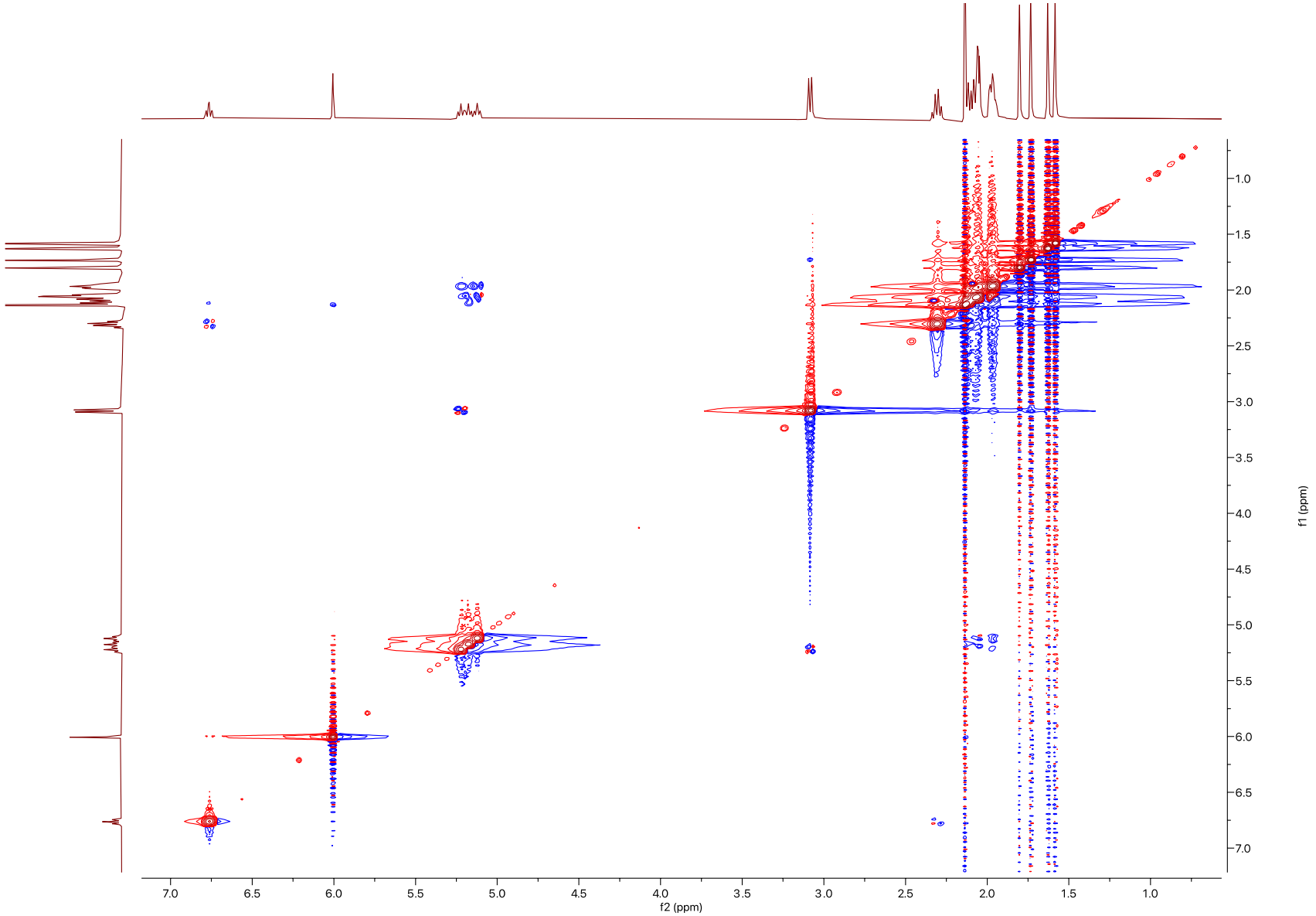

Figure S28. NOESY of compound **5** in acetone-d_6

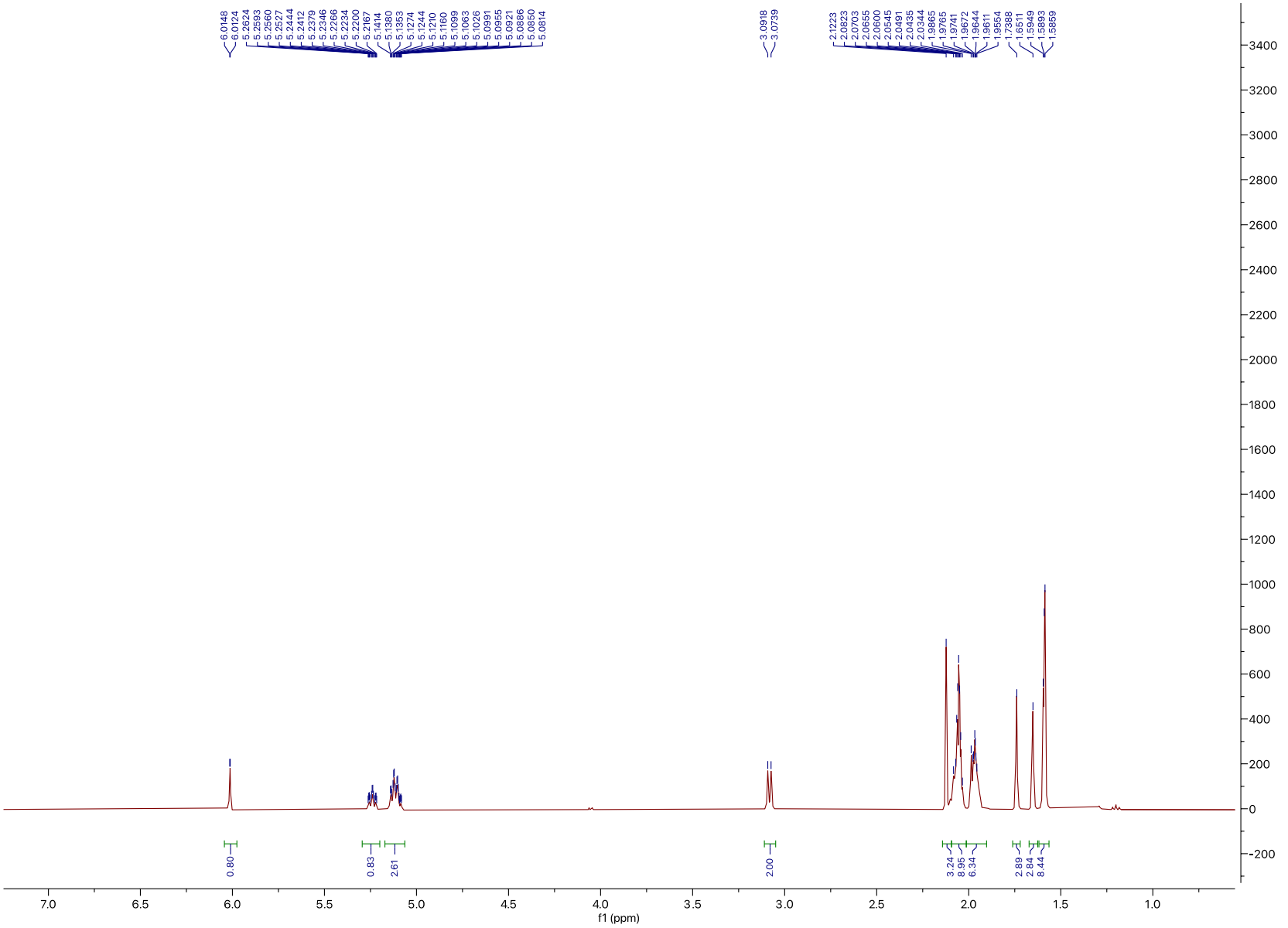

Figure S29. ^{1}H NMR of compound **6** in acetone-d_6

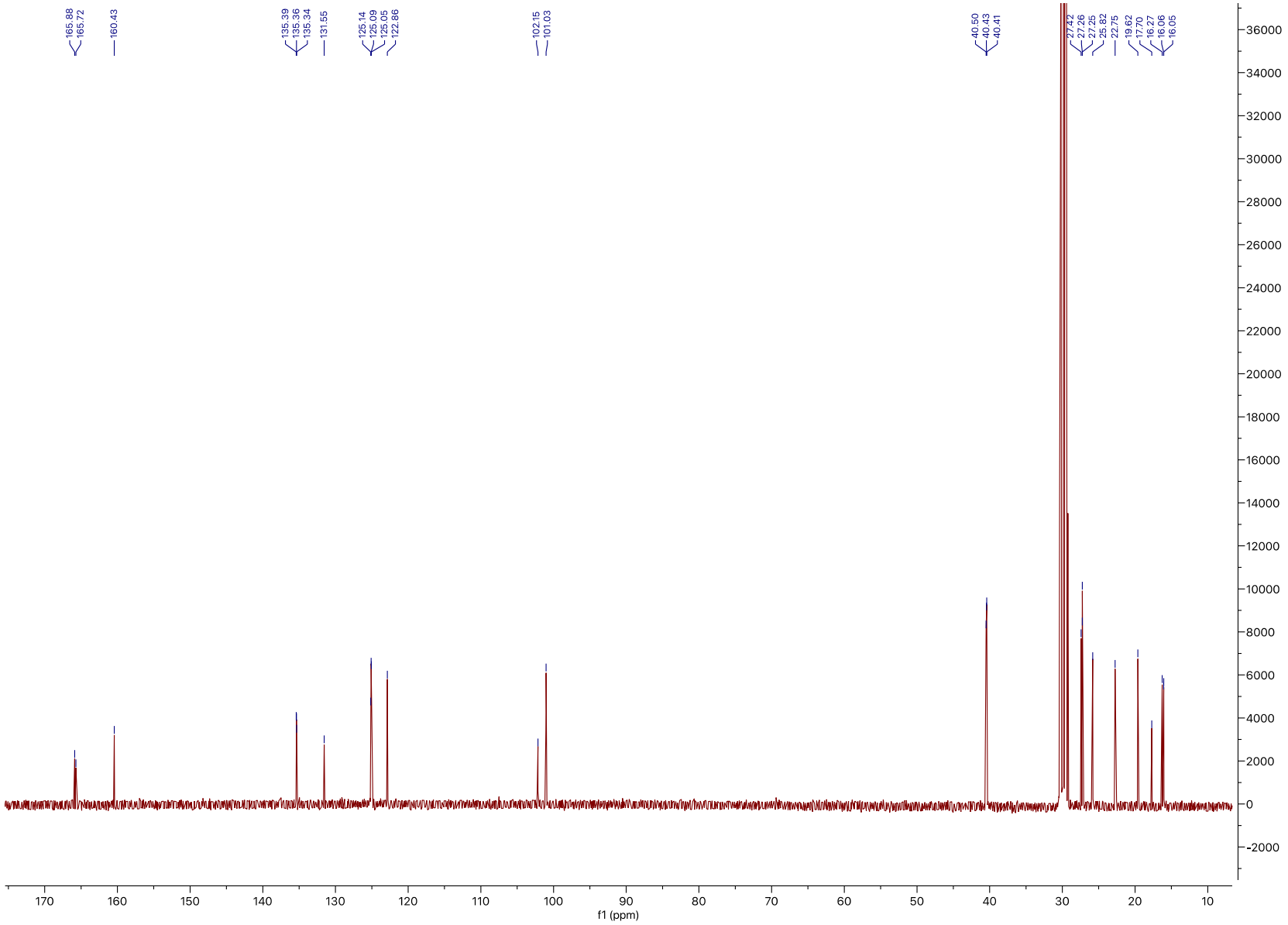

Figure S30. ^{13}C NMR of compound **6** in acetone-d_6

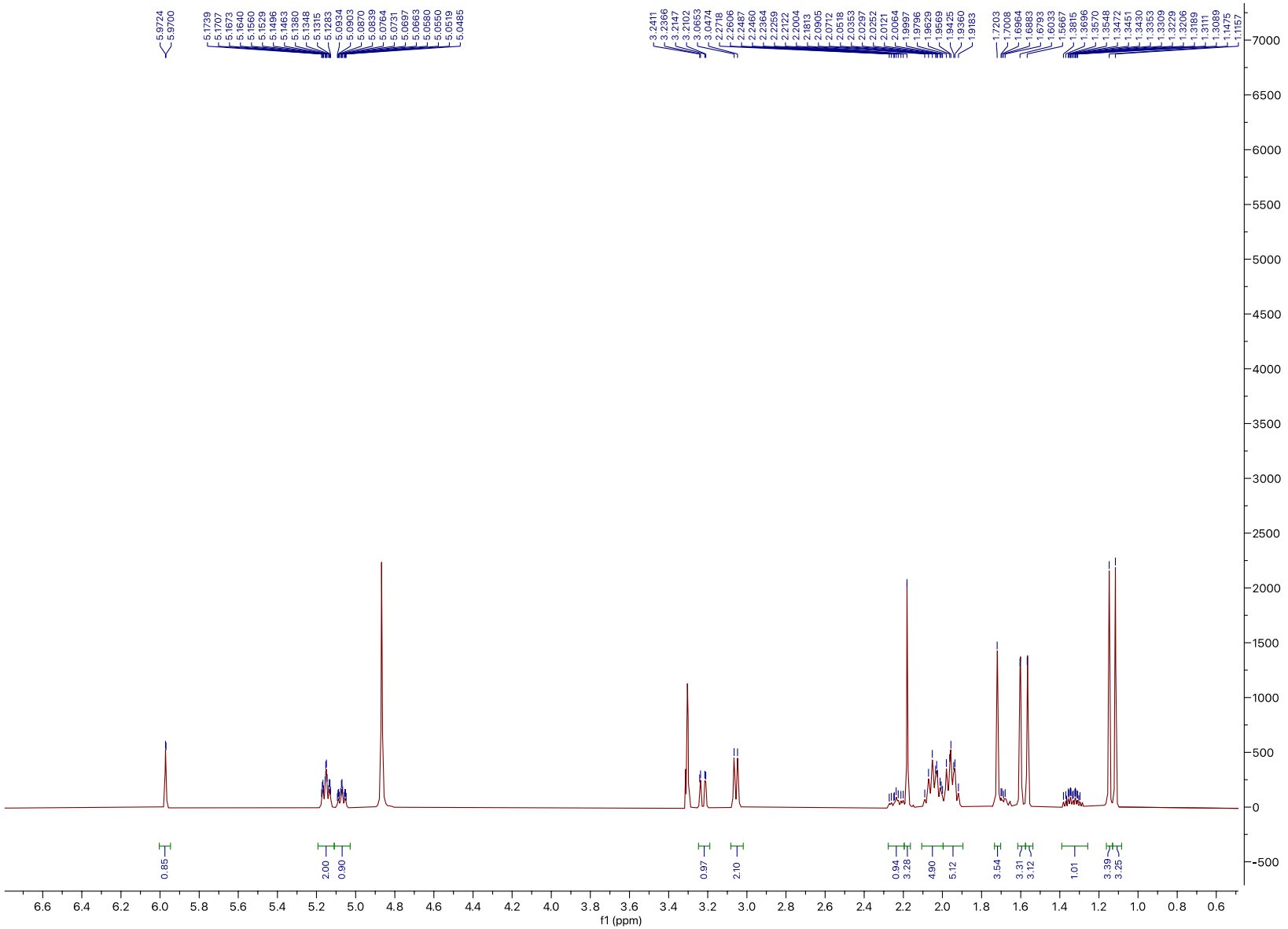

Figure S31. ^{1}H NMR of compound **7** in CD_3OD

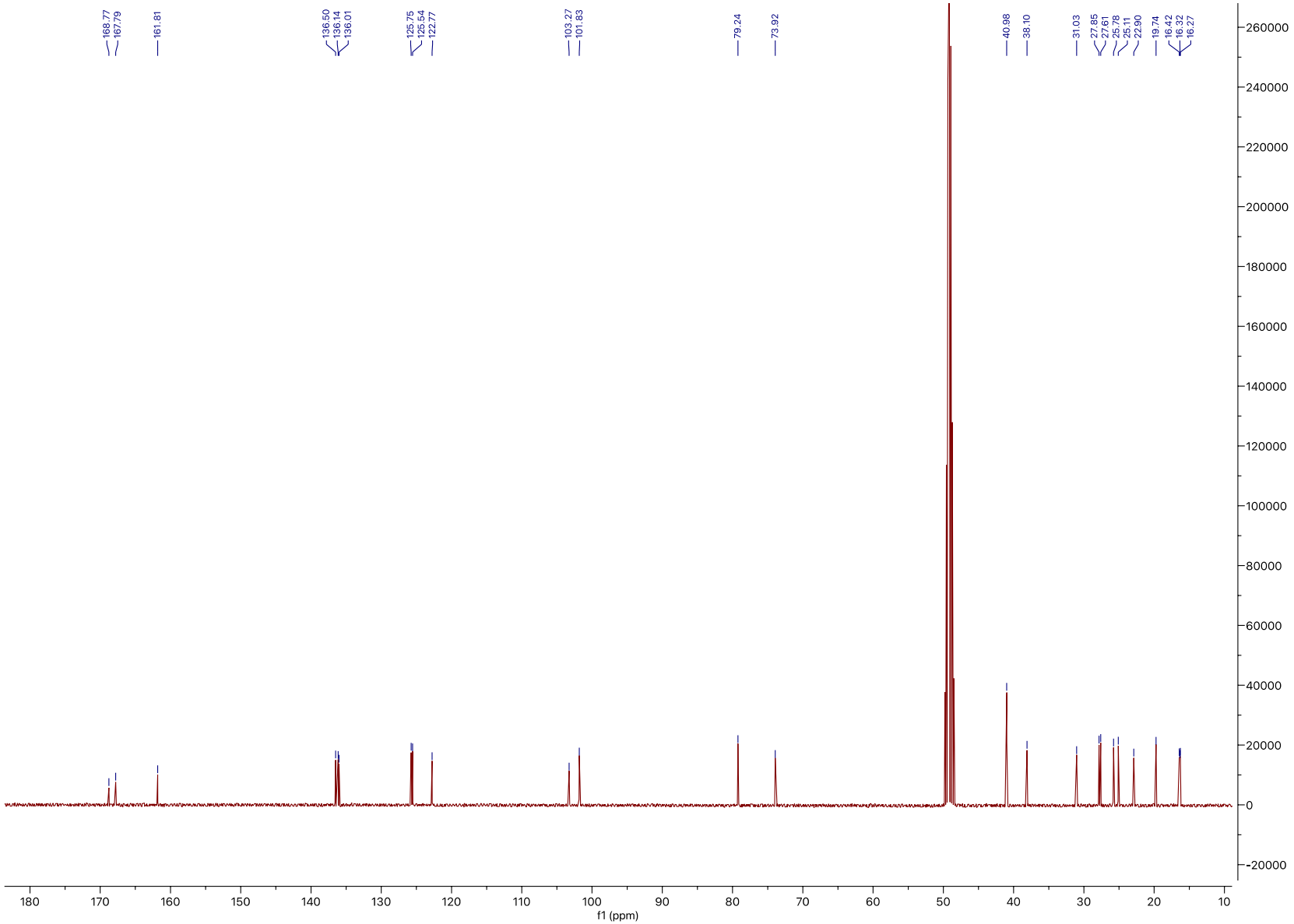

Figure S32. ^{13}C NMR of compound **7** in CD_3OD

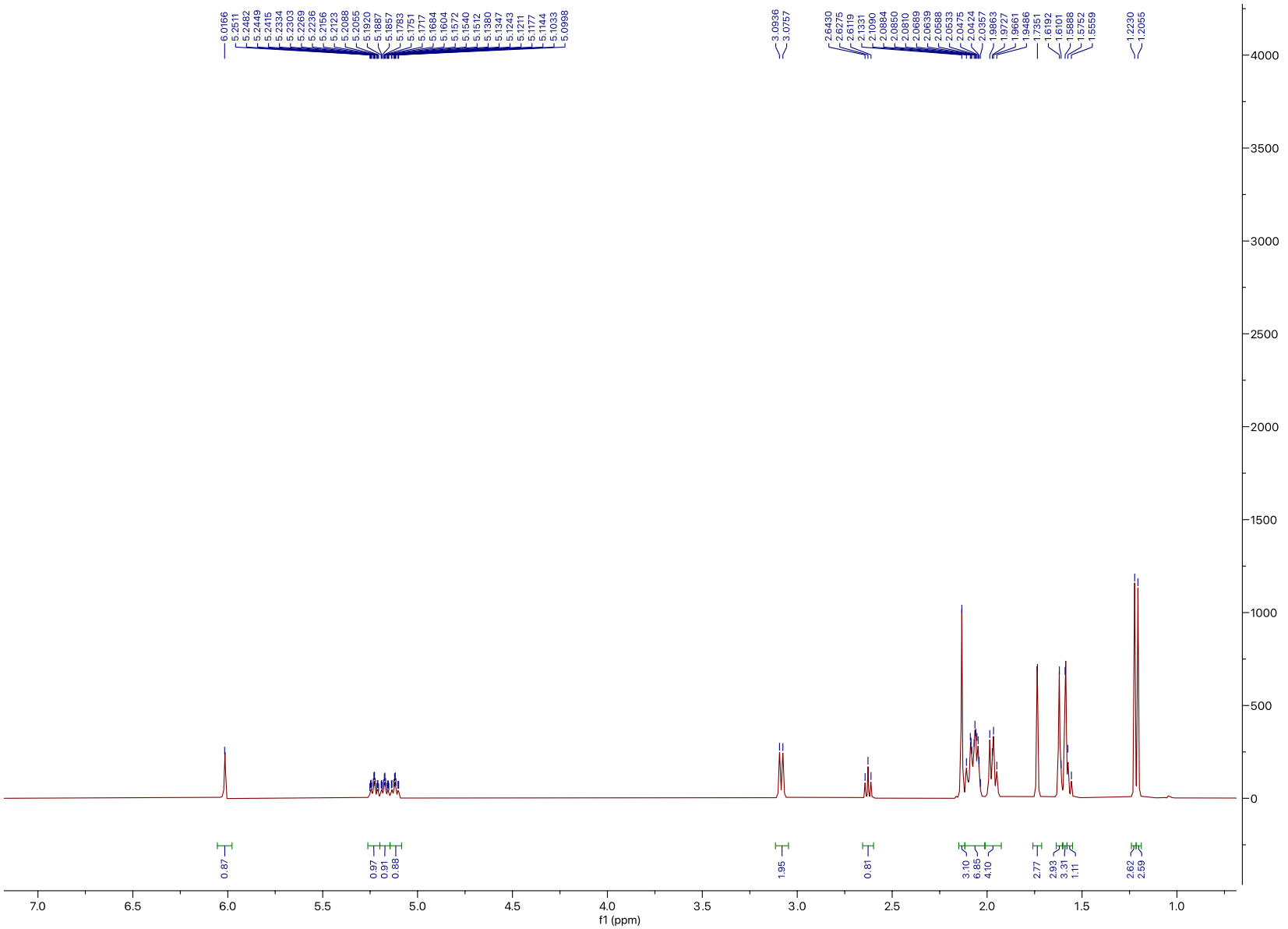

Figure S33. ^{1}H NMR of compound **8** in acetone-d_6

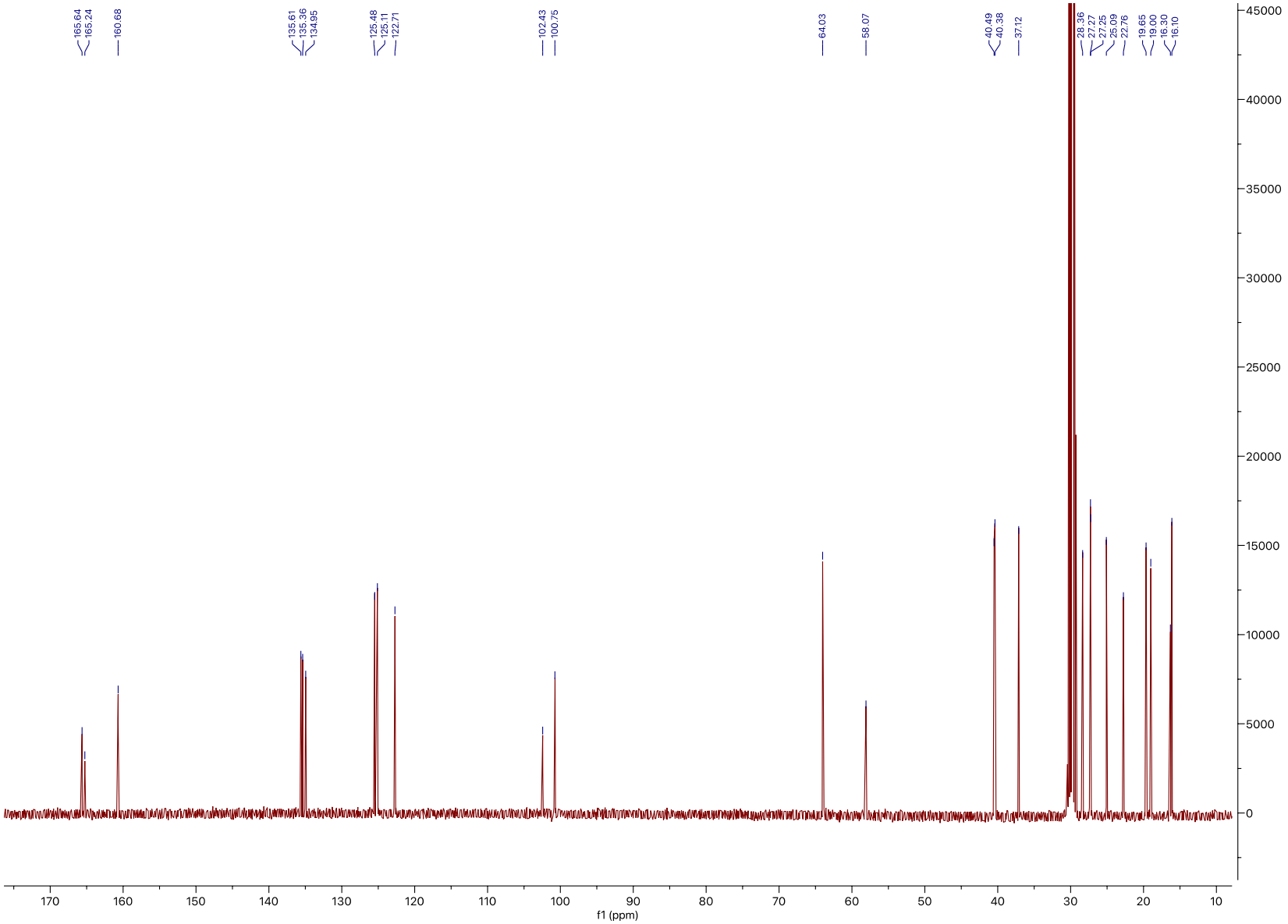

Figure S34. ^{13}C NMR of compound **8** in acetone-d_6

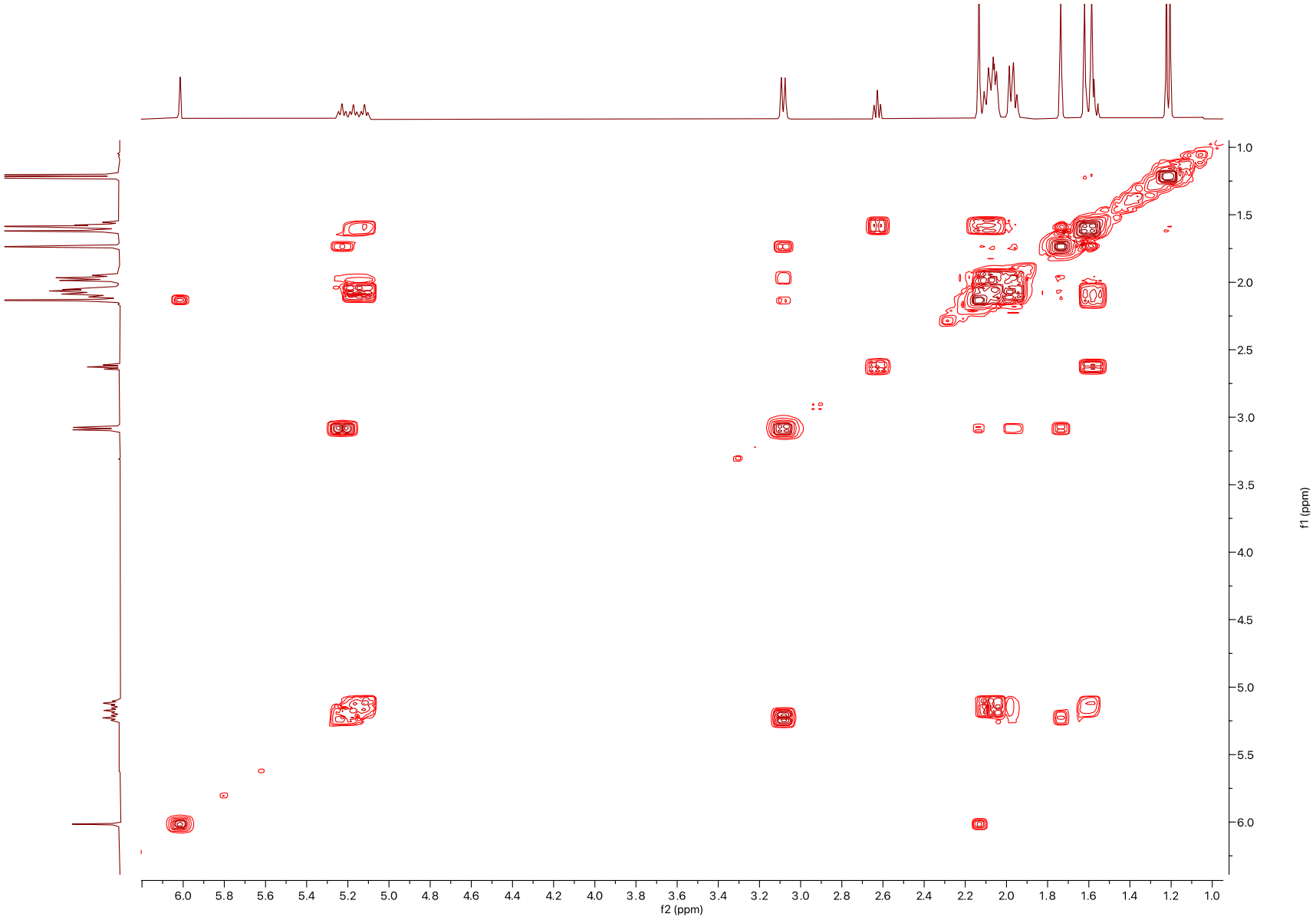

Figure S35. COSY of compound **8** in acetone-d_6

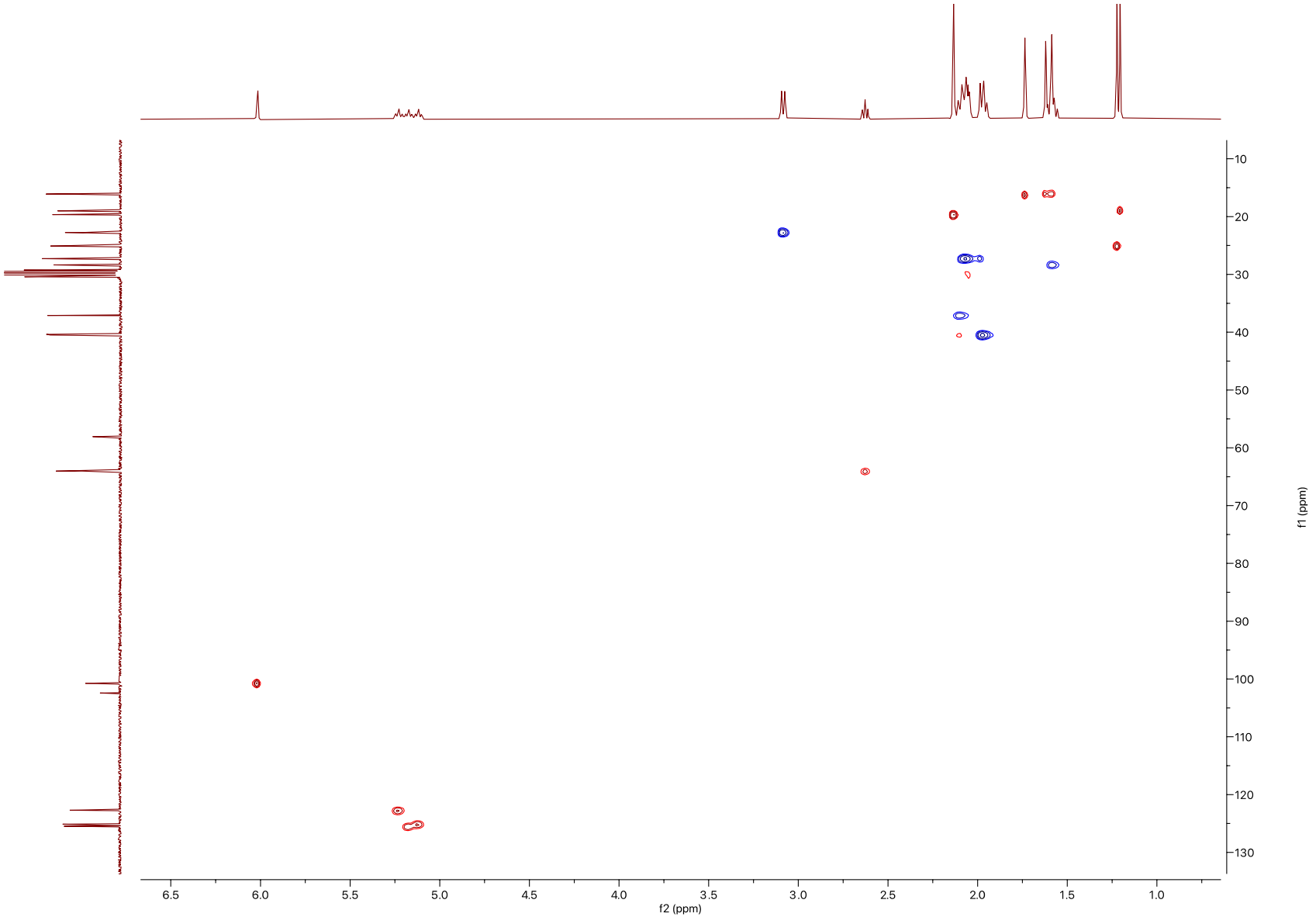

Figure S36. HSQC of compound **8** in acetone-d_6

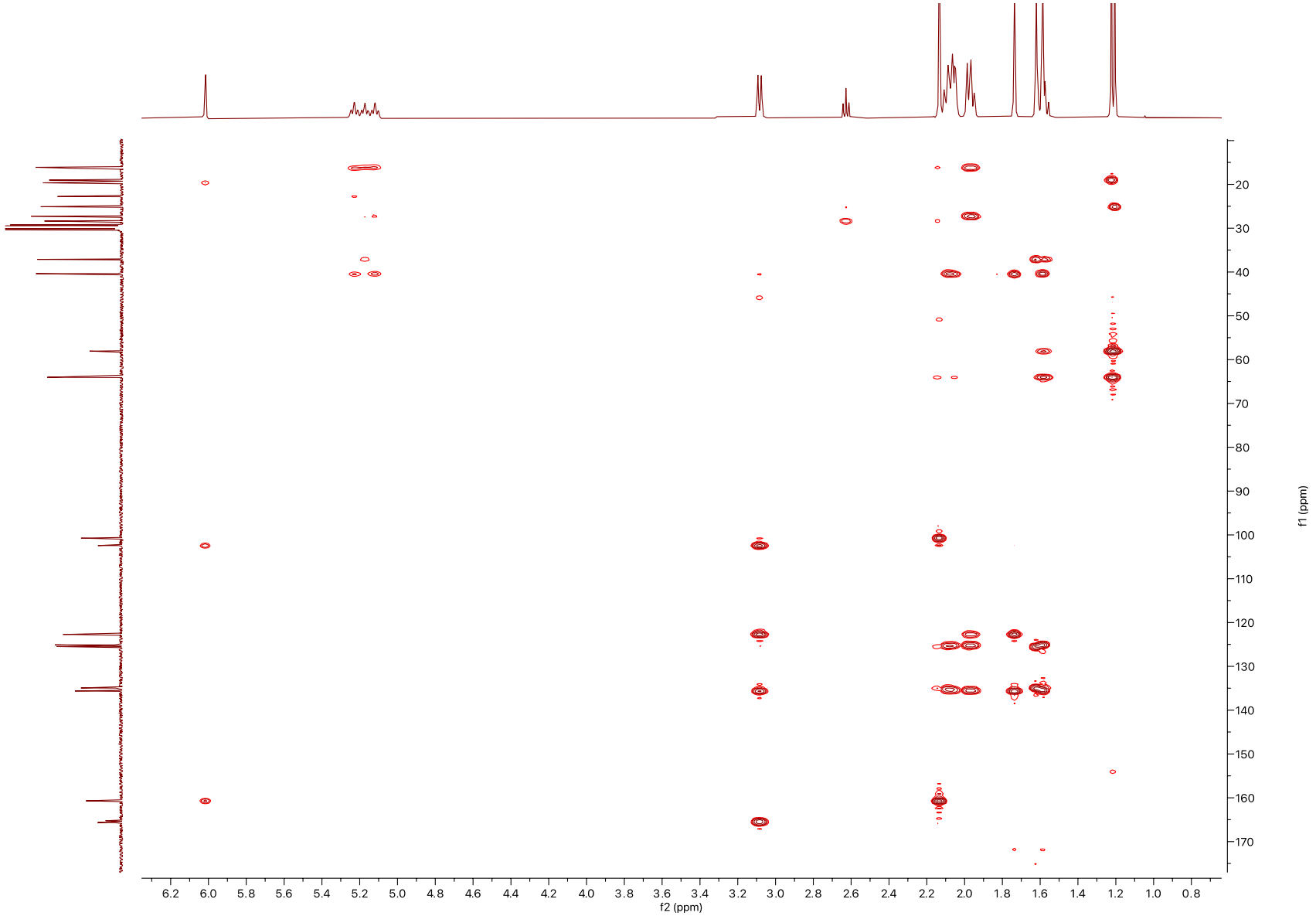

Figure S37. HMBC of compound **8** in acetone-d_6

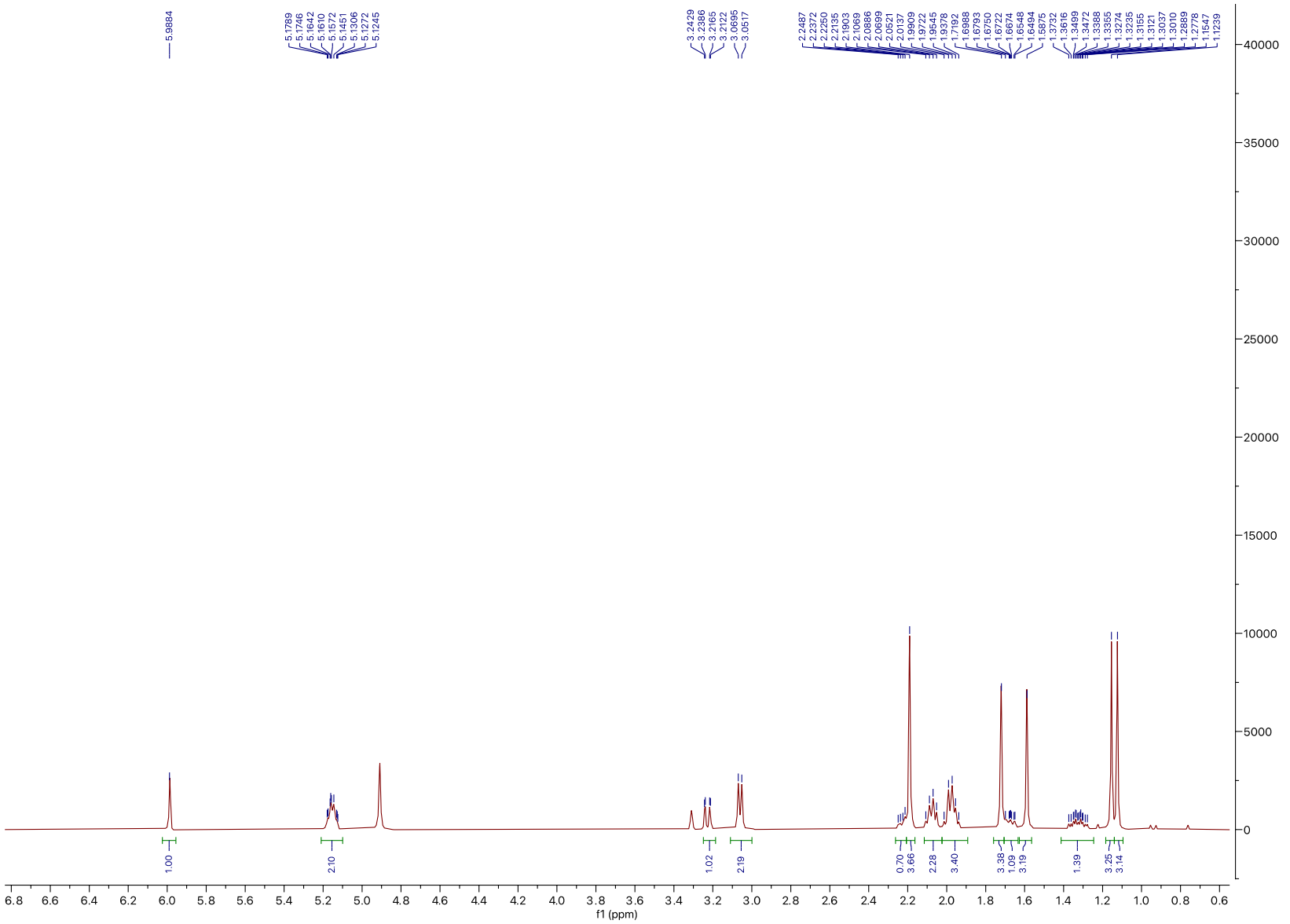

Figure S38. ^{1}H NMR of compound **9** in CD_3OD

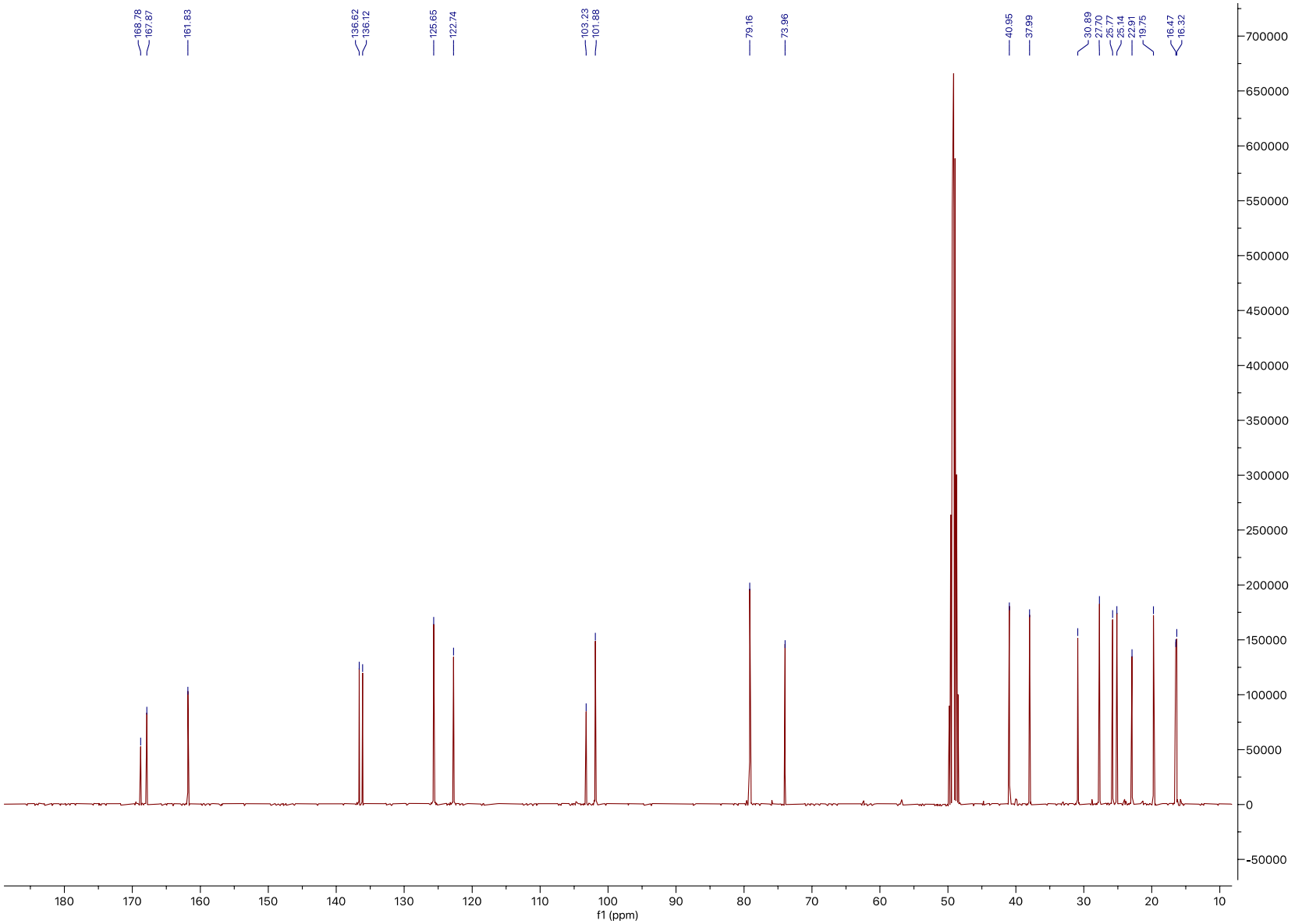

Figure S39. ^{13}C NMR of compound **9** in CD_3OD

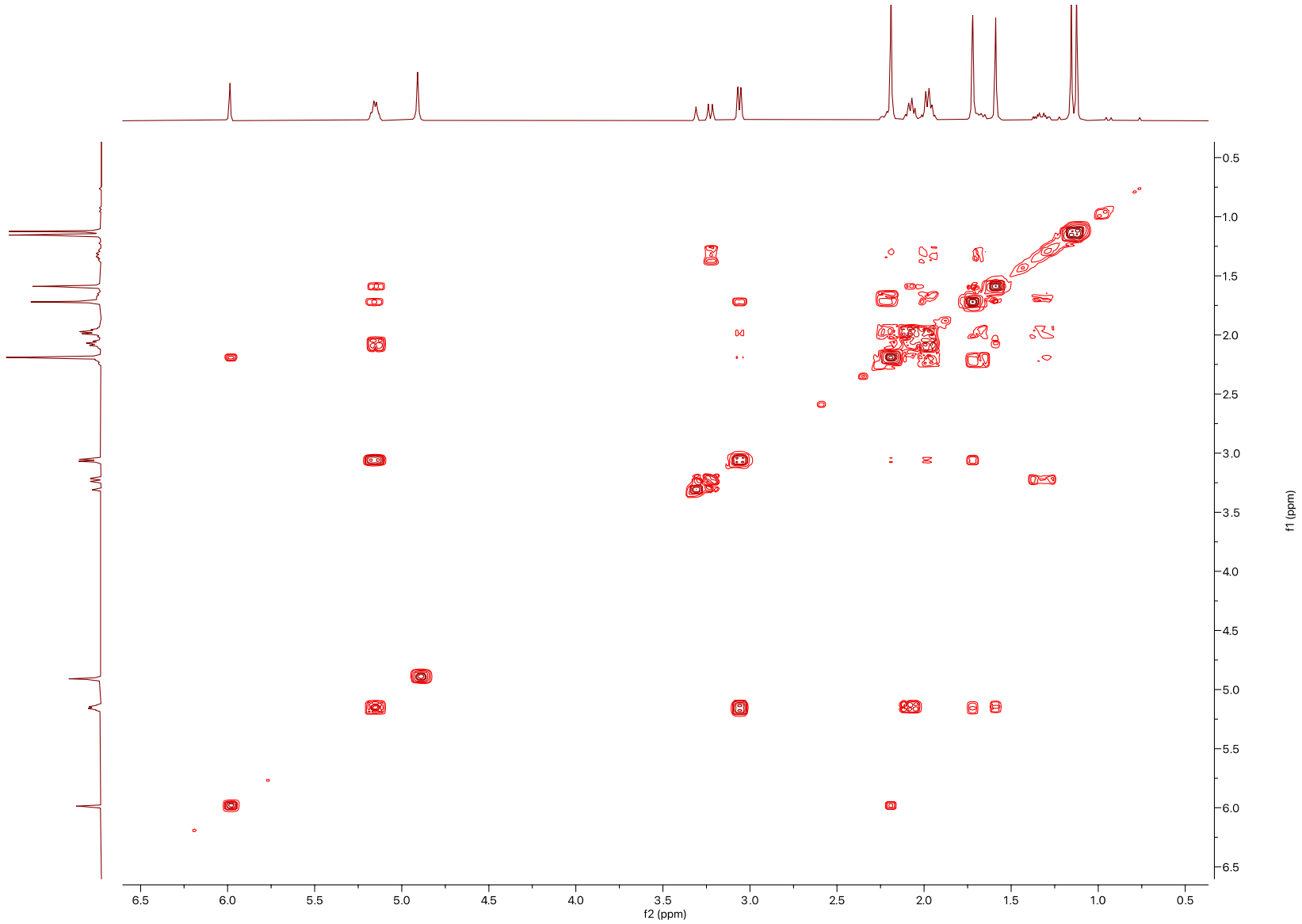

Figure S40. COSY of compound **9** in CD_3OD

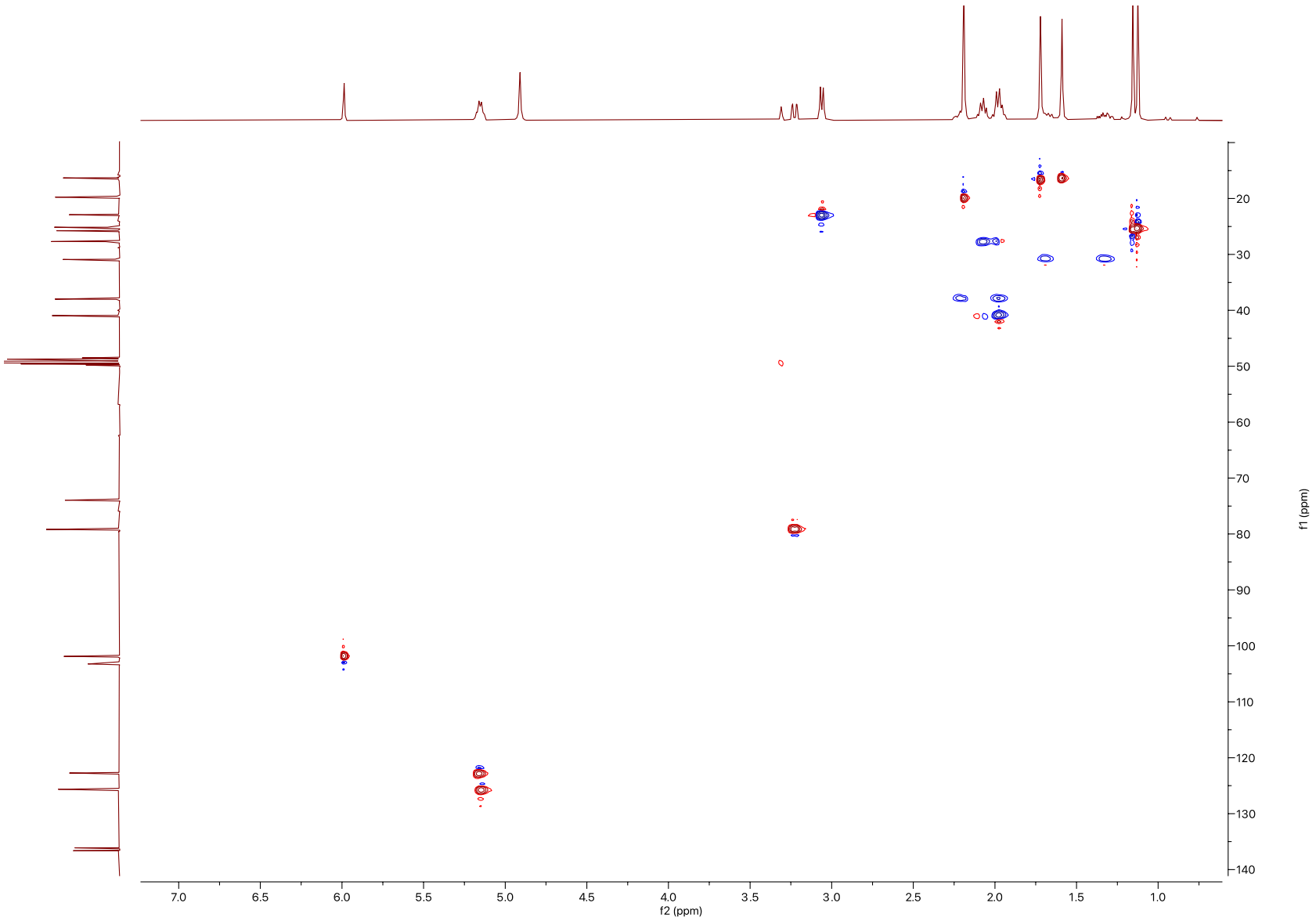

Figure S41. HSQC of compound **9** in CD_3OD

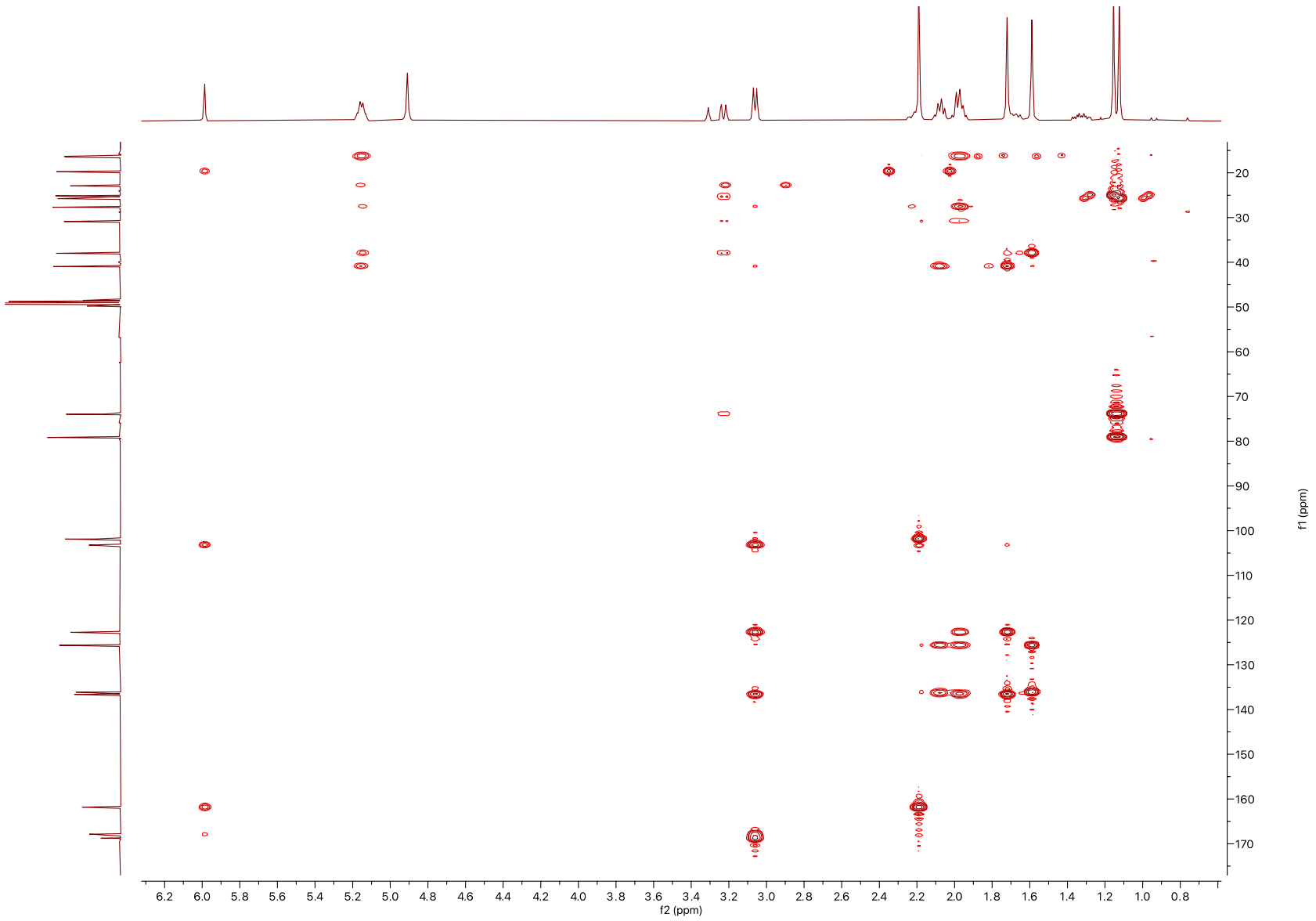

Figure S42. HMBC of compound **9** in CD_3OD

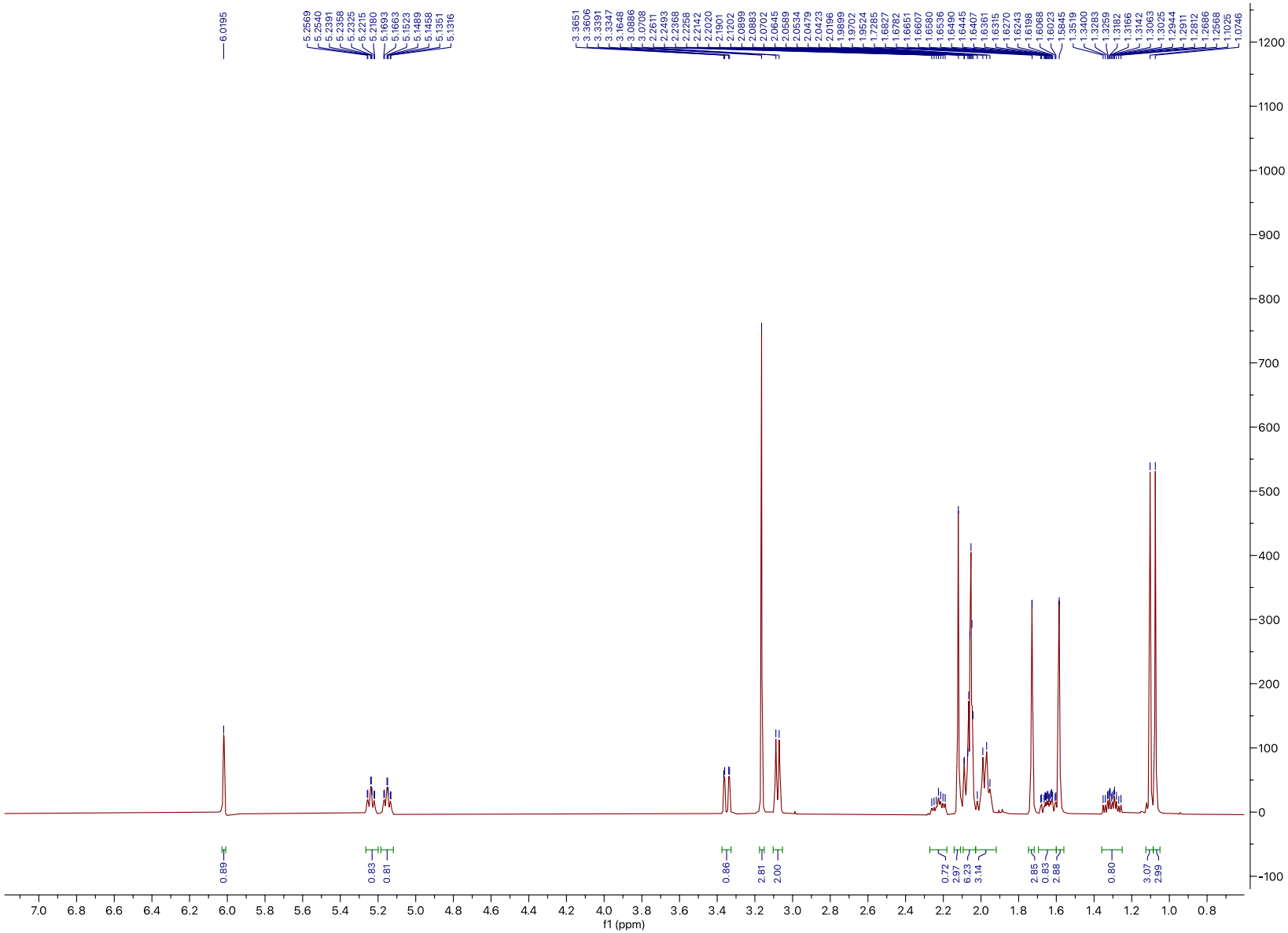

Figure S43. ^{1}H NMR of compound **10** in acetone-d_6

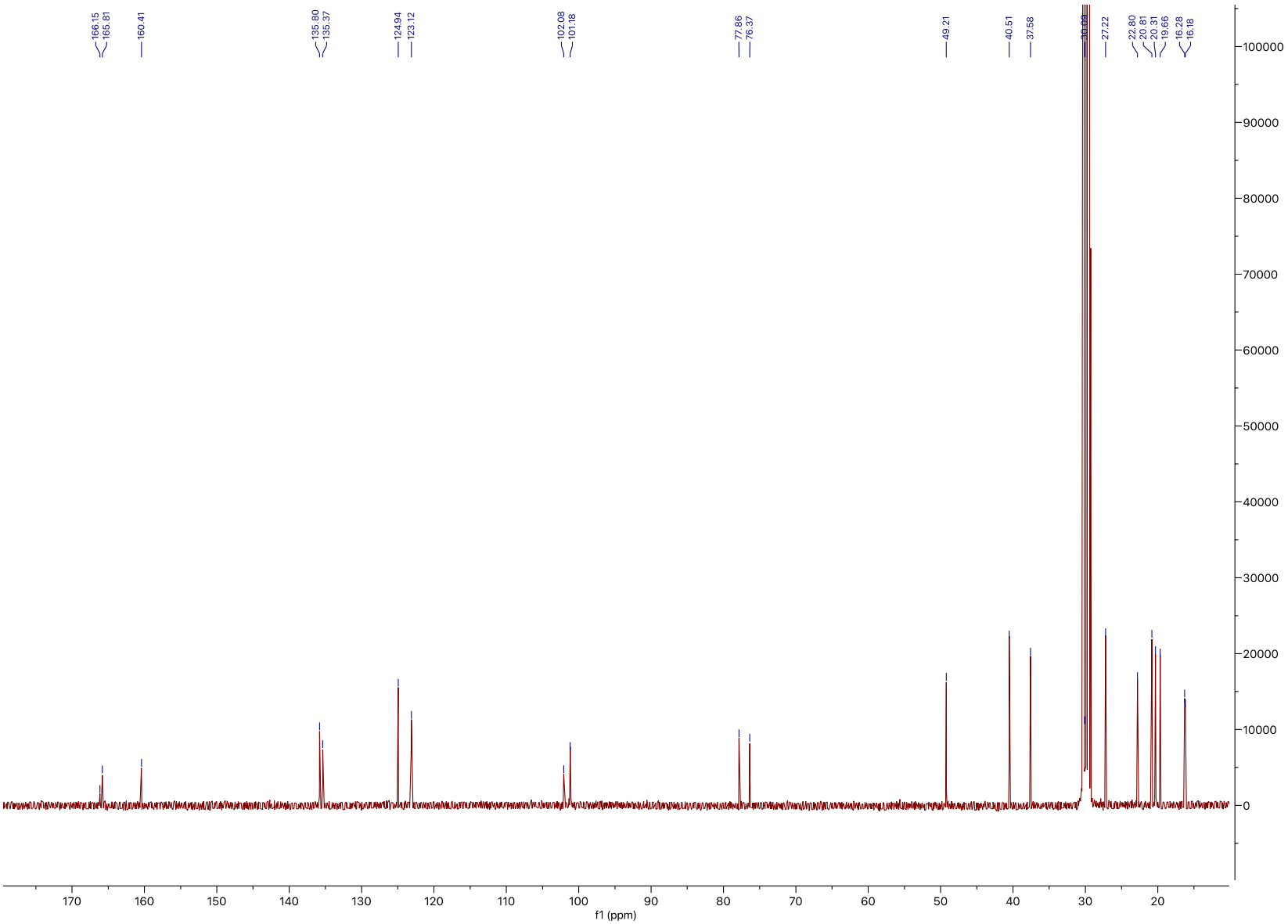

Figure S44. ^{13}C NMR of compound **10** in acetone-d_6

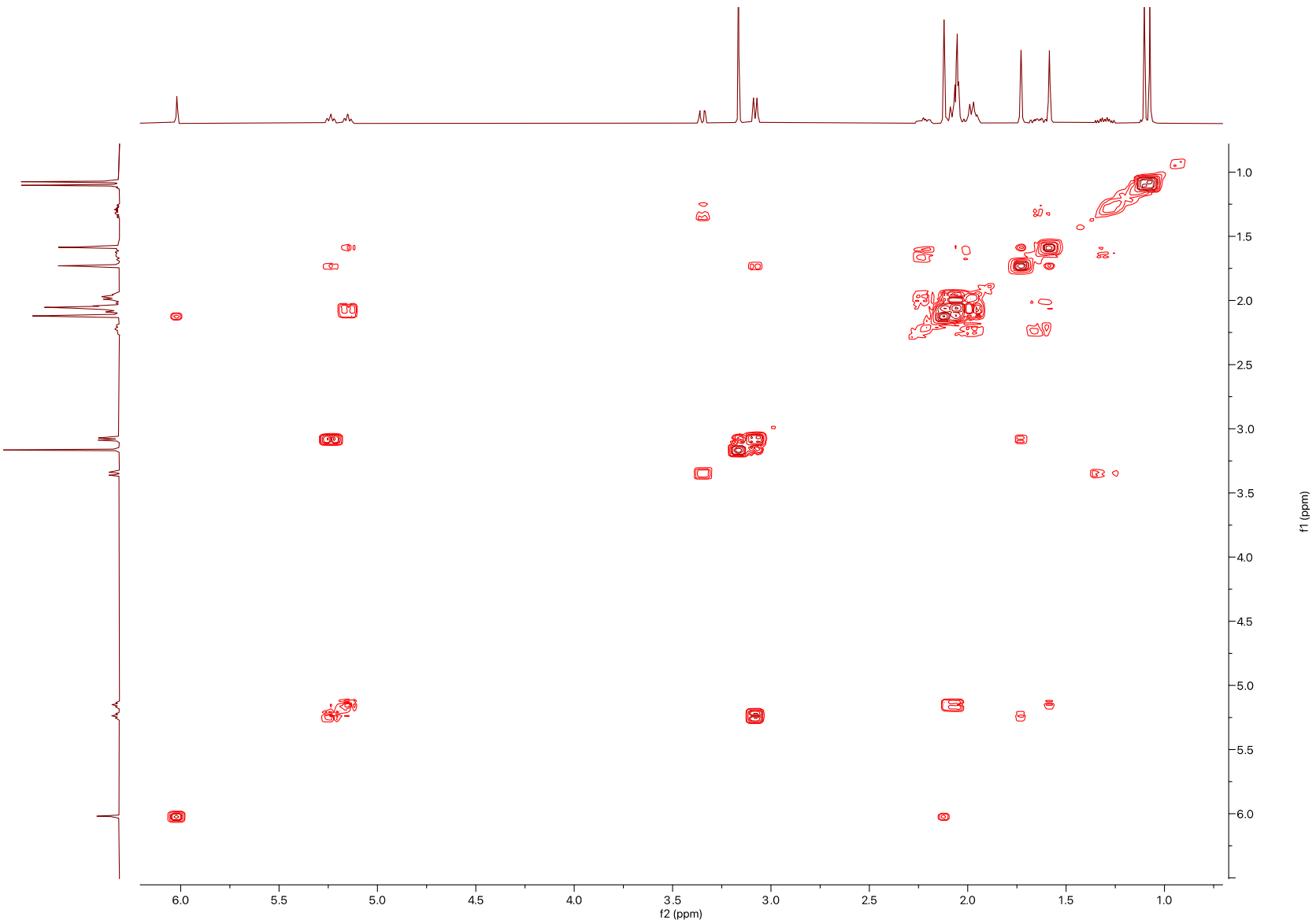

Figure S45. COSY of compound **10** in acetone-d_6

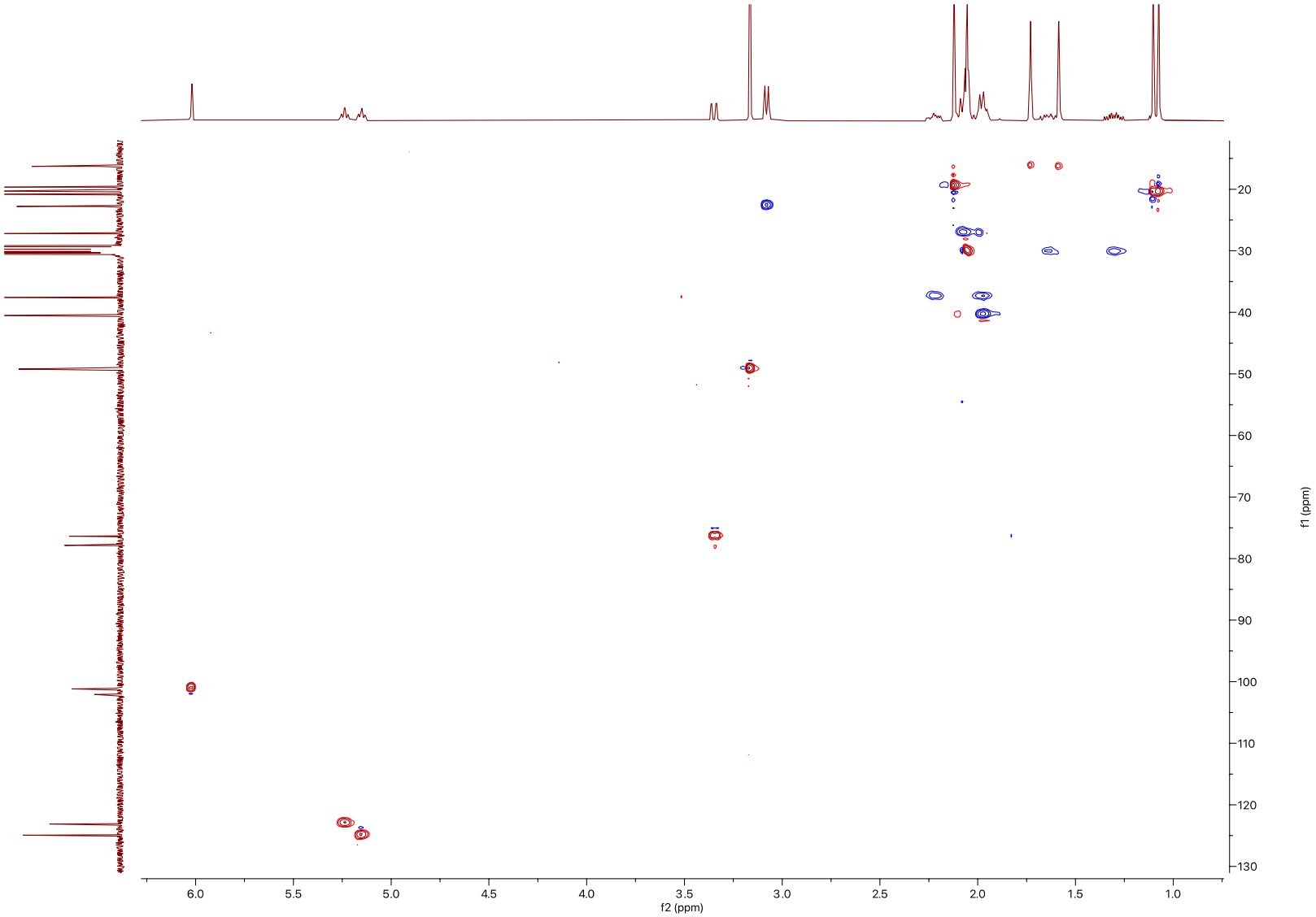

Figure S46. HSQC of compound **10** in acetone-d_6

Figure S47. HMBC of compound **10** in acetone-d_6

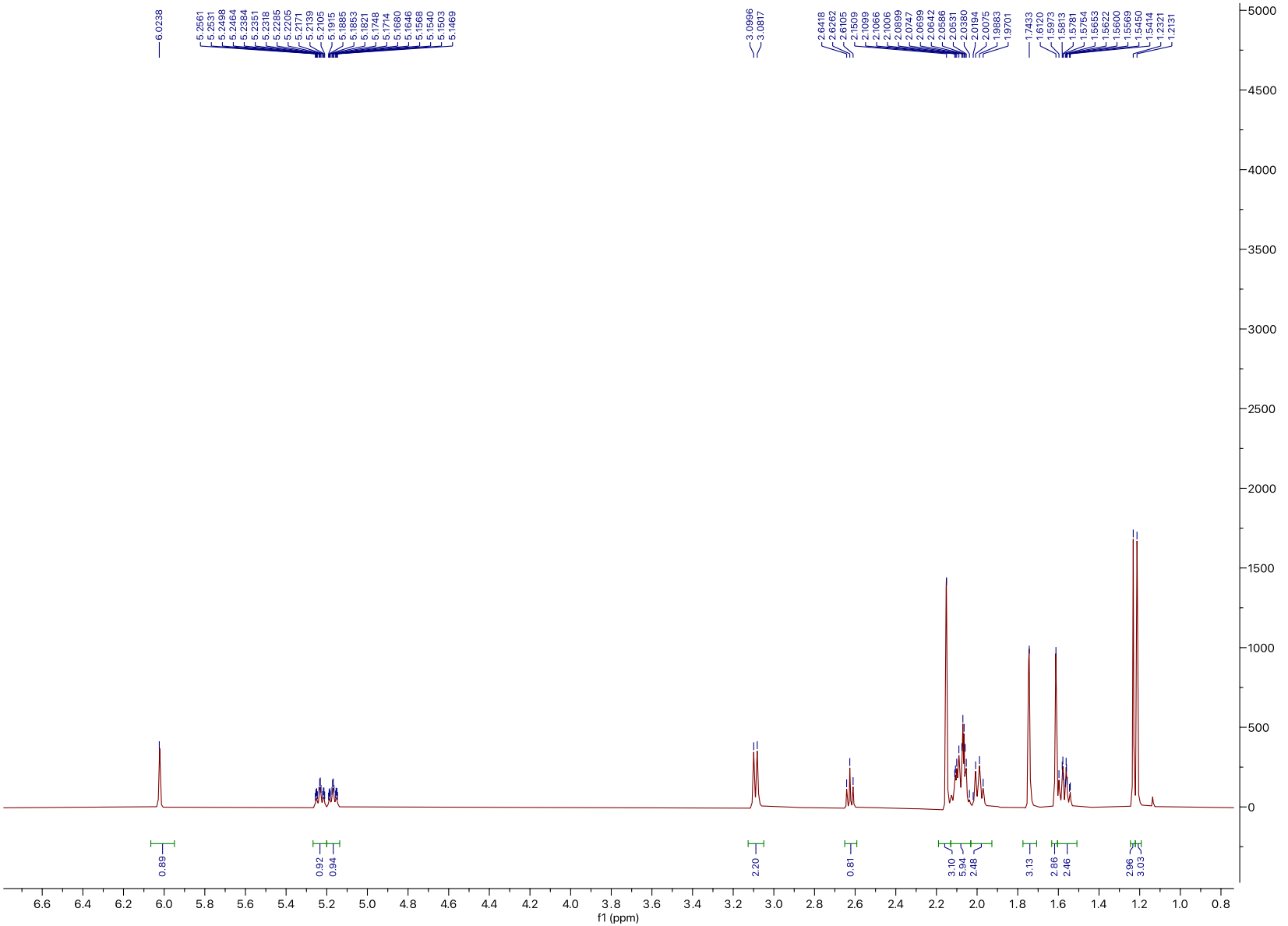

Figure S48. ^{1}H NMR of compound **11** in acetone-d_6

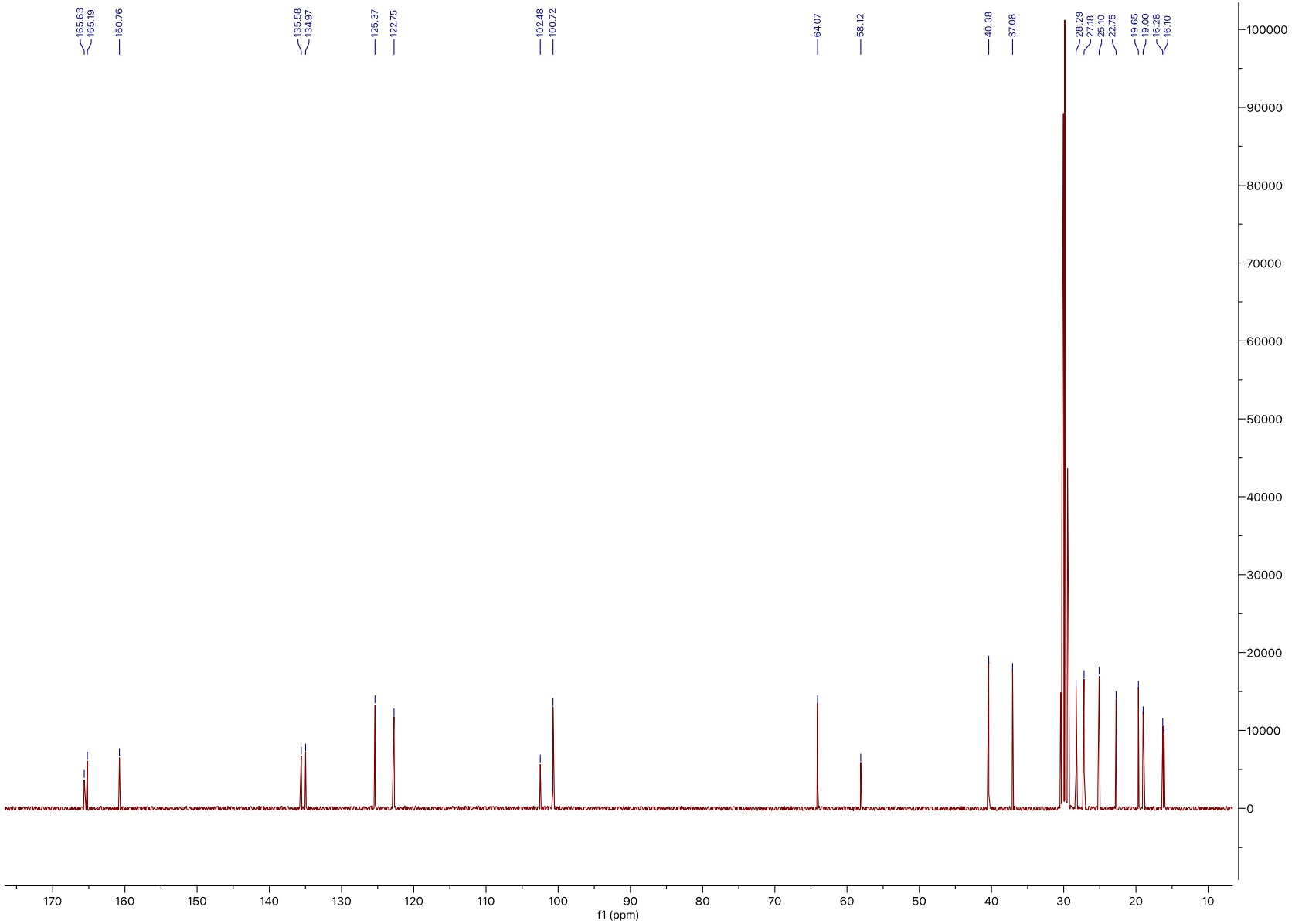

Figure S49. ^{13}C NMR of compound **11** in acetone-d_6

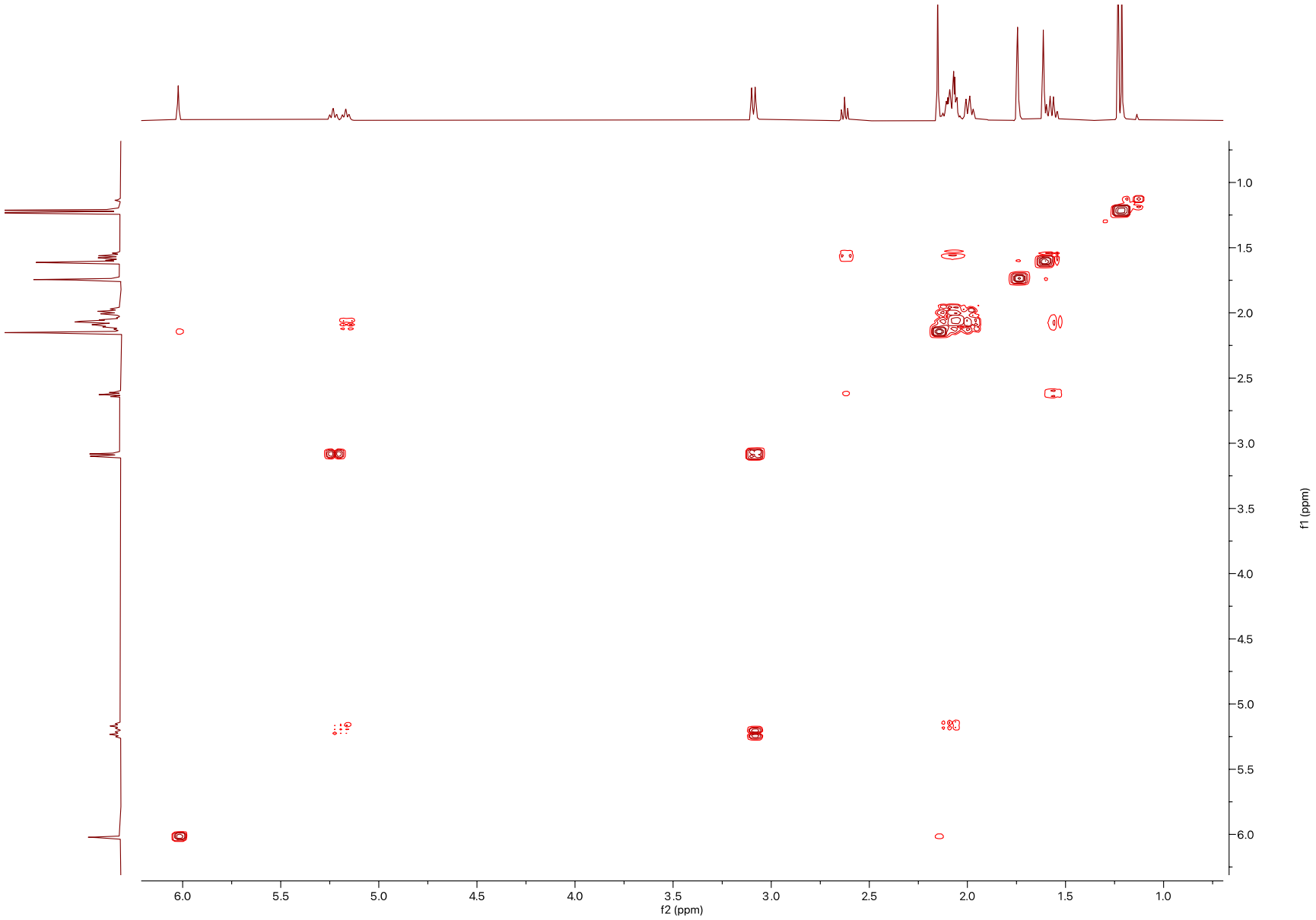
6.0
5.5
5.0
4.5
4.0
3.5
3.0
2.5
2.0
1.5
1.0
f2 (ppm)
1.0
1.5
2.0
2.5
3.0
3.5
4.0
4.5
5.0
5.5
6.0
f1 (ppm)

Figure S50. COSY of compound **11** in acetone-d_6

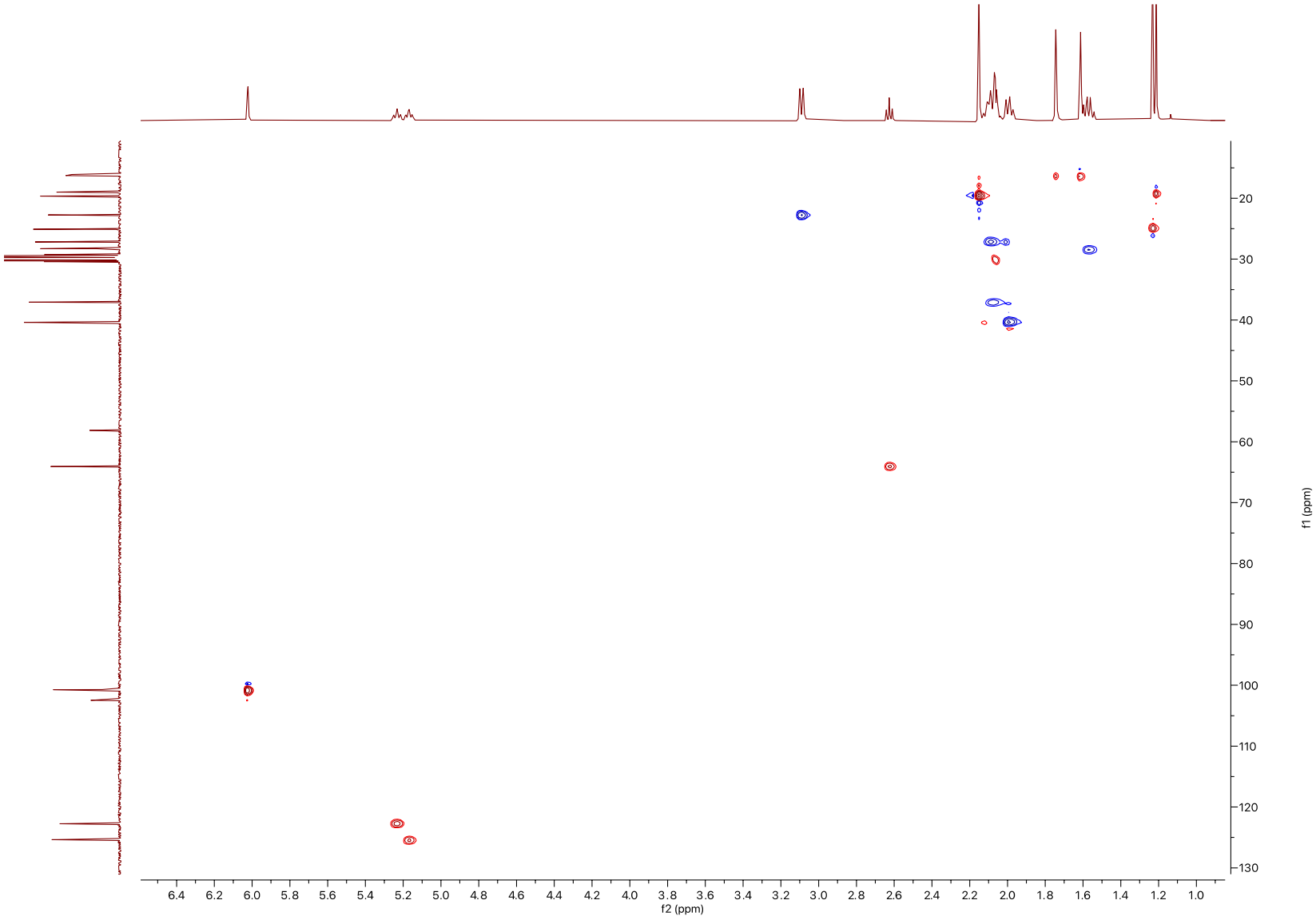

Figure S51. HSQC of compound **11** in acetone-d_6

Figure S52. HMBC of compound **11** in acetone-d_6

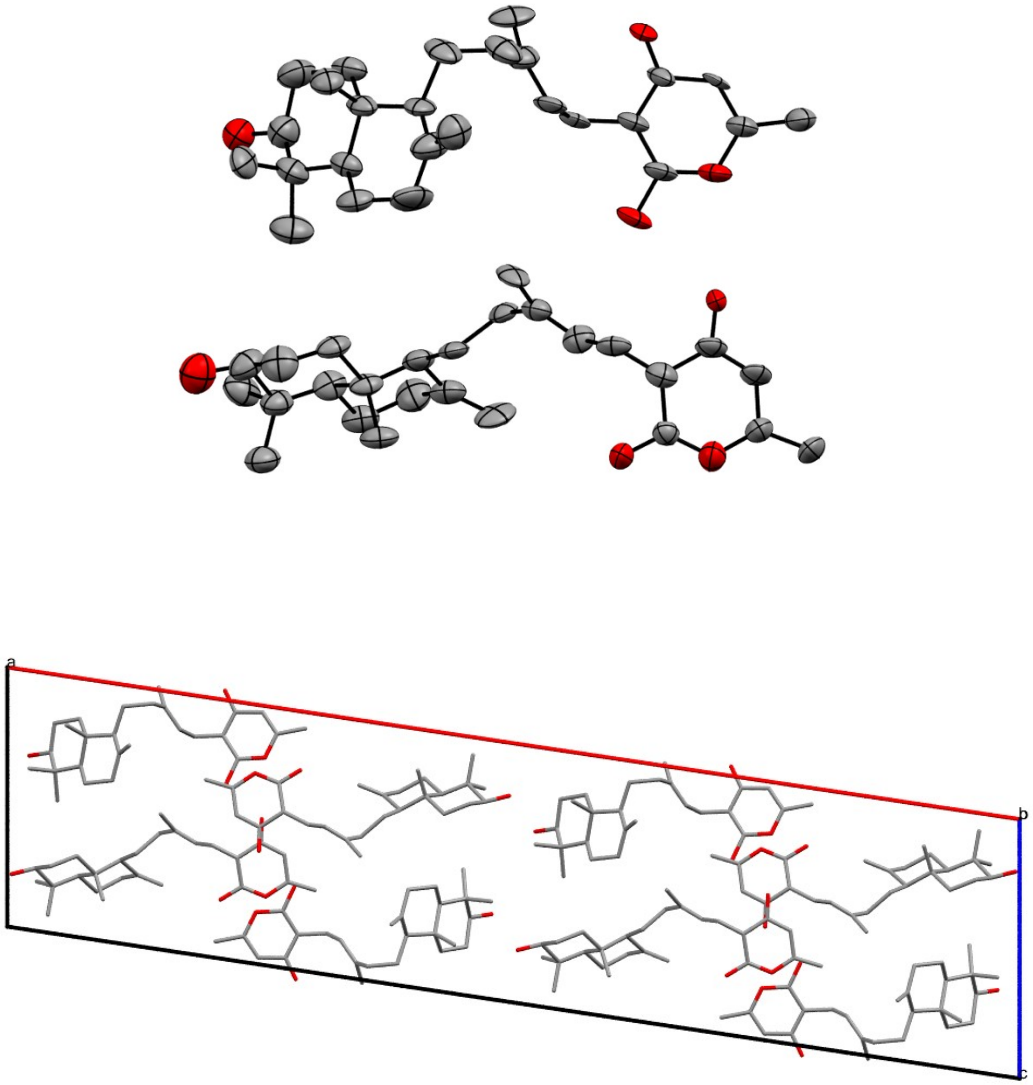

Figure S53. Crystal structure and unit cell packing of sartorypyrone F (**1**). Two molecules are present in the asymmetric unit. Thermal ellipsoids are drawn at 50% probability.

References

1 T. Wada, Y. Hayashi and H. Shibata, *Biosci. Biotechnol. Biochem.*, 1996, **60**, 120–121.

2 T. Nayak, E. Szewczyk, C. E. Oakley, A. Osmani, L. Ukil, S. L. Murray, M. J. Hynes, S. A. Osmani and B. R. Oakley, *Genetics*, 2006, **172**, 1557–1566.

3 E. Szewczyk, T. Nayak, C. E. Oakley, H. Edgerton, Y. Xiong, N. Taheri-Talesh, S. A. Osmani and B. R. Oakley, *Nat. Protoc.*, 2006, **1**, 3111–3120.

4 C. E. Oakley, H. Edgerton-Morgan and B. R. Oakley, in *Fungal Secondary Metabolism*, eds. N. P. Keller and G. Turner, Humana Press, Totowa, NJ, 2012, vol. 944, pp. 143–161.

5 H. Edgerton-Morgan and B. R. Oakley, *J. Cell Biol.*, 2012, **198**, 785–791.

6 L. J. Kim, M. Xue, X. Li, Z. Xu, E. Paulson, B. Mercado, H. M. Nelson and S. B. Herzon, *J. Am. Chem. Soc.*, 2021, **143**, 6578–6585.

7 W. Kabsch, *Acta Crystallogr D Biol Crystallogr*, 2010, **66**, 125–132.

8 G. M. Sheldrick, *Acta Crystallogr. Sect. A*, 2008, **64**, 112–122.

9 C. B. Hübschle, G. M. Sheldrick and B. Dittrich, *J. Appl. Crystallogr.*, 2011, **44**, 1281–1284.

10 G. M. Sheldrick, *Acta Crystallogr. Sect. C-Struc. Chem.*, 2015, **71**, 3–8.

11 S. Kaifuchi, M. Mori, K. Nonaka, R. Masuma, S. Ōmura and K. Shiomi, *J. Antibiot.*, 2015, **68**, 403–405.

12 A. Eamvijarn, N. M. Gomes, T. Dethoup, J. Buaruang, L. Manoch, A. Silva, M. Pedro, I. Marini, V. Roussis and A. Kijjoa, *Tetrahedron*, 2013, **69**, 8583–8591.

13 W.-G. Wang, L.-Q. Du, S.-L. Sheng, A. Li, Y.-P. Li, G.-G. Cheng, G.-P. Li, G. Sun, Q.-F. Hu and Y. Matsuda, *Org. Chem. Front.*, 2019, **6**, 571–578.

14 S. Bang, J. H. Song, D. Lee, C. Lee, S. Kim, K. S. Kang, J. H. Lee and S. H. Shim, *J. Agric. Food Chem.*, 2019, **67**, 1831–1838.